RSC Advances

REVIEW

View Article Online
View Journal | View Issue

Cite this: *RSC Adv.*, 2021, **11**, 36398

Received 24th May 2021
Accepted 9th October 2021

DOI: 10.1039/d1ra04060j

rsc.li/rsc-advances

Additive manufacturing technology of polymeric materials for customized products: recent developments and future prospective

Akhilesh Kumar Pal, [a] Amar K. Mohanty *[ab] and Manjusri Misra *[ab]

The worldwide demand for additive manufacturing (AM) is increasing due to its ability to produce more challenging customized objects based on the process parameters for engineering applications. The

[a]*Bioproducts Discovery and Development Centre, Department of Plant Agriculture, University of Guelph, Crop Science Building, 50 Stone Road East, Guelph, Ontario N1G 2W1, Canada. E-mail: mohanty@uoguelph.ca; mmisra@uoguelph.ca*

[b]*School of Engineering, University of Guelph, Thornbrough Building, 50 Stone Road East, Guelph, Ontario N1G 2W1, Canada*

Dr Akhilesh Kumar Pal is currently a postdoctoral fellow in Bioproducts Discovery & Development Centre, Department of Plant Agriculture at the University of Guelph. His current research emphasis on the development of novel bio-based composites their processing and utilization in various applications. He has authored 17 research articles in peer reviewed journals and 03 book chapters till date. He received his PhD degree in the Department of Chemical Engineering at Indian Institute of Technology Guwahati, India. He received Gandhian Young Technological Innovation Award from Society for Research and Initiatives for Sustainable Technologies and Institutions. He also received a national award from Technology Innovation in Petrochemicals and Downstream Plastics Processing Industry in India.

Dr Amar K. Mohanty is a Full Professor and OAC Distinguished Research Chair in Sustainable Biomaterials and is the Director of the Bioproducts Discovery & Development Centre at the University of Guelph. He is a former Michigan State University professor and is an international leader in the field of bioplastics, biocomposites and advanced biorefinery. His research focuses on engineering value-added uses of biomass wastes and industrial co-products from agro-food and biofuel industries. Circular economy, environmental sustainability, waste plastic valorization, biodegradable plastics as single-use plastic alternatives, biocarbon based composites and 3D printing of sustainable materials are other areas of his expertise. Prof. Mohanty is the Editor-in-Chief of Sustainable Composites, Composites Part C – Open Access (ELSEVIER). He has more than 800 publications to his credit, including 430 peer-reviewed journal papers, 6 edited books, over 400 conference presentations, 25 book chapters, and 67 Patents awarded/applied (His Google Scholar citations exceed 42 000). Prof. Mohanty is a Fellow of the Royal Society of Canada, the American Institute of Chemical Engineers, the Royal Society of Chemistry (UK) and the Society of Plastic Engineers. Prof. Mohanty has received many awards, including the: JL White Innovation Award from the International Polymer Processing Society; Synergy Award for Innovation from Natural Sciences and Engineering Research Council of Canada (NSERC); Andrew Chase Forest Products Division Award from the American Institute of Chemical Engineers and Lifetime Achievement Award from the Bio-Environmental Polymer Society (BEPS).

processing of conventional materials by AM processes is a critically demanded research stream, which has generated a path-breaking scenario in the rapid manufacturing and upcycling of plastics. The exponential growth of AM in the worldwide polymer market is expected to exceed 20 billion US dollars by 2021 in areas of automotive, medical, aerospace, energy and customized consumer products. The development of functional polymers and composites by 3D printing-based technologies has been explored significantly due to its cost-effective, easier integration into customized geometries, higher efficacy, higher precision, freedom of material utilization as compared to traditional injection molding, and thermoforming techniques. Since polymers are the most explored class of materials in AM to overcome the limitations, this review describes the latest research conducted on petroleum-based polymers and their composites using various AM techniques such as fused filament fabrication (FFF), selective laser sintering (SLS), and stereolithography (SLA) related to 3D printing in engineering applications such as biomedical, automotive, aerospace and electronics.

1. Introduction

Additive manufacturing (AM) is designated as one of the revolutionary innovations since the 19th century, which significantly reshaped the manufacturing industries.[1–3] AM, an advanced approach of materials fabrication, is a set of techniques, which use a layer-by-layer approach to construct complex shaped parts. Most commonly, it is ascribed as rapid prototyping (RP), free-form fabrication, with low energy consumption and high design flexibility.[4–6] The AM technique is versatile, adaptable, flexible, highly customizable and can be utilized in many sectors of industrial production.[7] Such characteristics have been acknowledged to be immensely advantageous in biomedical and automotive industries amongst others including construction, healthcare, dental and aerospace industries.[8,9] The advantageous side of AM is its nonrequirement of molding tools and its relatively less time consumption to fabricate customized parts, which are the most beneficial parameters for a robust manufacturing system. Computer-aided design (CAD) software is an integral part of AM technology, which helps to create personalized digital designs and 3D models to fabricate the prototypes.[5] In detail, such softwares prepare 3D models in the form of slices, which represent layers while polymer printing. Such digital files also comprise information about the material's properties and printing parameters used in various printing techniques.[10] Fundamentally, AM is completely different from the available traditional subtractive manufacturing-based techniques. This technique is based on the 'bottom-up' or 'top-down' approaches where a customized structure is fabricated using layer-by-layer model rather than casting or injection technologies. An extensive variety of materials such as metals, ceramics, polymers along with combinations in the form of blends, hybrids and composites can be utilized in AM technique. An excessive research work is required using AM to address the challenges associated with its two key technologies named 'materials' and 'metrology' to make this functional in prognostic and reproductive ways.[7] However, the interest in using AM technology at industrial scale has been increased exponentially due to its capability to produce real, complex shaped, innovative and robust products.

The production of complex geometries as per available advanced computer design software becomes an emerging research area in 3D printing. The limitations in printability and mechanical properties of neat polymers encourage the scientist community to develop high performance 3D printable polymer blends and composites, which have various advantages including cost effectiveness, high precision, reduction in polymer wastes, minimal chemical usage and customized complex geometries.[11] Such developed geometries can be utilized as per the demand in various domains of applications including

Dr Manjusri Misra is a professor and Tier 1 Canada Research Chair (CRC) in Sustainable Biocomposites in the School of Engineering and holds a joint appointment in the Department of Plant Agriculture at the University of Guelph. As well, she is the Research Program Director of the Bioeconomy Panel for the Ontario Agri-Food Innovation Alliance, a program between the Ontario Ministry of Agriculture and Rural Affairs (OMAFRA) and the University of Guelph. Dr Misra completed her Bachelors, Master's, and PhD at Utkal University in India focusing on chemistry with a specialization in polymers and natural fibres. Dr Misra's current research focuses primarily on novel bio-based composites and nanocomposites from agricultural, forestry and recycled resources for the sustainable bioeconomy moving towards Circular Economy. She has authored more than 750 publications, including 420 peer-reviewed journal papers, 21 book chapters, and 53 patents. She was the editor or co-editor of 4 books in the area of biocomposites and nanocomposites. She is a Fellow of the Royal Society of Chemistry (UK), the American Institute of Chemical Engineers (AIChE), and the Society of Plastic Engineers (SPE). Dr Misra has received many awards including the Synergy Award for Innovation from Natural Sciences and Engineering Research Council of Canada (NSERC); the Andrew Chase Forest Products Division Award from the American Institute of Chemical Engineers and the Lifetime Achievement Award from the BioEnvironmental Polymer Society (BEPS). In 2020, she was selected as one of Canada's Most Powerful Women: Top 100 Award Winner in the Manulife Science and Technology category from the Women Executive Network.

packaging, medical, tissue engineering, automotive, aerospace and electronics engineering.[12–14] Common techniques in 3D printing are fused filament fabrication (FFF), binder jetting 3D printing (BJP), selective laser sintering (SLS), and stereolithography (SLA) in which particle, fiber, and nanomaterial reinforced polymer composites can be utilized for the property's enhancement of individual polymer.[15–17] Wang *et al.*[14] has published a review article on 3D printing of polymer matrix composites in which various combinations of particle/polymer (*e.g.* iron/acrylonitrile butadiene styrene (ABS), copper/ABS, aluminium/nylon-6, tungsten/polycarbonate), fiber/polymer (*e.g.* short glass fibers/ABS, short carbon fibers/ABS, continuous carbon fibers/nylon, continuous carbon fibers/poly lactic acid (PLA)), and nanomaterial/polymer (*e.g.* TiO_2/ABS, graphene/ABS, montmorillonite/ABS, carbon black/nylon-12, silica/nylon-11) have been tabulated as polymer composites to enhance the mechanical, electrical, thermal, and other properties.

The problems related to oil exhaustion in the fabrication of non-biodegradable synthetic plastics have been developed exponentially and have unfortunately disturbed the ecosystem due to its accumulation in the environment based on the commercially available fabrication techniques.[18,19] This serious issue has motivated researchers to find a way in terms of sustainable material development and versatile techniques to replace the synthetic polymers as well as the conventional fabrication techniques such as injection molding, compression molding and thermoforming. In this direction, sustainable and biobased polymers have drawn attention because they can be produced from renewable resources and can be recycled but not biodegradable. Whereas, three-dimensional (3D) printing (as shown in Fig. 1) which is also known as additive manufacturing, is the latest developed technique and one of the best solutions for existing problems related to polymer wastes accumulation, landfill and disposal.[7]

The utilization of waste conventional plastic to develop 3D geometries is also an emerging area in which the used synthetic plastics can be mixed with sustainable fillers such as biocarbon, talc and renewable fillers such as cellulose,[20] and banana fibers[21] to meet the various required properties as per the targeted application. Recently, selective laser sintering and inkjet 3D printing techniques have been used widely for manufacturing complex 3D geometries by using various conventional polymers such as PET, nylon 6 [22] and renewable biobased materials such as wood flour, rice husk, and miscanthus fibers[23] respectively in powdered form. Hence, powder based additive manufacturing is one of the techniques, which may trigger the revolutionary changes at industrial scale due to its rapid tooling and prototyping in various manufacturing areas. An ideal packaging or implant material must be non-toxic, biocompatible, easily moldable, and mechanically durable.[24–26] A vast variety of application specific polymer objects such as fixation devices, scaffolds, bone like complex structures, implants, packaging materials, and automotive parts can be manufactured by 3D printers with relatively better efficiency, higher accuracy, minimal tooling cost, and time as compared with traditional manufacturing techniques such as injection molding and thermoforming.[27,28] At present, other materials such as metals and ceramics are used extensively in 3D printing in an industrial scale.[29–31] However, the use of sustainable polymers is limited at industrial scale due to their limitations such as processing window, brittleness, lower mechanical properties, compatibility with other conventional polymers and poor durability. On the other hand, bio-based

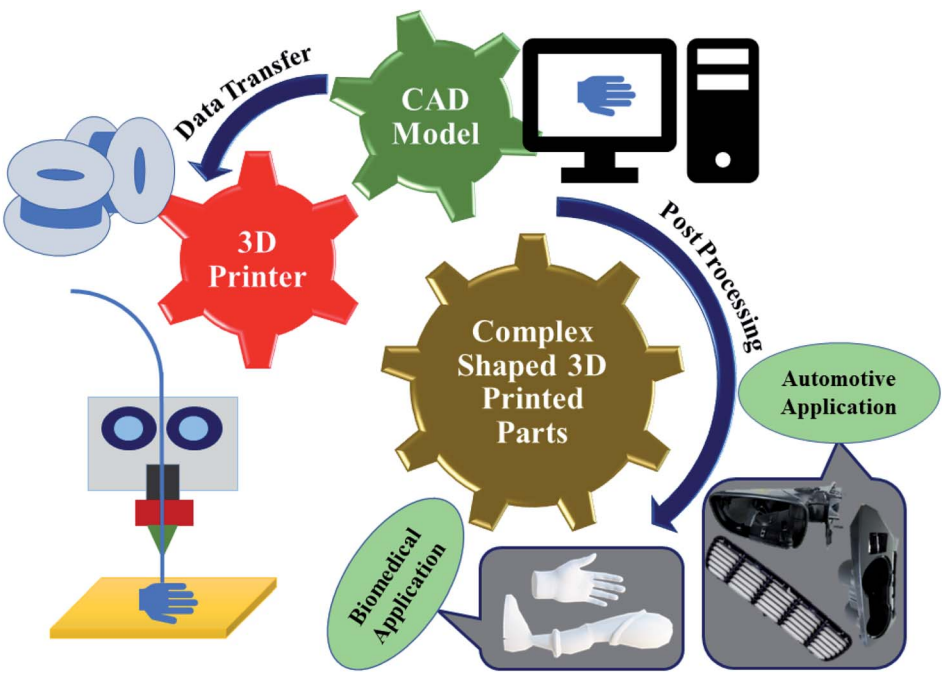

Fig. 1 Schematic representation of overall 3D printing process (drawn by authors).

Table 1 Various types of additive manufacturing techniques as per ASTM standard F2792-12a[36]

Technology	Process	Explanation
Fused filament fabrication (FFF)	Material extrusion	The material is extruded at a temperature more than its processing temperature and form products layer by layer
Electron beam direct manufacturing (EBDM)	Direct energy deposition	A metal wire is melted by using an electron beam and forms an object layer by layer
Selective laser sintering (SLS)	Powder bed fusion	A laser source is used to sinter the powder material and forms layer upon layer to build a product
Stereolithography (SLA)	Photo-polymerization	An ultraviolet (UV)-based laser beam is used to harden liquid photocurable resin and forms product layer by layer
Binder jetting 3D printing (BJP)	Binder jetting	A binding material is ejected by a movable inkjet and distributed over material's powder to form object in layers
3D plotting or polyjet printing (3DP)	Material jetting	A liquid photopolymer is jetted out very precisely which hardened in the presence of UV light and forms the object after stacking of the layers
Laminated object manufacturing (LOM)	Sheet lamination	The layers of adhesive-coated material are glued together, and a laser or knife is used to cut it in a shape

and/or biodegradable polymers namely poly(lactic acid) (PLA) and polycaprolactone (PCL) have been explored in 3D printing to develop biocompatible scaffolds for biomedical applications, *e.g.*, bone tissue scaffolds.[32,33]

In popular terms, additive manufacturing is not just one technique, it represents several technologies which have been recently developed. Other conventional techniques such as compression molding, injection molding, and thermoforming are called subtractive fabrication methodologies due to the final object being produced by subtracting the material.[34,35] Whereas additive manufacturing means the addition of new material to prepare the object. In 3D printing, there is a flexibility behind the addition of material in the form of layer by layer, which is highly efficient in terms of material usage.[31] Various types of 3D printing technologies exist based on the type of material usage and working principle. No matter the technology involved, all are additive. Additive manufacturing has been divided in several categories based on different variations. It is noteworthy to mention that the American Society for Testing and Materials (ASTM) have mentioned the division of the additive manufacturing technologies as shown in Table 1.

The first commercial instrument based on 3D printing was introduced in 1980, which has developed the technological and scientific impact of additive manufacturing on the society.[13] From the research point of view, the impact of this technique can also be justified from Fig. 2(a), which represents the number of publications per annum from 1990 to 2020 using the words such as "3D Printing", "Additive Manufacturing", and "Rapid Prototyping". It is concluded that the research work on 3D printing has been continued mainly from the last three decades. Now, the interest has been shifted towards biodegradable polymers from last 4–5 years.

Fig. 2(b) shows the percentage involvement or utilization of additive manufacturing in various industrial sectors. The market size of 3D printing was ~4.4 billion US dollars in 2013, which has been reached up to ~12 billion US dollars in 2018. Further, it is expected to drastically increase up to ~21 billion US dollars by 2021. This significant growth in 3D printing is mainly the result of increasing interest of researchers and industrialists in additive manufacturing related activities in multiple applications such as automotive, medical, aerospace, energy and customized consumer products. The worldwide market situation of 3D printing is growing exponentially as shown in Fig. 2(c).[37] The advances in 3D printing have not only made it a robust technique to use, but it can also be used to fabricate customized products from metals, ceramics, glasses and polymers.[13,38,39]

2. Injection molding *vs.* 3D printing technology

In this section, the widely used conventional injection molding technique is compared to the versatile 3D printing technique in terms of printing speed and cost effectiveness.[40] Such parameters are measured critically at industrial manufacturing scale, which are highly responsible to earn profits from the production. The injection molding process needs molds that are very costly and heavy. This means that the tooling and maintenance costs are higher for injection molding. Whereas 3D printing demands relatively lower fixed costs and operational cost as compared with injection molding for very small production runs. Such benefits help the industries/organizations to use 3D printing cost-effectively to complete custom-made orders and help niche markets. The amount of waste material in subtractive technologies in particular injection molding is higher because it utilizes multiple axis cutting machines to shape the plastics, metals and ceramics.[41,42] Whereas, being an additive manufacturing technique, 3D printing produces less/zero wastes *i.e.* no scrap, milling and sanding. For example, in metal applications, the generation of waste material has been reduced up to 40% in 3D printing as compared to that of subtractive technologies.[43] Some of the most important advantages in 3D printing are its printing quality, flexibility to produce customized designs, and recycling: all of which are not possible with an injection molding technique. Petrovic *et al.*[44] have mentioned that approximately 95–98% of wastes can be easily recycled using 3D printing and contributed significantly towards the development of sustainable plastics. Whereas the subtractive technologies create 96% wastes during the

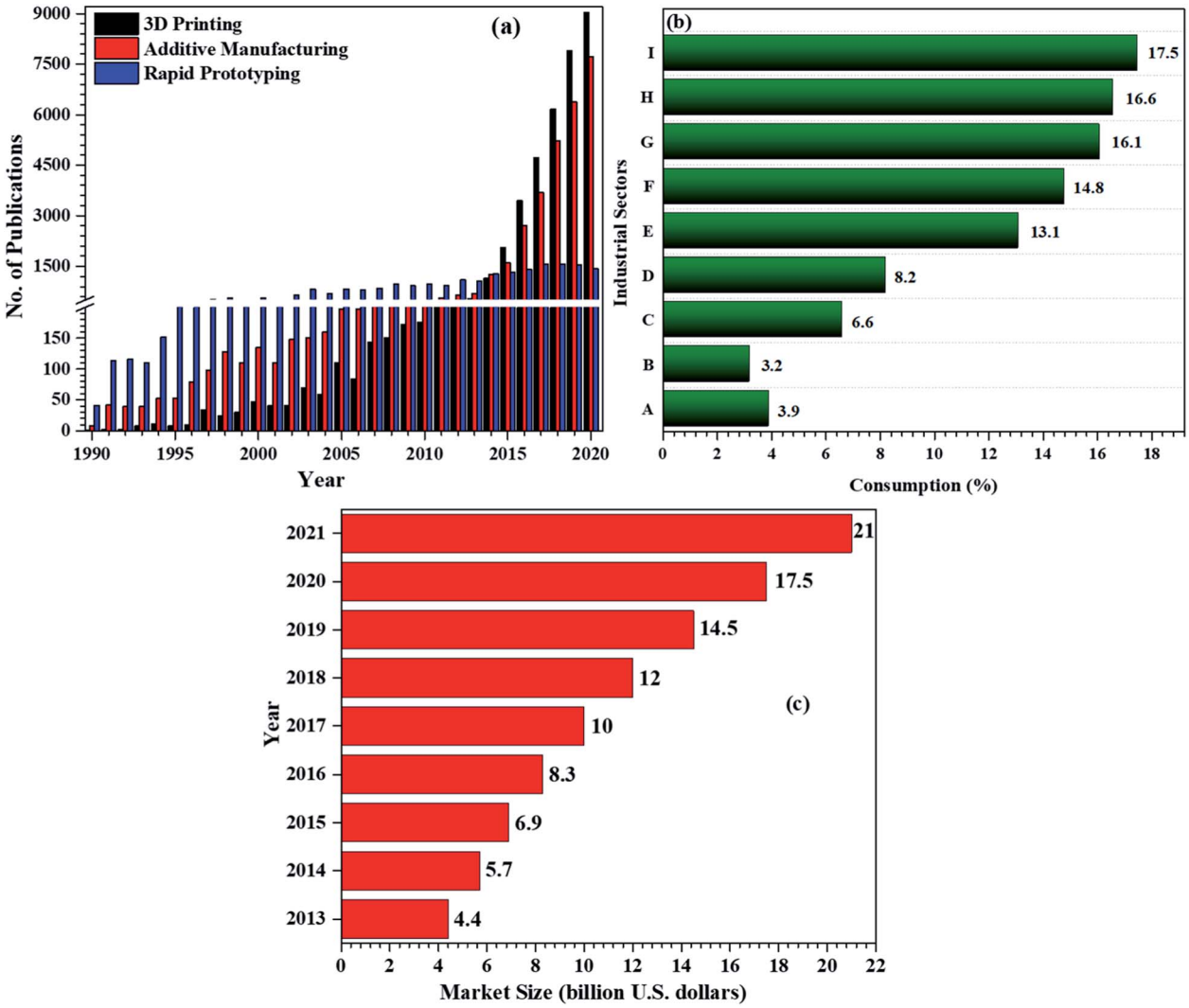

Fig. 2 (a) Number of publications per annum (data received from Web of Science, accessed on September 12, 2021); (b) utilization of 3D printing technique in various industrial sectors;[13] and (c) worldwide market size of 3D printing per annum[37] (data acquired from http://www.statista.com, accessed on September 17, 2021) (drawn by authors). Note: industrial sectors: (A) others, (B) architectural, (C) government/military, (D) academic, (E) medical/dental, (F) aerospace, (G) motor vehicles, (H) consumer products/electronics and (I) industrial machines.

production of parts. The variable costs per object do not change with the large production runs in 3D printing. This technique can prototype objects much faster as compared to that of conventional techniques including molding, milling and forging as no set-up time is needed to produce a product in 3D printing.[31] Further, the production of revised designs may take less time.[45]

3. Currently available additive manufacturing techniques

The selection of the most appropriate AM technique for a specific application can be difficult. An extensive variety of accessible 3D printing methods and materials often means that quite a lot of them can be feasible, however individual technique offers variations in dimensional precision, surface finish and post-processing conditions. Many institutions/companies have discovered new techniques and come up with their individual marketing terms for the new technique, though the fundamental technology might be the identical. As per ASTM standards, AM can be divided into the following seven categories based on creating individual layer. The aim of this section is to describe various types of currently available 3D printed techniques, their origin, working principle, advantages, limitations and summarize the differences among them.

3.1. Fused filament fabrication (FFF)

This technique was first described by S. S. Crump in 1991 and an US Patent 5121329 was granted in 1992 at Stratasys.[46,47] Among all existing AM technologies, FFF based 3D printing is a well-known inexpensive and scalable technology used to build customized products in layer by layer fashion after melting the thermoplastic filaments through extrusion and subsequently pushing the molten material out through the nozzle or

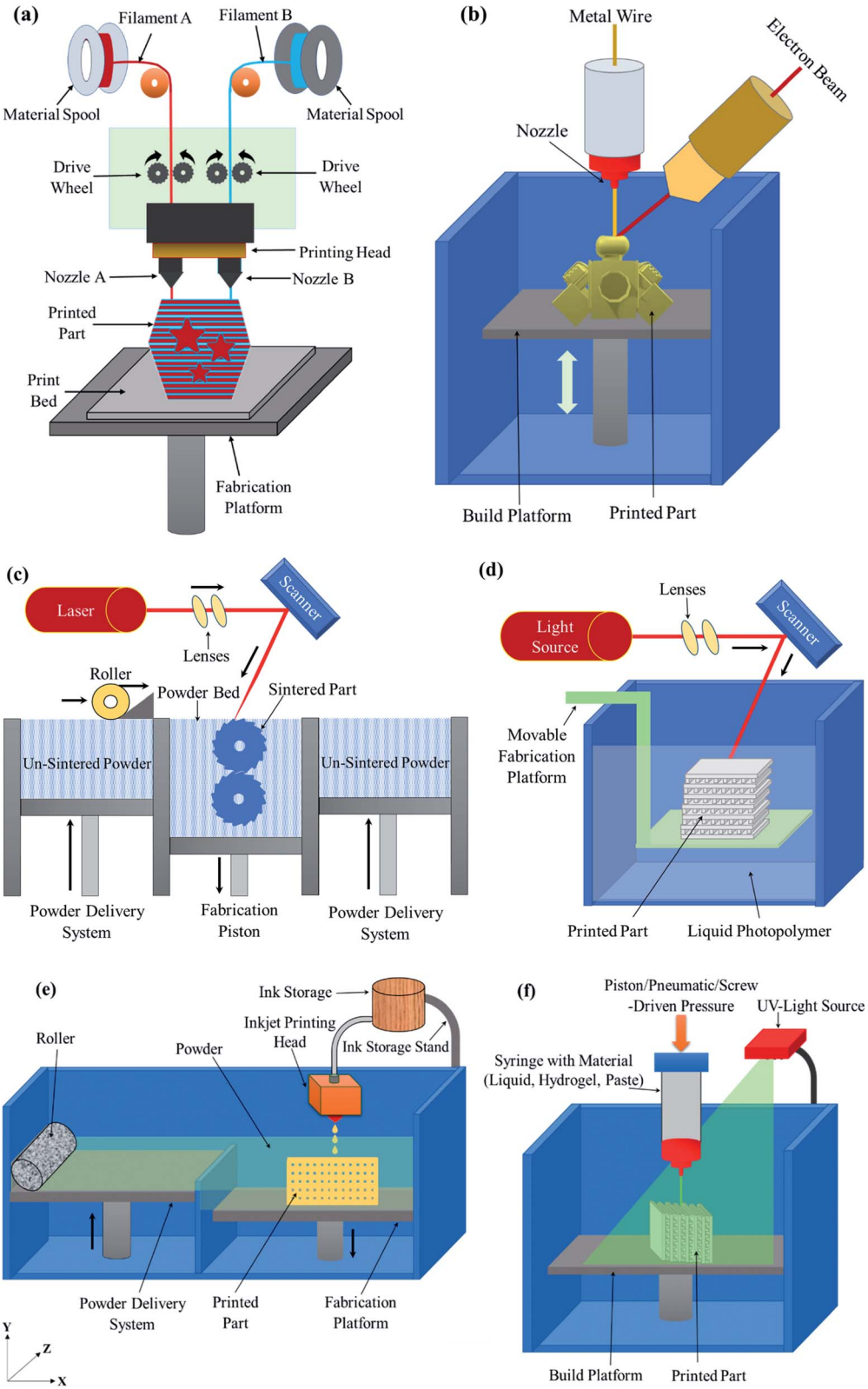

Fig. 3 Schematic representation of various AM techniques; (a) FFF-based 3D printing technique, (b) EBDM-based 3D printing technique, (c) SLS-based 3D printing technique, (d) top-down configuration of SLA-based 3D printing technique, (e) binder jetting 3D printing technique, and (f) 3D plotting technique (drawn by authors).

orifice.[48,49] It is also known as the "Free Form Fabrication" technique. 3D printers are designed on the basis of a Cartesian structure having three controlled axes and one/two hot extrusion head including a building platform.[50] In detail, FFF based 3D printers (as shown in Fig. 3a) can be divided into various components such as hot end (contains heating element and nozzle), cold end (motor mechanism to create the extrusion force), three axes (allow independent motion in x, y and z directions), print bed (flat surface to produce object), and motherboard (brain of 3D printer, controls all the parameters through a CAD software).[51] Multiple materials with different colors can then be printed simultaneously due to having multiple printing heads. The semi-molten material coming out of the nozzles solidifies immediately by cooling on the x–y axes of the build platform, followed by subsequent deposition of a fresh layer on top of previous layer by adjusting the print head or build platform automatically.[52,53] Further, the bonds formation between two deposited layers provide strength to the final product.[54,55] The resolution and performance of the produced products depend on various parameters such as processing temperature, raster angle, raster thickness, layer height, layer density, and printing velocity.[55,56] Advantages of 3D printing include low cost, customized product fabrication, easy removal of support structures, and surface coating possibility.[44] However, few limitations (as shown in Table 2) of FFF based 3D printing technology are vertical anisotropy, step structured surface, layer adhesion and nozzle clogging as compared to other traditional manufacturing methods.[2,7,55] The heterogeneity in the density and diameter of the filaments can also impart surface defects on the printed products. These limitations can be eliminated by applying various strategies such as increments in melting temperature, gamma irradiation of the final products, and thermally recyclable Diels–Alder reactions.[57,58] Thermal shrinkage is also one of the issues that deteriorates the interlayer adhesion and mechanical performance of the printed products[55] that can be controlled by the limited adjustment in the cooling rate of the temperature of the build platform.[59] The selection of inappropriate processing temperature and non-uniform diameter of filaments may also cause problems related to nozzle clogging of 3D printer, which can be minimized by softening the filament after increasing the printing temperature or by connecting additional printing tools at the top of the machine such as actuators or by using simplified configuration of FFF machines.[60,61] The analytical properties such as mechanical and thermal of 3D printed parts have often found lower as compared to that of injection molded parts.[62] It is due to the anisotropic effects caused by the directionality of 3D printed layers. Another most common limitation of FFF based technique is the need of filament fabrication from feedstock materials by melt extrusion before 3D printing.[63] Feedstock materials generally include conventional materials, polymers, polymer blends, and composites. The melt extrusion process is generally carried out for the new feedstocks to prepare the filaments. Sometimes, it is challenging to extrude filaments from feedstocks due to the challenging mechanical, thermal and rheological properties.[64] The extruded filaments must sustain uniform diameter and low melt viscosity to enhance the consistent flow.[14] However, it is noteworthy to mention that the viscosity and modulus of the molten filament is adequately high to self-support the developed structure and to avoid buckling.[65] Hence, the mechanically and rheologically balanced feedstock materials can only be used for 3D printing. Whereas, additives such as plasticizers and compatibilizers are usually mixed with the feedstock materials to balance the rheological properties, homogeneity, components adhesion, and mechanical friction between molten filament and extruder.[66] The cost-effective 3D printers are made commercially available by various manufacturers such as Lulzbot, Flashforge, Makerbot, Prusa, Ultimaker, and Stratasys – all of which are widely used for various industries and private users.[67] These printers can be used only for a limited variety of materials such as ABS, PLA, thermoplastic polyurethane (TPU) and polyamides (PAs) as compared to other conventional manufacturing techniques such as injection and thermoforming. The resolution of printing objects from such polymers is an inevitable parameter, which can be adjusted by optimizing the printing speed.[28] The modern 3D printers show a resolution up to 40 μm, which can be improved by faster printing rates.[61]

3.2. Electron beam direct manufacturing (EBDM)

Electron beam direct manufacturing, also known as electron beam melting (EBM) is one of the types of additive manufacturing that is used to fabricate metal parts.[68] In this technique, the metals or metal alloys are positioned under vacuum and fused together with the help of heat produced by electron beams.[49] Based on the type of raw materials used, it is divided in to two parts: (i) metal wire-based manufacturing and (ii) metal powder-based manufacturing. Metal wire-based manufacturing is based on the melting of welding wires by electron beam and its conversion into a desired metal part, collected on the build platform as shown in Fig. 3b. This technique is very similar to FFF based 3D printing technique, the differences are (i) in the utilization of metals in place of plastics and (ii) FFF heats the material through the nozzle-head, while the EBAM uses the electron beam coming from electron gun (another point of the machine). With this process, the metallic feedstock (metal wires) is melted with high energy electron beam sources. This highly efficient power source can focus precisely on drawing the product with high resolution.[69] This process can only run at high vacuum environment (10^{-4} torr or greater), which provides a contamination free work zone.[70] In such a way, no additional inert gases are required to avoid contamination and the purity of the printed metal parts will also be very high. The metal powder-based manufacturing technique is used to produce metal parts by using metal powder unlike metal wire.[71] An electron beam under high vacuum is used as a heat source to melt the metal powder and convert it into solid mass. The density of the fabricated metal (with this technique) is higher than that of fabricated parts from other technique *i.e.*, metal wire-based manufacturing. The 3D CAD model is used to design metal parts in the form of successive layers of powdered material. Further, these layers are melted together by the electron beam and builds the metal parts with

targeted microstructural and mechanical properties.[72] This technique can be used at high temperature (up to 1000 °C) to produce metal parts from highly reactive materials such as titanium and niobium.[73] It can only be possible under high vacuum so that the reactive materials can't form metal oxides in the presence of oxygen.

3.3. Selective laser sintering (SLS)

Selective laser sintering, an advanced additive manufacturing technique, uses a focused laser as a power source for sintering powdered materials including polyamide and polypropylene.[74] In this technique, the laser aims automatically at the special coordinates, defined by a 3D digital model. The high energy of laser transfers to powdered material in the form of heat, which melts the material and binds it to fabricate a solid structure. SLS technique was patented by Carl Deckard at the University of Texas in 1988.[42] Commercially available powdered materials including metals, and polymers such as polystyrene, polycarbonate, polyaryletherketones (PAEK) and polyamides are suitable for SLS 3D printing.

Recently, new applications for 3D printed materials emerged such as packaging, visual aids, or decorative parts for example. The high volume of material is required for most of these applications, as the volume of waste generated is more. Generally, used materials are fossil-based polymers in solid or porous/foamed state, which are neither recyclable nor biodegradable when their useful life concludes.[75,76] For that reason, the use of biomass waste (biomaterials or agricultural residues that are biodegradable under certain conditions) in SLS type (as shown in Fig. 3c) of 3D printing in powder form could further increase the environmental benefit and reduce the cost of the printed pieces.[23] To produce the plastic-biomass composites, one interesting option for SLS 3D printing is to perform a dry-blending step as all the materials can be obtained in a powder form.[77] It's also possible that the developed polymer composites *via* synthesis route followed by milling processes may produce the material in powder form. Moreover, dry blending of various solid components is a simple and low-cost technique, which doesn't require previous melting information. Dry blending avoids high capital, maintenance, and operational costs while at the same time limiting the mechanical, thermal and oxidative degradation of the matrix as well as reinforcement phase.[78] Dry-blending of polymer mixtures is used in most of the rotational molding industries and is also used to produce foams and composites.[79] So, this is a fascinating option for biomaterials which are highly sensitive to thermal degradation.[80]

3.4. Stereolithography (SLA)

Stereolithography was developed by Chuck Hull in 1986,[81] and is a fascinating 3D printing technique which works on selective crosslinking of various types of materials such as thermosetting polymers, elastomers, ceramic-based resins and bio-inks (bio-inks are prepared by combining numerous biocompatible materials with cells, which are subsequently 3D printed in definite shapes layer-by-layer to produce tissue-like, 3D structures) in the presence of ultraviolet (UV) light/visible light and forms layer-by-layer assembly.[82–84] SLA (as shown in Fig. 3d) is a laser induced forward transfer printing technique, which doesn't heat the donor polymer layer. It requires an intense laser light or digital light projector to initiate the photolytical crosslinking of bio-inks which enables crosslinking one layer in single printing plane.[85] SLA based 3D printing shows various advantages such as higher resolution, reduced printing time and higher cell viabilities as compared to other bioprinting techniques.[86] The SLA technique is based on photopolymerization, which is defined as a technique in which a UV light or laser is guided in a predefined design over a path of photopolymerizable polymer in liquid form followed by cross-linking it into a hardened layer.[87] As each individual layer is polymerized, the printing platform further moves up/down (based on top-down or bottom-up configuration) into a polymer ink solution, which allows for several cycles to construct a 3D structure. This process is used predominantly when the solutions of curable acrylics and epoxies are consumed as photopolymerizable material.[88] These photopolymerizable liquid polymers show a higher degree of fabrication along with high accuracy (as shown in Table 2) as compared with other techniques. Stereolithography is used in biomedical applications *e.g.* to make computerized tomography (CT)-based molds for producing artificial heart valves.[15] The main drawbacks of SLA are the necessity of UV radiation, visible light intensity, required longer post-processing time, and its compatibility with fewer materials.[15,89]

3.5. Binder jetting 3D printing (BJP)

This technique is based on the processing of the combination of powder and liquid that does not require any predesigned masks[90] as shown in Fig. 3e. It uses the programmable digital files to print the complex designs. In this technique, an organic/inorganic liquid binder (1 to 100 picoliters) with low viscosity (below 10 mPa S)[91] and surface tension (in the range of 28 to 350 mN m^{-1})[92] is used to facilitate the jetting process from the inkjet printhead.[93,94] First, a layer of powdery material is spread uniformly by a roller on the build platform and the liquid binder is dropped from the inkjet printhead (moves only in x–y direction) over the powder layer in a selective pattern to form a two dimensional layer of desired design.[14,95,96] After the completion of single layer, the build platform travels downward direction and a new layer of powder spreads over the formed single layer with the help of roller and the excess powder is removed into an overflow box. The same process is repeated to form the second layer. Finally, the unbounded powder is cleaned to achieve the final product. The structure of the printed product is adjusted by controlling the volume of deposited binder. The eminence of the printed product depends on various factors such as powder particle size, liquid binder viscosity, interfacial interaction between powder and binder, and the binder deposition speed.[97] This technique is assumed as an ideal technique to produce small

and medium products volumes. It is basically used in the design of soft scaffolds, human fibroblast, smooth muscle cells, cartilage, and microbatteries.[98–101] However, Inkjet 3D Printing (IJP) is completely different from binder jetting 3D printing as only liquid materials are used in IJP. Based on the binder generation mechanism, inkjet 3D printers are divided into two major groups: (i) continuous inkjet 3D printers and (ii) drop on demand inkjet 3D printers.[102] In continuous inkjet 3D printers, a continuous stream of binder droplets (~100 μm in diameter) are produced for fabricating object and unused liquid binder is reused. The size and spacing of the binder droplets are managed by applying pressure wave pattern.[28] Whereas in drop on demand inkjet 3D printers, the individual droplets (25 to 50 μm in diameter) of the binder are produced on demand when required and mostly used in tissue engineering applications. A voltage and pressure pulse are the two parameters which direct the binder droplet on demand, which helps to eliminate the need for the separation of waste liquid binder.[103] The printing quality depends on the positional accuracy of binder droplets. Hence, the three main factors that are responsible to prepare the suitable binder formulations are: (i) droplet generation, (ii) interaction between droplet and substrate and (iii) drop solidification.[104,105] The liquid binder properties differ depending on the variation in the powder substrates and the mechanism related to drop formation at inkjet print head. The phase transformation of binder droplet from liquid to solid defines the shape and size of the printed objects.[94] The unsupported objects such as bridges and overhangs can't be printed using inkjet 3D printing. The major advantages of binder jetting 3D printing techniques are processing at room temperature and flexibility in material selection. This technique can be used to print any polymer material in powder state and the support structures can be easily removed in this technique as compared to that of other techniques as mentioned in Table 2. On the other hand, the disadvantages of this technique are the binder contamination, nozzle clogging, printing resolution, bulging, and coffee-ring effect.[27,40] The optical transparency of the printed objects is not significantly good due to the incomplete interaction between liquid binder and powder material. Such incomplete interactions may create partially bounded powder particles in the printed object, which increase the porosity and surface roughness in the finished materials.[28]

3.6. 3D plotting or polyjet printing (3DP)

3D plotting or polyjet printing was patented by Objet in 1999[106] and was further acquired by Stratasys. This technique is a completely different additive manufacturing technique to binder 3D printing as shown in Fig. 3f. In this technique, ultraviolet (UV) sensitive photocurable resins are used in place of binding agents.[67] The photopolymer resin is jetted through print heads on the selective locations as predefined by the digital model and is cured instantaneously using UV light to form a continuous layer.[107] The build platform moves in a downward direction after hardening of the first layer. The same curing and printing process are repeated multiple times until the completion of the desired object.[108,109] Multiple materials can be printed individually and simultaneously by choosing various photocurable resins and by spraying them and cured, which is not possible in the case of BJP and IJP.[110–112] Such types of printing can create a complex shaped multi-material object with position specific properties. The multi-material object drawing from this technique has been widely used in medical applications to fabricate the anatomical models, which can be used in pre-surgical planning.[113,114] The resolution and dimensional stability of the fabricated objects are higher when compared to that of binder jetting 3D printing as mentioned in Table 2. The modular strength of the objects varies due to the utilization of multi-photopolymer resins.[115] The UV source is fixed just next to the print head or jetting nozzle. This position helps in curing the resin instantaneously. This additive manufacturing technique is relatively new as compared to other techniques. Various types of photopolymer resins such as ABS like, fullcure, verodent, and veroclear can be used in polyjet printing.[116] The removal of the support structure from the final object is difficult due to its waxy nature, which limits the complexity and dimension of the printed object.[46] Finally, the key advantages of 3D plotting technique are material flexibility and curing speed.[14]

3.7. Laminated object manufacturing (LOM)

First patented by Feygin and Pak[117] in 1999, LOM technique is one of the sheet lamination techniques that is completely different than all other additive manufacturing techniques. In this technique, some of the objects are fabricated by trimming the thin sheets of metal, plastic, or paper followed by binding all the sheets together using heat activated glue[118] and forms layer by layer assembly.[119,120] Further, a laser or knife is used to cut the layers in a desired shape. This technique is easy to use, fast and cost-effective.[67] The technique is used in multicolor prototyping. However, the resolution of the printed object from this technique is lower as compared to other additive manufacturing techniques such as FFF, SLS and SLA. During object preparation, the excess material offers good support for thin-walled sections.

3D printing technology has various advantages such as on-demand printing, customized complex shaped products, cost-effectiveness, and rapid prototyping.[121] The internal tensions in LOM parts are very low as compared to other rapid prototyping machines, which prevents the deformation and shrinkage of the printed objects. The parts with extra large dimensions can be manufactured by this technique as mentioned in Table 2, which sustain high durability, toughness, and fragility. LOM technique can be used for processing various structurally different organic (paper and plastics) and inorganic materials (metals, calcium carbonate and talc). It should be noted that non-toxic and non-reactive materials that are used for LOM printing can be easily handled and disposed of adequately.[122] The supporting structures are not required in this case, which makes it simple and easy to handle. There are negligible chances for deformation or phase change in material during printing. However, the lack of diversity in the available biomaterials limits this technique to be used in medical applications.

Table 2 Advantages and limitations of existing additive manufacturing techniques

3D printing technique	Advantages	Limitations	Sources
FFF (resolution range: 50–200 μm)	Simple, multi-material structures capability, overall low cost (for thermoplastic materials), high speed, high tensile strength	Anisotropic nature, materials clogging, uniform diameter, high cost (for glass and metal), limited materials (only thermoplastics), layer-by-layer finish	14, 31, 123 and 124
SLS (resolution range: 80–250 μm)	Fine resolution, high quality, good strength, easy removal of support powder, no need for support material	Slow printing, powdery surface, expensive, limited mechanical properties	14, 31, 123 and 124
IJP (resolution range: 5–200 μm)	Low cost, quick printing, easy removal of support powder, flexible to many materials	Maintaining workability, binder jet clogging, coarse resolution, binder contamination, layer-by-layer finish, lack of adhesion between layers, limited material ink compatibility	14, 31, 123, 125 and 126
SLA (resolution range: 10 μm)	Simple, high printing resolution, biocompatible resins available	High cost, single material, very limited materials, slow printing, cytotoxicity, postprocessing to remove support material	14, 31, 123, 124 and 127
3DP (resolution range: 80–250 μm)	Versatile, high printing resolution, soft material capability, compatible with a wide range of materials	Slow, low mechanical strength, requires post-processing, low resolution, high porosity	14, 31, 123, 124 and 126
LOM (resolution range: depends on laminates thickness)	Versatile, low cost, broad range of materials, reduced tooling and manufacturing time, excellent for larger structures manufacturing	Limited mechanical properties, design limitations, dimensional accuracy, inferior surface quality	31 and 124

4. 3D printing in various engineering applications

4.1. Automotive sector

The automotive sector is one of the many applications of AM to fabricate complex shaped components by various types of 3D printing such as FFF-based 3D printing, SLS-based 3D printing.[13,63] Few of aerospace and automotive components consist of complex geometries and are highly costly and time consuming when prepared using conventional techniques such as injection molding.[128] Thus, 3D printing is an extremely appropriate technique for the manufacturing of such components. Components such as motor blades and engine exhaust were mostly 3D printed using metals due to its higher strength and flame retardancy properties as compared with polymer materials.[129] However, the fuel consumption in automotive was higher due to the higher weight of the printed metal components as compared to that of polymer materials. Hence, several researchers have explored different ways to include 3D printed polymers and polymer composites in automotive and aerospace applications due to their lightweight, chemical resistance, and lower fuel consumption. In this direction, the components such as propeller and airfoil were 3D printed using photopolymer/glass fibers or carbon fibers composites by UV-assisted 3D printing technique and demonstrated.[130] Excellent repeatability and reproducibility of 3D printed polymer composites were observed and have shown potential to be used in automotive and aerospace components. This was due to excellent interlayer bonding between adjacent layers which provided the required mechanical properties and dimensional stability. The researchers have developed 3D printed polymer composites which showed a heat resistance of 250 °C with 50% lighter in weight as compared with aluminum. Polyphenylene sulfide (PPS) is one of the high-performance engineering thermoplastic polymers, offers high thermal stability, high mechanical strength, good chemical resistance, high fatigue resistance and good dimensional stability due to its semicrystalline nature, molecular chains arrangement, rigidity, embracing sulfur atoms and benzene ring in an alternate position in chemical structure.[131–135] PPS can also be used in 3D printing using FFF technique. The mechanical properties and impact behavior of 3D printed PPS specimens were analyzed by changing filament extrusion and alignment parameters.[131] The internal voids between PPS filaments can be removed and the mechanical strength was improved by declining load direction and filament alignment. Therefore, 3D printed polymer composites with lightweight and higher mechanical strength properties have shown potential to replace the traditional metal-based 3D printed components used in automotive and aerospace applications.

4.2. Electronics sector

The complex designed electronic prototypes can be produced with higher resolution and accuracy in reduced time by using advanced 3D printing technology.[136] When a mixture of an electrically conductive material and polymer matrix is used for 3D printing, the prepared polymer composite behaves like an electronic device, which can then be utilized in many ways.[137,138] Leigh *et al.*[139] developed various types of PCL/carbon black composite-based electronic sensors which covered a wide range

from piezoresistive to capacitive sensors with the help of FFF-based 3D printing. Different types of sensors are used for different purposes. Piezoresistive sensors are capable to monitor mechanical flexing on the basis of change in electrical resistance. However, capacitive sensors are used as a part in custom interface devices or can be printed on a vessel to detect the presence of liquid. Likewise, epoxy/carbon nanotubes (CNT) nanocomposites were 3D printed by using ultraviolet-assisted direct write technique to fabricate piezoresistive sensor with electromechanical sensitivity.[140] Such developed sensors have shown the potential of 3D printing technology in electronic applications. Traditional electrical circuits were printed by using 2D flat surface printing.[141] The electrostatic printing was used to print conductive circuits on flexible substrates with the help of conductive toner made of silver composite particles, which showed a conductivity of $\sim 10^{-4}$ Ω cm.[142] Though, more authenticated prototype designs with embedded electrical circuits may be needed in real-world applications.[136] Many efforts have been made by researchers to develop customized 3D electrical structures. Recently, a connector has been printed by a digital light processing printer with the help of cross-linked photopolymer and silver particles.[143] The dipping of oil-in-water emulsion into the silver nanoparticles solution followed by sintering was used to fabricate conductive percolation paths of porous structures. The critical properties such as porosity, pore dimension, surface area and conductivity can be adjusted by controlling the processing conditions. 3D electronic structures were also printed using PLA/CNT nanocomposites by depositing CNT homogeneous dispersion in PLA followed by its evaporating.[61] This formulation was further used to develop an electrical circuit and fabricated a prototype of commercial light emitting diode (LED), which was an example of the applicability of 3D printing in microelectronics. 3D electronic devices have also been made by metal wire encapsulation into polymer matrix during printing, which is very similar to 3D printing of continuous fibers reinforced composites. Such two-phase composites system was also used in the fabrication of pressure sensitive membranes.[144]

4.3. Biomedical sector

Since 1989, AM has developed exponentially in biomedical engineering applications due to its individualized customizability.[145] This powerful tool can be utilized at clinics to print patient specific medical products, which can increase the response to surgery and also increase the creativity of the products required by the surgeons.[54,146] The concept of 3D printing at clinics has evolved due to the tremendous progress of various types of 3D printing techniques and its freedom to produce any shape and size of customized products.[147] The four levels of printing at clinics are conferred, which cover from surgical implants to direct 3D printing during surgery. The rapid implementation of 3D printing at clinics greatly depends on the fabrication of customized prosthetics, implantable scaffolds, and tissue repair. It is supposed that the 3D printing of any product at clinic will be a cost-effective service in the coming decades.

4.3.1. 3D printed biomedicines. After the development of a 3D printed bladder with the help of real cells by Professor John Hunt in 1993, AM has achieved substantial progress in the biomedical industry.[147] Another research area such as biomedicines has also been developed enormously due to the rapid evolution of 3D printing. As for biology and medicine, the development of 3D printing has been divided into four stages.[148] In first stage, the development of 3D medical structures and devices were incorporated for *in vitro* use without biocompatibility requirements.[149] The second stage consists of the development of implants with good biocompatibility by using non-biodegradable polymers for permanently use *in vivo* such as the development of orthotics, arthroplasty, and auxiliary supporting.[150] The third stage consists of 3D printing of degradable implants as replacement by using polymers or other materials with good biocompatibility with the human body which can encourage tissue regeneration, *in vivo*.[151] The fourth stage consists of printing customized implants, tissues, or organs using extracellular matrix and cells as materials.[152] 3D printing has improved the surgical success rates due to the onsite printing at clinics. Moreover, facilities related to cadavers and surgical training are very expensive however 3D-printed prosthetics have provided a new economical approach to resolving this issue.[153] Therefore, it is noteworthy to mention that 3D printing has been proved as a possible solution for the global scarcity of donor organs.[147]

4.3.2. 3D printed prosthesis. The multistep processes involved in the fabrication of human organ models is expensive and time-consuming.[154] The successful utilization of 3D printing technology has made it possible to fabricate organ replicas in a cost-effective matter.[146] In some cases, the doctors can also make prosthetics for the patient instantly. Surgeries always carry a risk factor for unforeseen complications, which is why it is vital for doctors to have a complete knowledge about the patient's health condition and surgical implementation. However, computer-aided simulation-based 3D printing can also solve this problem.[119] The models for surgical aids prepared by 3D printing is often successful due to its customizable property, inexpensive cost, and broad accessibility. In this direction, a virtual model has been developed for bone reduction clamp using online available software, which can be used in finger fractures.[155] Similarly, an exoskeletal of cortex cast was designed by Jake Evill, which was used as a support for localized trauma zone. The prepared cortex cast is ultralight, recyclable, fully ventilated, and hygienic.[156] In recent years, the scientific development in the technologies related to the prosthetics fabrication has provided a sustainable solution to fulfil the growing medical demands. Currently, additive manufacturing has been exploited for all possible applications using a variety of materials such as thermoplastic filaments, powder or liquid, and hydrogels. From the available variety of materials, biodegradable polymers are often used in biomedical applications to fabricate prosthetics and rehabilitation devices.[157] Hence, this versatile 3D printing technique can be applicable to numerous applications in prosthesis manufacturing.[147]

4.3.3. 3D printed implants. The ability to produce artificial implants by 3D printing and their reliability have been tested to

gain insight about their performance. Such implants can be produced using 3D printers with the help of virtual files of abnormal tissues. Such implants act as a bridge to support and accelerate the healing process.[158] Various types of 3D printed implants from biomaterials have been manufactured. However, three types of implants including surgical fillers, implantable medical devices, and degradable bioactive implants are mostly used for tissue replacement in clinical applications. The upgradation of the defects in patients using 3D printed prostheses is a simple application of implants.[159] Incredible progress in the area of 3D implant-based research has been observed in last decades. The use of implantable medical devices as physical tools is the best example of it. On the other hand, non-degradable surgical fillers play an important role for reshaping faces in the area of plastic surgery. However, more attention has been paid to develop degradable bioactive implants with required physical and biological properties. In contrast, 3D printers have been considered as a new and innovative way to produce surgical implants. Before printing biomaterial-based implants, the selection of biocompatible material is necessary and depends on its biodegradable properties. After printing, sterilization of implants is necessary in order to make it free from any contaminations.[160] After implantation, the size of the implanted device should be measured continuously to evaluate its performance.[161]

4.3.4. Tissue engineering. Biomaterials with higher porosity have been explored broadly in various orthopedic applications. The scaffolds prepared from porous materials help to stimulate cellular responses and accelerate osteogenesis.[162] Various cellular responses such as adhesion, proliferation, penetration and nutrition diffusion are performed on the basis of porosity and composition structure of scaffolds.[163] Tremendous successful efforts have been taken by researchers to develop various innovative technologies for the production of distinct porous structures made of polymers, ceramics, glasses and metals with improved properties.[164] The biological,

Table 3 Mechanical properties of polymers and their composites prepared by various 3D printing techniques used in different applications

Materials used	Tensile strength (MPa)	Elongation at break (%)	Young's modulus (MPa)	Sources
PP	32.2	12	841	166 and 167
PP/PE	20	6.2	1150	168
PP/polyamide 6	25	—	—	169
High density polyethylene/cenospheres	10.7	5.1	1569	170
ABS	37.0	—	2000	171 and 172
ABS/short glass fibers	58.6	—	—	173
ABS/short carbon fibers	70	—	18 000	172
ABS/cellulose nanocrystals	33.1	—	—	174
ABS/montmorillonite	37.1	—	—	175
Polyamide 66/continuous carbon fibers	464.4	—	35 700	176
Polyamide 12	41.38	—	1006.28	171 and 177
Polyamide 12/ZrO_2/tricalcium phosphate	36.71	—	1382.34	177
Polyamide/ABS/poly(styrene-maleic anhydride)	51.8	0.5	310	178
PTT/EBA-GMA/SA-GMA	35.3	—	1773	179
Methacrylate polymer/functionalized graphene oxide (GO)	60	6	—	180
Acrylic photocurable component	35.1	1.8	2600	130
Acrylic photocurable component/glass fibers reinforced dual core polymer	41.7	1.6	3500	
Polycarbonate	68.0	100	2200	181
E-waste polycarbonate	22.2	—	673	182
Polyurethane	30.4	599.7	16.7	183
Polyurethane/cellulose nanofibers	31.4	618.2	19.1	
Polyurethane/organosolv lignin	24.50	269	11.59	184
Polyurethane/organosolv lignin/graphene nanoplatelets	27.35	273	12.68	
PLA	63.8	4.7	3105	56
PLA/wood flour	35.5	—	3642	185
PLA/modified pulp fibers	21.5	—	—	186
PLA/sugarcane bagasse fibers	57.1	—	—	187
PLA/lignin	41.3	1.88	2390	188
PLA/MWCNTs	78.4	94.4	134.4	189
PLA/graphene	64.0	6.21	12.35	190
PLA/polyurethane	—	717	45.56	191
PLA/polyurethane/graphene oxide	—	602	79.96	
PLA/carbon fibers	185.2	0.95	19 500	192
PLA/jute fibers	57.1	1.85	5110	
PLA/melamine polyphosphate/Cloisite 30B	70	2.32	3910	193
PLA/PA11/Joncryl	57	3	3400	194
PP/PLA/bamboo fibers	21.83	14.20	—	195

physiochemical and mechanical properties are the main focus to design and fabricate porous scaffolds. Artificial bone formation *in vivo* is also an emerging area of research in which pore size distribution, pore morphology, and pores interconnectivity are critical properties at macroscopic scale.[165] However, at microscopic scale, interaction among proteins and absorption-delivery of therapeutic agents are the factors which can decide the cellular pattern and microtextured surfaces.[38]

A tabular form of analyzed mechanical properties of 3D printed specimens from various petroleum-based polymers, and their composites is shown in Table 3, which can be used to analyze and compare with the mechanical properties of the polymer products obtained from other conventional processing techniques.

5. Traditional plastics in additive manufacturing

The consumption of virgin and recycled petroleum-based polymers such as acrylonitrile butadiene styrene (ABS), polypropylene (PP), polyethylene (PE), and polyethylene terephthalate (PET) in additive manufacturing opens the door of material's sustainability and reusability at industrial scales.[196,197] The use of additive manufacturing at industrial scale has significantly reduced the polymer wastes generation during and after processing along with production time and cost.[3,198] It also supports the concept of polymer recycling, which is the prime focus to reduce landfilling. However, the required properties such as mechanical and thermal of 3D printed products limits the number of polymer recycling.[199] On the other hand, the use of plastics such as PLA, poly(butylene succinate) (PBS) and poly(hydroxyalkanoates) (PHAs) as replacement of traditional petro-based plastics in additive manufacturing without affecting the required properties are crucially demanded.[200] The utilization of biodegradable polymers in various applications can reduce the carbon footprint as a result of a decrease in plastics waste generation and avoid landfilling due to their biodegradable nature.[201] This section describes in detail the utilization of traditional plastics-based composites in various applications through 3D printing.

5.1. Acrylonitrile butadiene styrene (ABS)

ABS is a common amorphous thermoplastic and has been prepared by the polymerization reaction between styrene and acrylonitrile in the presence of polybutadiene.[202] ABS is a tough light-weight polymer with high impact strength, rigidity, gloss, and electrical insulation properties. It is chemically resistant to concentrated phosphoric acid, hydrochloric acid, alcohols, alkalis, and vegetable oils.[203] However, ABS can swell after mixing it with glacial acetic acid (CH_3COOH), carbon tetrachloride (CCl_4) and aromatic hydrocarbons. ABS can easily dissolve in ethylene dichloride, esters, and ketones. It is one of the commonly used polymers in 3D printing due to its good printability. The printability of ABS has been analyzed with variations in printing conditions such as processing temperature, bed temperature, and printing speed. Morales *et al.*[204] have analyzed the outcome of interlayer cooling speed on the mechanical properties of ABS specimen printed by FFF-based 3D printer. It has been observed that the effective yield strength reduces with the reduction in interlayer cooling speed between two layers. The ultrasonic treatment of 3D printed specimens can also improve the mechanical properties of ABS.[205] As a result, 11.3 and 16.7% improvement were observed in tensile strength and Young's modulus respectively of ABS specimens after the ultrasonic treatment controlled by strengthening pressure and time. Similar research has been performed by Tofangchi *et al.*[206] to check the effect of ultrasonic vibrations during 3D printing of ABS. It has been concluded that the interlayer adhesion strength of ABS has been improved by 10% with the effect of ultrasonic vibrations, which imparts the increment in the relaxation of the polymer chains from secondary interactions at interface between two adjacent layers. In continuation, the effect of infill density and printing pattern on various properties such as mechanical and thermoelectrical of ABS have been analyzed after blending with conductive zinc oxide (ZnO).[207] The increment in infill density has improved tensile strength, Young's modulus, dynamic storage modulus, and electrical conductivity. However, elongation at break, loss modulus and damping factor have been reduced gradually with increase in the infill density from 50 to100%. ABS can also be blended with a variety of materials such as styrene ethylene butadiene styrene, ultrahigh molecular weight polyethylene,[208] montmorillonite clay,[209] layered silicates,[210] and other petroleum-based and biobased materials. In this article, the latest research on 3D printing using ABS has been focused. ABS is a versatile polymer and can be used in various applications such as automotive, electrical,[211,212] custom-fit prosthetics,[213] aero-space, energy and gas storage,[214,215] artifacts complex designs,[216] multi-purpose sensor designing,[217,218] and dielectric devices.[219] ABS was reinforced with polycarbonate (PC) in various proportions (10, 20 and 30 wt%) and the prepared ABS/PC composite filaments were used for FFF-based 3D printing.[220] The mechanical properties of 3D printed pure ABS, pure PC, and ABS/PC composites samples were measured and compared. The improved flexural modulus, tensile, and flexural strength were observed for ABS/PC based composites as compared with pure ABS and PC due to the modification in void formation and improved interfacial bonding as shown in Fig. 4(A) and (B). Chen *et al.*[221] have analyzed the scratch resistance and mechanical performance of 3D printed ABS specimens before and after the addition of poly(methyl methacrylate) (PMMA). The significant improvement in scratch resistance, hardness, melt flow rate, mechanical performance, and surface glossiness of ABS have been observed after the addition of 30% PMMA. The toughness of ABS/PMMA blends have also been improved by adding small quantities of methacrylate-butadiene-styrene (MBS), which acts as toughness modifier. Ren and Yin[222] have utilized carbon loaded ABS polymers to design a low cost absorber with dielectric resonator for microwave absorption with the help of FFF-based 3D printing, which showed the absorption capacity more than 90% over the whole frequency range from 3.9 to 12 GHz. Basic research was conducted on ABS blended with carbon nanotubes and short carbon fibers to

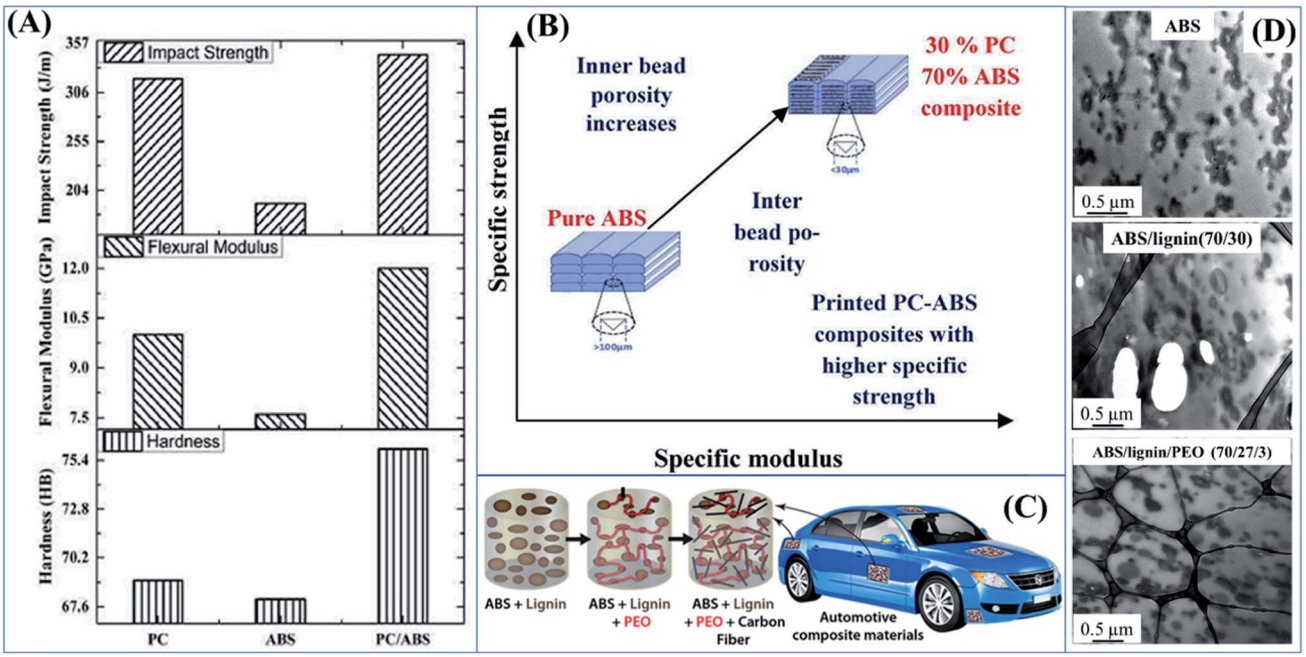

Fig. 4 (A) Comparison of mechanical properties of polycarbonate (PC), ABS and PC/ABS-based specimens and (B) schematic representation of the difference in strength and modulus for 3D printed pure ABS and its composites using FFF technique (adapted with permission.[220] Copyright 2019, Springer Nature, License Number: 5151470621307). (C) Schematic representation of ABS composites formulation using lignin, poly(-ethylene oxide) (PEO) and carbon fibers in automotive and (D) transmission electron microscopy images of neat ABS, ABS/30% lignin and ABS/27% lignin/3% PEO blends (adapted with permission).[225] Copyright 2015, American Chemical Society.

prepare composite specimens using 3D printing to analyze the interfacial strength between polymer matrix and reinforcement phase.[223] The in-plane tensile strength of ABS-based composites has been observed to be higher when compared to the virgin ABS specimen. However, the matrix fracture, fiber pull-out, and interfacial debonding between matrix and fibers have also been detected. The interlayer fracture toughness of ABS specimens was determined after reinforcing with chopped carbon-fibers and printed by FFF based 3D printing technology and observed that the fracture toughness of ABS has been reduced after adding the poorly wetted chopped carbon fibers.[224] The 3D printed ABS composites filled with carbon black have been manufactured by Dawoud *et al.*[217] for its use in strain sensor applications for health monitoring purposes. In this direction, Cardoso *et al.*[212] have fabricated low-cost multiuse electrochemical cells and sensors using ABS as well as conductive graphene-doped polylactic acid by 3D printing technology. The 3D printed cells have shown similar electroanalytical performance as compared with existed carbon-based electrodes. Additionally, a triboelectric touch sensor has also been manufactured using ABS and polyamide (PA) as rigid polymers as well as elastomer Tangoblack as a soft active triboelectric layer with the help of 3D printing technology.[218] Weng *et al.*[209] have used ABS polymer with montmorillonite clay modified by benzyldimethylhexadecylammonium chloride to fabricate nanocomposite filaments by a single screw extruder followed by FFF technique-based 3D printing and received the significantly improved mechanical properties, thermal stability and linear shrinkage ratio. In another research, FFF-based 3D printing of ABS with biomass-derived lignin (10, 20 and 30 wt%) was studied after compatibilizing with 10 wt% poly(ethylene oxide) (PEO)[225] as shown in the form of schematic representation in Fig. 4(C). It was concluded that the addition of lower lignin% in ABS tensile strength was again decreased after increasing lignin content. However, PEO inclusion in ABS/lignin composites reduced the activation energy of the blend due to improved plasticization of the hard phase. The dispersion and dimension (300–1000 nm) of lignin in ABS was also responsible for better mechanical properties. The dimension of lignin particles was further decreased in the range of 200–500 nm (as shown in Fig. 4(D)) after adding PEO as interfacial adhesion promoter. Furthermore, chopped carbon fibers (20 vol%) were added in the ABS/lignin/PEO composite system and exhibited superior mechanical strength (77–80 MPa) of 3D printed samples, which demonstrated its use in the fabrication of automotive parts. Significant research has been done with one of the most used polymers (ABS) in biomedical applications. In this direction, Arulmozhi *et al.*[213] fabricated a custom-fit finger splint with a blend of ABS with flex PLA by using FFF based 3D printing. This initiative has been taken to improve the biobased content in the petro-based polymers without affecting the performance of the 3D printed objects. A simple, comfortable, and inventive lightweight design for finger splint with appropriate properties was fabricated, which mainly supported patients to perform their daily activities. It varies patient to patient with finger deformity. Apart from the significant utilization of ABS in biomedical applications, it is also used for gas storage after blending with metal organic framework materials (MOFs) to

prepare ABS-metal composites.[215] MOFs are the crystalline materials mostly used in gas storage, catalysis, filtering, and sensing due to their large surface area, which can be easily processed after the addition of ABS using 3D printing. Similar work has been conducted by Kreider *et al.*[226] by utilizing ABS-MOF composites to develop hydrogen storage devices *via* 3D printing. The used MOF composition was of 10% or below in ABS to develop the composite. It is noteworthy to mention that the 3D printing has also been used in food applications to develop a high precision viscous chocolate printer. Electrostatic inkjet 3D printers have been fabricated in this line of research. The printing accuracy of the materials have been improved by modifying the nozzle structure of the printer by using ABS resin microfibers due to its non-toxic and insensitive nature towards electric field.

The recycling of conventional polymers is the key focus for the researchers and industrialists to develop a sustainable solution by reducing the accumulation of polymer wastes in the environment. 3D printing is one of the easiest and most used technology to produce the recycled complex shaped objects with the lowest production cost. Woern *et al.*[227] followed the same polymer recycling approach and utilized the most common waste plastics as well as printing polymers (*i.e.* PET, PP, PLA and ABS) in their research work and compared the mechanical properties of recycled polymers with virgin PLA printed by fused particle fabrication 3D printing at optimized properties. Lee *et al.*[228] have also used filaments for 3D printing made from recycled thermoplastic resins such as ABS and PLA, which helps to reduce the production cost and green house gas emissions. They have fabricated the value-added products by combining the recycled PLA or recycled ABS with carbon nanotubes or polydopamine to improve the strength as well as conductivity.

5.2. Polypropylene (PP) and polyethylene (PE)

Polypropylene is a tough thermoplastic polymer, which belongs to the polyolefin family and manufactured from its monomer unit by using chain-growth polymerization. It is a non-polar, semi-crystalline and high chemical resistant polymer with slightly better hardness and heat resistant properties as compared to that of PE.[229,230] It is consumed in various commodity applications such as packaging, labelling, automotive, medical, laboratory plasticware, and textiles.[231] Polypropylene is one of the commercially available petroleum-based plastics, consumed in the form of powder in selective laser sintering based 3D printing. Tan *et al.*[232] utilized PP powder to develop feed channel spacers (net like structures) used in spiral wound membrane modules for the treatment of wastewater in

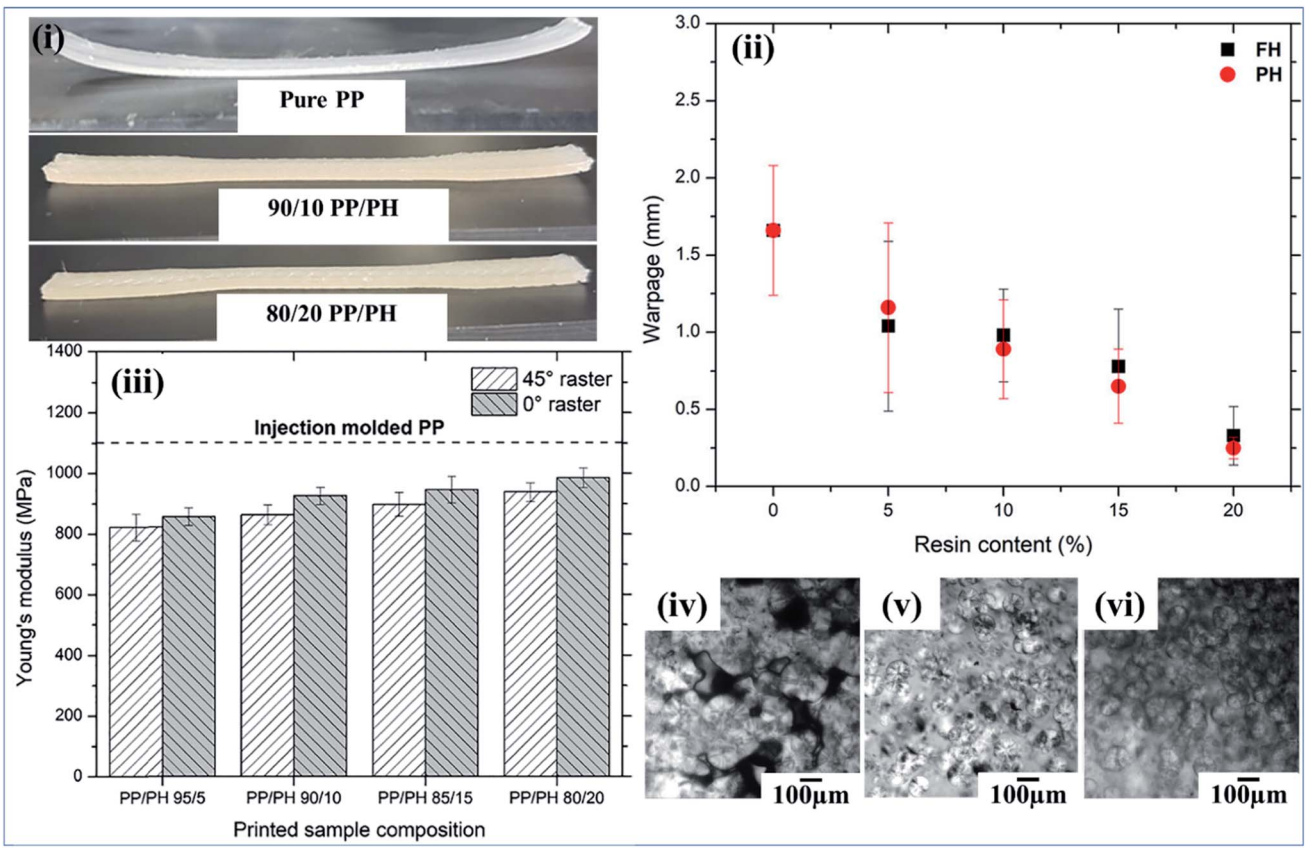

Fig. 5 FFF-based AM with PP and hydrocarbon resins blends, (i) 3D printed specimens from pure PP, PP/PH(90/10) and PP/PH(80/20) blends, (ii) warping observed in 3D printed parts of PP/FH and PP/PH blends with increase in resin content, (iii) effect of raster angle print orientation on Young's modulus of PP/PH blends and POM images for (iv) pure PP, (v) PP/PH(80/20) blend and (vi) PP/FH(80/20) blend taken at hot stage condition (adapted with permission).[233] Copyright 2020, American Chemical Society.

water industry. PP-based feed channel spacers are required to support and protect the thin membrane from damaging and puncturing due to its stiffness, flexible and chemical resistant properties. Various processing constraints such as laser intensity, scan pattern, layer thickness, bed temperature, and energy density related to SLS-based 3D printing were optimized for successful printing of PP-based specimens having feed channel spacers type of infill design. It was also concluded that Young's modulus of PP materials was directly correlated with the dimensional accuracy of the 3D printed objects. A positive relationship of edge energy density was observed with modulus and mechanical strength. Young's modulus and mechanical strength of 3D printed tensile bars having net type structure were increased linearly with an increase in edge energy density. In other research work, PP was utilized with hydrocarbon resins (fully hydrogenated (FH) and partially hydrogenated (PH)) to fabricate FFF-based 3D printed PP/FH and PP/PH specimens.[233] The specimens were 3D printed using various proportions (5, 10, 15 and 20 wt%) of FH and PH into PP matrix and clearly observed warping issues during 3D printing with pure PP as shown in Fig. 5(i). The effect on warpage was observed by changing FH and PH content and observed significant reduction in warping with increment in FH and PH loadings (as shown in Fig. 5(ii)) due to increased adhesion between build platform and first printed layer. The effect of raster angles (0 and 45°) on Young's modulus of 3D printed PP/PH blends was also observed and the results showed no significant change in Young's modulus by changing raster angle in this case as shown in Fig. 5(iii). The polarized optical microscopy (POM) analysis of pure PP (Fig. 5(iv)), PP/PH(80/20) (Fig. 5(v)) and PP/FH(80/20) (Fig. 5(vi)) blends was performed and showed an improved nucleation sites and a clear interference in the morphology of PP/PH and PP/FH blends due to the reduction in spherulites size. PP is also used as reactionwares fabricated using 3D printing for chemical synthesis due to its chemical resistant property. Kitson *et al.*[234] developed a detailed protocol for the development of reactionware device, which will be capable to produce a PP-based 3D printed sealed reactor that will be proficient to carry out a multistep organic synthesis. A schematic route of reactionware fabrication has been presented in Fig. 6(A), which represents the need of 3D printing technology in the fabrication of reactionwares to perform chemical experiments. The fabricated reactionware device with multiple options to place starting materials, reagents and purification columns has been showed in Fig. 6(B)–(D). PP was also used with other fillers to prepare 3D printed composites using a SLS-based 3D printing methodology. The research on the suitability of blends/composites with enhanced analytical properties in additive manufacturing is in demand. In this direction, PP was modified by adding fillers such as carbon fibers,[235] bamboo fibers,[195] cellulose,[236] and glass spheres[237] while the printability of PP-based composites has been checked. Short carbon fibers (CF) were used as reinforcement in the PP matrix to enhance the mechanical strength of the composite due to increment in anisotropic property.[235] The carbon fibers (10 volume%) oriented along with the flow direction of the filament in extrusion-based additive manufacturing technique, which resulted in a homogeneous dispersion of fibers as well as strong fiber-matrix adhesion in the presence of compatibilizer (PP-*grafted*-maleic anhydride). Such anisotropic behaviour of the fabricated composites enhanced the mechanical properties and thermal conductivity due to the preferential alignment of CF in printing direction. Parandoush *et al.*[238] fabricated various complex designed objects based on PP as a matrix with glass fibers as reinforcement. Fabricated objects have shown excellent interfacial bonding without the formation of voids. The mechanical properties of SLS-based 3D printed specimens were found superior as compared to that of FFF-based 3D printed PP/short fiber composites and found comparable properties to that of compression molded samples. Spoerk *et al.*[237] used different sizes of borosilicate glass spheres as a reinforcement phase in PP matrix to fabricate 3D printed objects using FFF-based AM technique and observed the effect of filler dimension and chamber temperature during printing on various properties

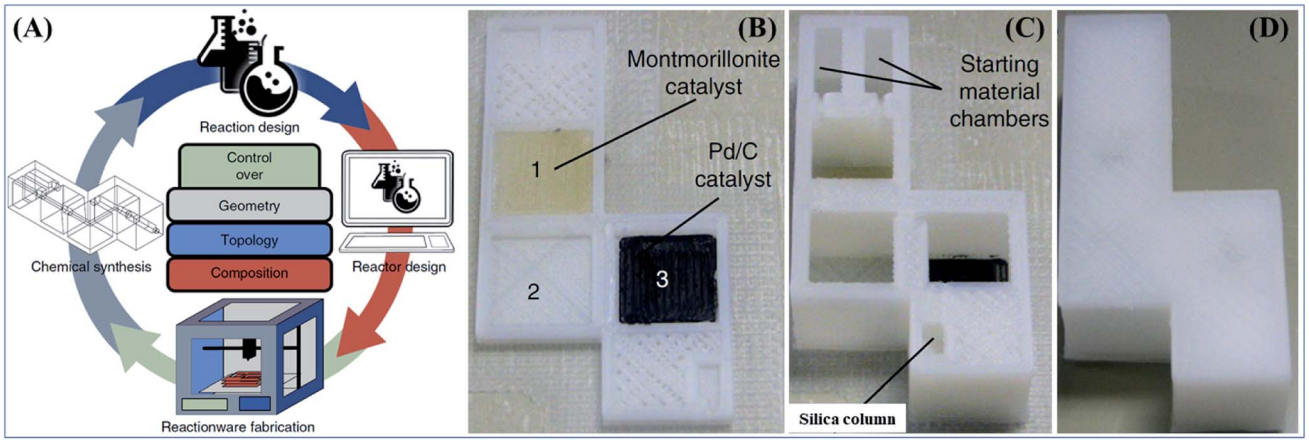

Fig. 6 (A) Illustration related to the involvement of 3D printing technology to fabricate reactionware, (B) first pause: base architecture of reactionware after 3D printing of catalyst beds, (C) second pause: printed device for introducing starting materials, reagents and purification column essential for reactionware testing and (D) completely 3D printed reactionware device ready for use (adapted with permission).[234] Copyright 2016, Springer Nature, License Number: 5151560599663.

such as mechanical, thermal, impact, crystallinity, morphology, and warpage. The glass spheres (<12 μm) were found to be the best among others as all the properties were better in this case. However, the increment in printing chamber temperatures (55 °C) promoted the annealing of 3D printed parts during printing with improved dimensional accuracy. PP was also modified by blending with other petroleum-based polymers such as polystyrene,[239] styrene-(ethylene-butylene)-styrene (SEBS) block copolymers,[240] polypropylene,[231] thermoplastic polyurethane (TPU)[241] and bioplastic particularly poly(lactic acid) (PLA)[242] to enhance the 3D printability and the related properties. In this direction, the FFF-based 3D printing was performed using a blend of PP, PLA, and treated bamboo fibers to impart the sustainability, mechanical, and thermal strength in the printed composite. However, the compatibility between PP matrix and bamboo fibers was improved with the addition of maleated polypropylene (MAPP), which works as compatibilizer to enhance the interfacial adhesion between polymer matrix and treated bamboo fibers. As a result, the tensile, flexural, and notched impact strengths of 3D printed PP/PLA/treated bamboo fiber were improved by 13, 11.7 and 23.5% respectively.

Expanded polypropylene (EPP), a versatile closed-cell bead foam containing CO_2 gas, is another form of PP, which was used to develop porous polymer structures by FFF-based 3D printing technique.[243] Similar to PP, EPP also has various desirable properties such as light weight, heat resistance, shock absorption, chemical resistance, and weather resistance, which are required for various commodity applications. The mentioned properties may vary with the expansion ratio of PP, printing speed, laminate thickness, and nozzle temperature. The increment in foaming ratio resulted with the increased number of pores and porosity without affecting the pore size.

Similar to PP, polyethylene (PE) also belongs to the polyolefin family and sustains comparable properties as that of PP. PE is a thermoplastic petroleum-based polymer and is primarily used in packaging applications in the form of plastic films, plastic bags, membranes and containers due to its high ductility, impact strength, excellent water barrier and chemical resistance properties.[244] Based on the chemical structure, density, and branching, PE is classified as low density polyethylene (LDPE), linear low-density polyethylene (LLDPE), high-density polyethylene (HDPE), high molecular weight polyethylene (HMWPE), and ultra high molecular weight polyethylene (UHMWPE).[245] Among various types of PE, UHMWPE is widely used in additive manufacturing as a feedstock to develop the various complex shaped objects such as antifriction products in mechanical engineering, and medicines.[244] The complex shaped objects are not only printed using FFF-based 3D printing but also with the other 3D printing techniques such as SLS-based 3D printing. HDPE powder with copper was used as a feedstock to develop next-generation miniaturised devices in electronic application such as flexible 3D circuits with conductive tracks.[246] SLS-based 3D printing with higher input power and lower scanning speed might responsible for the evaporation of HDPE, which generated the granular structure and therefore answerable with poor conductivity. Recycling of petroleum-based plastics is currently a prime concern to convert the waste plastics to value-added products by using various processing techniques. 3D printing is one of the most advanced processing techniques for recycling with low process cost and minimum wastes produced as compared to that of traditional manufacturing processes. The usability of recycled HDPE in the fabrication of various products is highly recognized as compared to that of ABS. The comparable thermal stability, water rejection, and chemical inertness make HDPE an alternative in place of ABS pellets or powder.[247]

5.3. Polyethylene terephthalate (PET)

PET is a colorless, semi-crystalline, thermoplastic petroleum-based polymer and belongs to the polyester family. PET is used in various applications such as fibers for clothing in textile, liquid and food containers in packaging, thermoformed products, engineering plastic in electronics and substrate in solar cell.[248] PET is manufactured using condensation polymerization (after esterification/transesterification) and is generally recycled after end use due to its non-biodegradable characteristic. PET is widely used in AM techniques as a feedstock to fabricate complex shaped objects due to its mechanical properties, better ductility, low friction resistance, high abrasion resistance, high dimensional stability and high tracking resistance.[249,250] The bulk tensile strength of PET lies in the range of 47 to 90 MPa, whereas it is lower in the case of 3D printing and lies in the range of 27 to 45 MPa.[227] On the other hand, the recycled PET shows the average tensile strength of ~40 MPa (also comparable with the commercial ABS), which suggests that the recycling of PET *via* FFF-based 3D printing doesn't affect the strength of the material.[251] The recycling of waste plastics in additive manufacturing may reduce the operational cost and increase the sustainability of the materials by converting it into value-added products. It was also detected that the % elongation of recycled PET was comparable to the injection molded counterparts. The properties such as barrier, optical clarity and flexibility of 3D printed parts are significantly affected with the variation in crystallinity. The problems such as warping and discontinuity in molten filament during 3D printing are mainly related to the material's crystallinity and non-uniform diameter of the filament, which can be further resolved by the addition of fillers, compatibilizers and impact modifiers.[252] On the same concept, Idrees *et al.*[253] has developed a novel, low-cost three-dimensional recycled polyethylene terephthalate (PET)/biocarbon composite with improved thermal and mechanical properties using 3D printing technology. The PET polymer and biochar were collected from used Aquafina water bottles and packaging wastes respectively. The recycled postconsumer PET bottles were used as matrix, which was filled with the biochar (~100 μm) as filler as shown in Fig. 7(A). The biochar was prepared from pyrolysis of packaging wastes at higher temperature (1100 °C) and autogenic pressure (150 bar).[253] The observed coefficient of linear thermal expansion (CLTE) value for pristine recycled PET was observed 53.2 ppm $°C^{-1}$ as shown in Fig. 7(B). However, CLTE values for recycled PET/biochar composites were observed in the range of 37 to 50.8 ppm $°C^{-1}$, which means that the incorporation of biochar

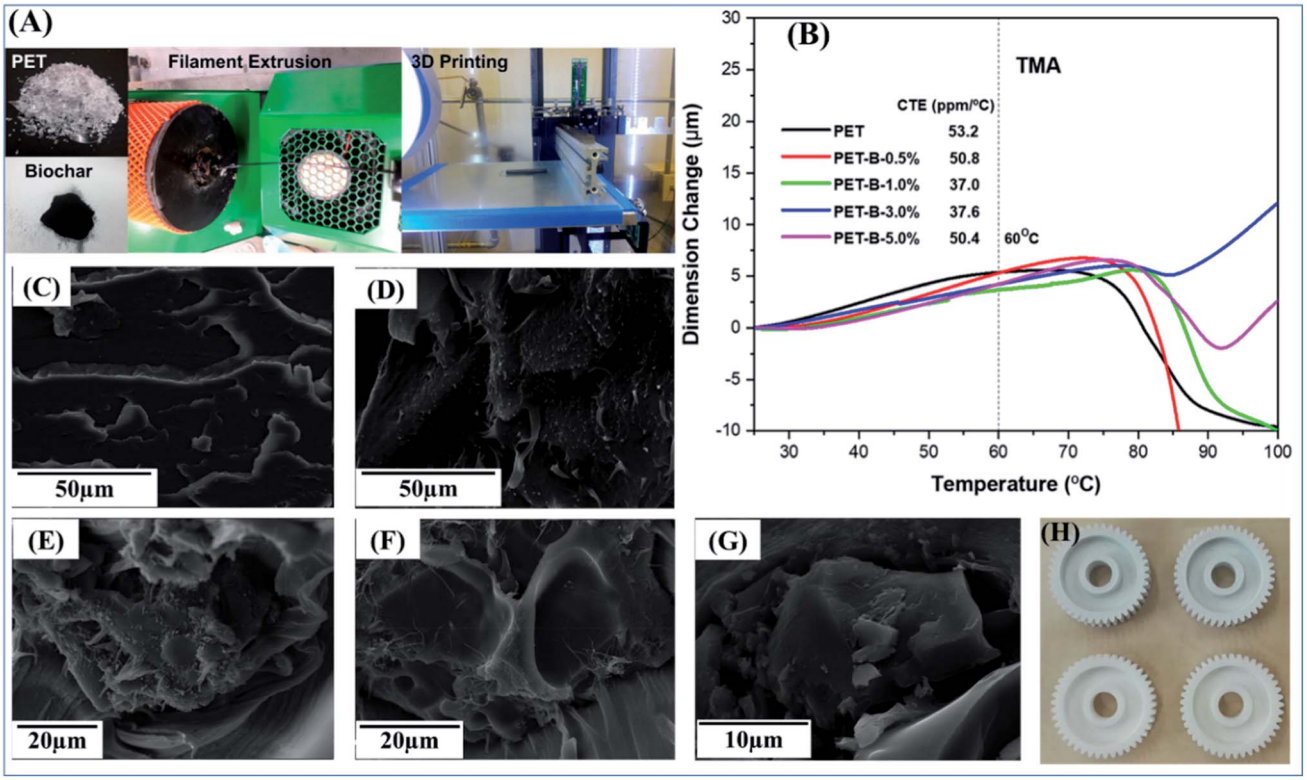

Fig. 7 (A) Illustration of recycled PET/biochar composite fabrication and its 3D printing, (B) the variation in CLTE values of 3D printed recycled PET by increasing biochar content; SEM micrographs of fractured surface of 3D printed (C) recycled PET, (D) recycled PET/biochar(0.5%), (E) recycled PET/biochar(1.0%), (F) recycled PET/biochar(3.0%), (G) recycled PET/biochar(5.0%) (adapted with permission.[253] Copyright 2018, American Chemical Society) and (H) SLS-based 3D printed spur gears using PET and PA12 powders: top two printed gears are from PET; bottom two printed gears are from PA12 (adapted with permission).[254] Copyright 2017, John Wiley and Sons, License Number: 5143581211176.

improved the dimensional stability. The lower CLTE values indicate the minimized thermal stress during 3D printing and restricts the deformation during cooling. Scanning electron microscopy (SEM) images showed relatively brittle fracture in virgin recycled PET as shown in Fig. 7(C). However, excellent interactions between PET and biochar were observed in composites as PET forms a fibrous structure and infiltrated through biochar pores as shown in Fig. 7(D)–(G). PET was also used in the powder form to fabricate complex shaped objects such as spur gears by using SLS-based 3D printing[254] as shown in Fig. 7(H). As per the literature survey, polyamide 12 (PA12) is the best polymer for SLS-based 3D printing. However, polypropylene was recently added due to its improved performance. It was observed that the highly crystalline PET showed good printability with SLS-based 3D printing without using the optimized particle shape and size. The printed parts with highly crystalline PET sustained good surface finish and gloss as compared to that of PA12. One important benefit of using PET powder was its well-maintained retention of properties such as molecular weight and crystallinity even after keeping it inside build chamber for prolonged period (~4 h).

5.4. Polycarbonate (PC)

Polycarbonates represent a group of thermoplastic polymers with the attached carbonate groups in their chemical structures.[255] PCs are produced by a reaction between bisphenol A and phosgene with tough, strong, temperature resistance, impact resistance, and optical transparent properties. PCs are used in various commodity and engineering applications such as electronics, construction materials, data storage devices, complex shaped parts for automotive, medical and phone body due to its easier thermoformed and moldable properties. Unlike most of the available thermoplastics, PC can undergo large plastic deformations without cracking. PCs are used to fabricate parts by 3D printing technique for above-mentioned applications. In this way, Shemelya *et al.*[256] fabricated 3D printable tungsten-doped polycarbonate composites specifically designed for X-ray radiation-shielding for space-based devices *e.g.* cube satellites. The X-ray radiation-shielding of 3D printed tungsten-doped polycarbonate composites were improved by ~10% only after the addition of ~0.3% tungsten. The storage modulus and complex viscosity of PC were improved by increasing the tungsten content without affecting tensile strength, elongation, impact, and glass transition temperature. As it was mentioned earlier, polycarbonate covers a wide range of applications and is also used in the medical field. Alaboodi *et al.*[257] fabricated biocompatible polycarbonate based scaffolds using color jet 3D printing technology for medical bone application. The scaffolds were printed with various percentage of porosity (0, 1, 5, 11, 19 and 30%) and the compression test was conducted in terms of

yield strength, elastic and plastic modulus. It was analyzed that the yield strength, elastic and plastic modulus were reduced with increment in porosity. Blaya *et al.*[258] designed a sustainable and recyclable orthopedic product (custom-made arm splint) with FFF-based 3D printing by using polycarbonate and PLA as feedstock materials. Polycarbonates were also used with other polymers to fabricate polymer blends with improved properties. Blanco *et al.*[259] examined the effect of polyetherimide (PEI) on the thermal properties of 3D printed polycarbonate samples to figure out the range of processing widow. The thermal and surface morphology results showed partial miscibility between PC and PEI. However, the addition of PC in the blend lowered the viscosity and hence, improved the processing window. Similarly, Peng *et al.*[260] used polycarbonate with Surlyn (an ionomer of partially zinc-neutralized polyethylene-*co*-methacrylic acid) in various ratios (25, 45 and 55%) to fabricate filaments using coextrusion process (as shown in Fig. 8(A)) followed by 3D printing of impact and tensile samples with four different orientations (*i.e.* 0, 15, 30 and 45°). It was observed that PC/Surlyn blends formed a simple core–shell morphology which triggered the synergistic effect between used polymers and improved the impact performance due to efficient energy dissipation. The stress *vs.* strain curve presented immediate failure after yield strength of pristine PC samples on uniaxial stretching as shown in Fig. 8(B). However, 3D printed Surlyn showed lowest tensile stress and modulus as compared to PC/

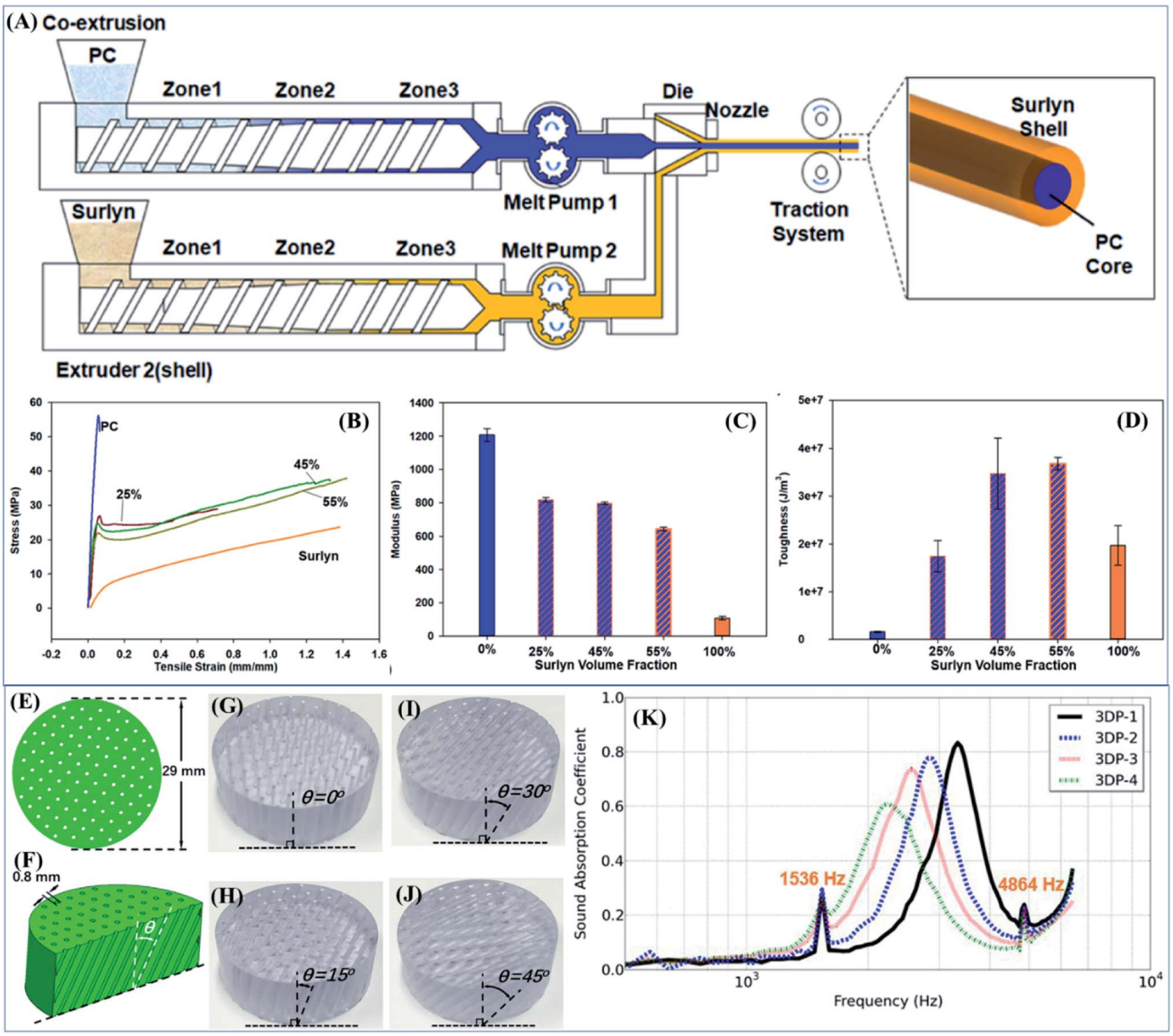

Fig. 8 (A) Schematic representation of coextrusion process to formulate core–shell structured PC/Surlyn filaments for 3D printing, (B) stress *vs.* tensile strain curves for 3D printed PC/Surlyn, (C) variation in Young's modulus of PC as a function of Surlyn volume fraction, (D) variation in toughness of PC as a function of Surlyn volume fraction (adapted with permission.[260] Copyright 2018, American Chemical Society); (E & F) CAD designs of porous PC samples, (G) 3D printed PC with $\theta = 0°$, (H) 3D printed PC with $\theta = 15°$, (I) 3D printed PC with $\theta = 30°$, (J) 3D printed PC with $\theta = 45°$ perforation angles, (K) sound absorption coefficient *vs.* frequency curves for 3D printed porous PC materials (adapted with permission).[261] Copyright 2016, Elsevier, License Number: 5143590471284.

Surlyn blends. The modulus for 3D printed Surlyn was lowest due to the exceptionable deformation of printed specimen at relatively lower applied loads as compared to pure PC and PC/Surlyn blends as shown in Fig. 8(C). However, ~25% reduction in the modulus of 3D printed PC was observed after the addition of 25 and 45% Surlyn, which was also responsible for incredible improvement in impact properties with core–shell structured filaments. The highest toughness was observed for 3D printed PC/Surlyn (55%) blend due to its core–shell structure and improved synergy between PC and Surlyn as compared with pure PC and other blends as shown in Fig. 8(D). Liu *et al.*[261] created CAD designs (as shown in Fig. 8(E) and (F)) and utilized porous polycarbonate material for fabricating an entirely different device using 3D printing at different perforation angles (0, 15, 30 and 45°), which had sound absorbing capacity. The printed samples with different perforation angles have been shown in Fig. 8(G)–(J). It was observed that the sound absorption capacity can be attained significantly in the lower frequencies by adjusting perforation angle, porosity and airgap during printing. Fig. 8(K) showed the highest sound absorption coefficient for 3D printed PC at $\theta = 0°$ at 3328 Hz due to the increment in the acoustical mass of the holes. The results clearly suggested that the increment in perforation angle and constant porosity resulted in the reduction in sound absorption capacity. Rohde *et al.*[262] utilized polycarbonate and ABS for 3D printing of mechanical specimens at different raster and build orientations (flat, on-edge, and up-right) in order to check and optimize the shear properties. It was observed that the ABS based specimens showed strong anisotropy as compared to that of PC based on build orientation. However, PC based specimens revealed strong anisotropy as compared to that of ABS based on raster orientation. Recycled polycarbonates were also utilized in 3D printing in order to check the effect of recyclability on the mechanical and thermal properties and its utilization in various applications. In this direction, Reich *et al.*[199] used recycled PC in particle/granular form for 3D printing and optimized various parameters namely nozzle temperature and velocity of molten polymer. The results suggested that the tensile strength (64.9 MPa) of 3D printed parts from recycled PC particles was comparable to that of commercially printed parts. It was also concluded that recycled PC particles-based 3D printed parts can sustain high mechanical strength and high heat resistant at low costs.

5.5. Thermoplastic elastomers (TPE)

Thermoplastic elastomers belong to a class of copolymers in which one is usually plastic and other one is rubber. It means that TPE has both thermoplastic and elastomeric properties.[263] Whereas, most of the elastomers come under the category of thermosets. The advantage of thermoplastic elastomers is their stretch ability up to moderate elongations and shape memory, which provide longer service life and better physical properties.[264] The difference between thermoplastic and thermoset elastomers is only based on crosslinking bond type in their chemical structures. The type of crosslinking is a critical factor that affects the elastic properties of the materials. Various types of commercial TPEs are available in the market such as styrene block copolymers (SBC), thermoplastic polyolefinelastomers (TPPOE), thermoplastic vulcanizates (TPV), thermoplastic polyurethanes (TPPU), thermoplastic copolyesters (TPCP), and thermoplastic polyamides (TPPA) to be used in various applications based on their properties. TPEs can be recycled also as they can be extruded and molded like plastics. In this direction, Gao *et al.*[263] prepared thermoplastic vulcanizate (TPV) by using PLA with poly(1,4-butanediol/2,3-butanediol/succinate/itaconic acid) (PBBSI) and analyzed the elongation properties by varying the amount of bio-based 2,3-butanediol. It was concluded that elastomeric properties were improved by the increasing the amount of 2,3-butanediol in PBBSI copolyester due to the decrement in the crystallization behaviour. The prepared TPV with good rheological and elasticity properties can be used as feedstock material in 3D printing. TPEs can be used in various applications such as electronics, robotics, and prosthetics due to its high flexibility. Christ *et al.*[64] fabricated flexible and conductive sensors by utilizing TPPU as a matrix with multiwalled carbon nanotubes as fillers using FFF-based 3D printing. The incorporation of multiwalled carbon nanotubes enhanced the stiffness of the composites and improved the 3D printing capability due to the excellent interlayer adhesion. It was concluded that TPPU based composites have potential to be used as an excellent piezoresistive feedstock in wearable electronics. Farstad *et al.*[265] fabricated prototype of wheels (as shown in Fig. 9(A(i–x))) with various grades of TPEs (*i.e.* NinjaFlex having shore hardness of 85A, TPE90A having shore hardness of 90A and SemiFlex having shore hardness of 98A) using 3D printing to check the surface friction and concluded that TPE based composites can be a good option for such applications where high friction is required for functionality. It was also mentioned that 3D printed components with TPEs can bend without break or permanent deformation. The friction properties of softer materials were found better as compared to that of standard rigid polymers such as ABS and PLA. The softest material *i.e.* NinjaFlex in this study was observed best quality for 3D printing and showed highest friction coefficient for all type of printed wheels. Wang *et al.*[266] used FFF-based 3D printing techniques to fabricate peristaltic microfluidic systems (horizontal and vertical diaphragm shown in Fig. 9(B)) with the help of TPEs as the traditional micromolding process involves intermediate steps such as molding and bonding, which takes excess time and energy. It was observed that the 3D printed microfluidic system (as shown in Fig. 9(C)) from TPEs can successfully detect low level of insulin concentration as the results were comparable with the conventional polydimethylsiloxane (PDMS) based systems. Another observed advantage over PDMS that the surface of 3D printed TPEs was hydrophilic, which supports the compatibility with biological materials. Ellson *et al.*[267] developed tough thiourethane thermoplastics as feedstock material for FFF-based 3D printing which can be used in applications where large thermal operating ranges and self-healing properties are required to promote the interlayer adhesion. The tough thiourethane thermoplastic was synthesized by thiol-isocyanate polymerization. The synthesized material was highly tough and sustained low melting point with well-suited thermal properties for 3D

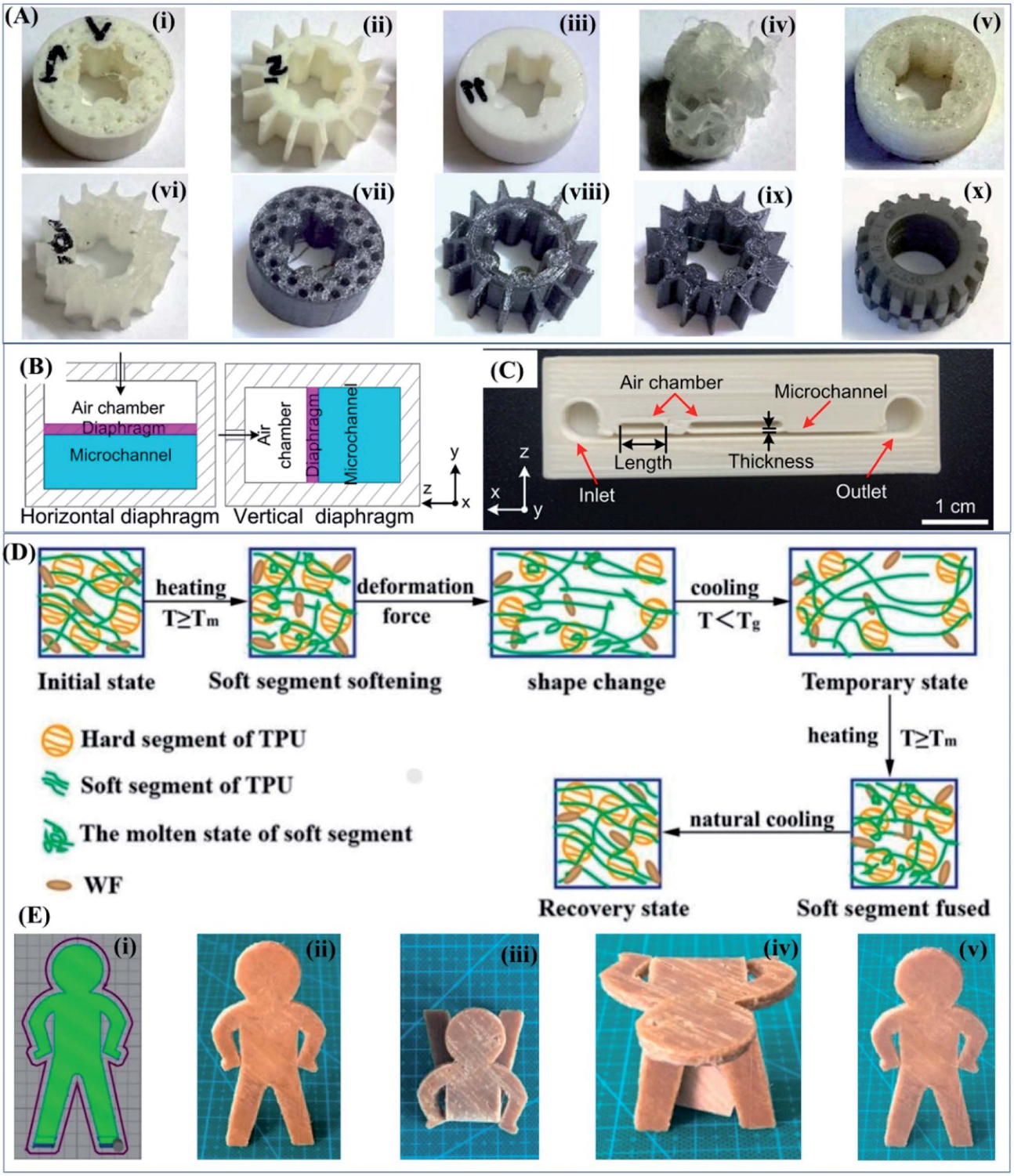

Fig. 9 (A) FFF-based 3D printed wheels prototype and termed as (i) NinjaFlex holes, (ii) NinjaFlex thin fins, (iii) NinjaFlex original, (iv) TPE90A thin fins, (v) TPE90A original, (vi) TPE90A spikes, (vii) SemiFlex holes, (viii) SemiFlex thin fins, (ix) SemiFlex spikes and (x) Lego wheel as reference (adapted with permission).[265] Copyright 2017, Elsevier, License Number: 5143590853429; (B) illustration of configurations for horizontal and vertical diaphragm, (C) demonstration of 3D-printed micropump (adapted with permission.[266] Copyright 2017, Springer Nature, License Number: 5151570227181); (D) schematic representation of heat-induced (60 °C) shape memory effect mechanism of TPU/WF composites and (E) a demonstration of shape memory effect using 3D printed man model: (i) digital design of a man model using software, (ii) 3D printed man model, (iii) started recovery state of 3D printed model at 2 min, (iv) at 20 min and (v) at 50 min (adapted from MDPI.[268] open access 2021).

printing technique. The yield strength of polythiouretahne was unaffected with the stress applied during printing. However, the commercial material lost 45% yield strength under stressed conditions. The biomass was also used with TPEs to improve the sustainability of the material and support the circular economy approach. Bi *et al.*[268] utilized TPU with wood flour (WF) and various loading of ethylene propylene diene monomer-*grafted*-maleic anhydride (EPDM-*g*-MAH) as compatibilizer for fabricating composites with improved mechanical, thermal, and shape memory properties with the help of hot-melt extrusion followed by 3D printing. The addition of 4% EPDM-*g*-MAH in TPU/WF composite formulation enhanced the tensile elongation and thermal stability as compared to that of unmodified composites. Fig. 9(D) showed schematic representation a mechanism for heat-induced (60 °C) shape memory effect of TPU/WF composites. The mechanism explains about deformation and recovery phenomena of the used material. In detail, the polymer chains of the soft segment of TPU were extended and oriented under external forces at higher temperature, which deforms the material to any shapes. However, the temporary shape was maintained, and the molecules stay in a glassy state, when the deformed material was cooled lower than the glass transition temperature of the soft segment. Further, the temporary shape of the material was retained after eliminating the external forces. After increasing the temperature more than glass transition temperature again, the soft segment started to melt partially, and the printed material recovered gradually due to conformation hysteresis. When the temperature was increased more than melting temperature, the soft segment started melting and as a result, the deformed 3D printed material could start regaining its original shape automatically. This shape memory phenomenon was practically examined on a man model as shown in Fig. 9(E(i–v)).

5.6. Polyamide (PA)

Polyamide is a macromolecule in which the repeating units are connected by the amide bonds. Polyamides are synthesized using step growth polymerization and are commonly used in various applications such as automotive, textiles, kitchen utensils, carpets, and sportswear due to its strength and durability. Few examples of polyamides are nylons (PA6 and PA66) and aramids, which are mostly used in additive manufacturing. Polyamides and their performances were investigated extensively with various fillers such as bioceramics (zirconia, hydroxyapatite, tricalcium phosphate),[177,269] graphene,[270] graphene oxide,[271] copper,[272] carbon black,[22] carbon, and glass fibers[273] and also with the various types of 3D printing technologies. FFF-based 3D printing was utilized to fabricate the specimens from PA12 after adding bioceramic fillers such as zirconia and hydroxyapatite to analyze the effect on the mechanical and thermal properties for the composite's end-use in biomedical application.[269] It was evident that the mechanical properties of 3D printed PA12 based composites was lower as compared with injection molded ones. However, in the case of 3D printed PA12 samples, the melting temperature, toughness, and flexibility were reduced after the addition of bioceramic fillers. On the other hand, thermal stability was improved without/slightly affecting the tensile strength. Hence, it was inferred that 3D printed PA12 based composites can be used in medical implants for non-load bearing applications. In a similar fashion, Abdullah *et al.*[177] also prepared hybrid ceramics (zirconia and β-tricalcium phosphate) filled PA12 based complex parts *via* FFF-based 3D printing for craniofacial bone reconstruction and observed mechanical and cytotoxicity properties. The effect of fillers in various loadings (zirconia: 15% and β-tricalcium phosphate: 30, 35 and 40%) were analyzed and human periodontal ligament fibroblast cells (HPdLF) were consumed to estimate the cytotoxicity of the printed materials using (3-(4,5-dimethylthiazol-2-yl)-2,5-diphenyltetrazoliumbromid) (MTT) assay. The results suggested that the impact strength and tensile modulus were improved by 98–181% and 8–31% respectively, as compared to that of unfilled PA12. However, the slight reduction in tensile strength of PA12 was observed after the addition of hybrid ceramics. The cell viability of the prepared composites was also improved significantly. The incorporation of graphene nanoplatelets in 3D printed PA12 by FFF-based technology can improve the thermal conductivity (51.4%) and elastic modulus (7%) as compared to that of compression molded parts.[270] Such improvements were observed due to the alignment of graphene nanoplatelets in the printing direction without compromising the ultimate tensile strength. The rate of consumption of polyamides is higher in the case of SLS-based 3D printing as compared to FFF-based 3D printing. Brugo *et al.*[274] manufactured polyamide based complex parts using SLS-based 3D printing to observe fracture mechanics and concluded that all the printed layers of specimens with a portion of crack showed better mechanical properties. In other study, the PA12 with different chemical structure than PA6 was utilized to prepare specimens using SLS-based 3D printing.[275] The problem like warping of PA12 based specimen during printing were focused, which was explained with the help of isothermal and non-isothermal crystallization kinetics. It was observed that nonuniform crystallization occurs when the molten PA12 comes out from the nozzle and warping occurs for the printed parts. This happens because the volume of the semicrystalline polymers shrinks when cooled down from the melt. Apart from this problem, the mechanical behaviour of SLS-based 3D printed PA12 specimens were analyzed and the visco-elasto-plastic response was observed on the basis of compression, shear, tensile and relaxation testing by using various instruments.[276] It was concluded that the SLS-based 3D printed PA12 specimens can be reproducible under controlled printing parameters except elongation at break and relaxation behaviour. Compression test conformed that the PA12 can be a bi-modular material.

The innovation related to 3D printing is moving towards the development of multifunctional and light weight materials. In the direction, the SLS-based 3D printing technology was used to develop a metal-free electric motor made from the composite of polyamide coated with graphene oxide nanosheets.[271] The compression and tensile modulus were reduced slightly as compared to that of pristine PA. In other research, the commercial PA6/carbon fibers, PA6/glass fibers and PA6/Kevlar

fibers were used to fabricate specimens in atmospheric as well as low pressure conditions.[277] The microscopic images of cross section of PA6/carbon fibers, PA6/glass fibers and PA6/Kevlar fibers filaments are shown in Fig. 10(A)–(C) along with the instrumental image of vacuum chamber as shown in Fig. 10(D) to produce low pressure during printing. The results concluded that 3D printing of specimens as shown in Fig. 10(E) at low pressure helped to reduce the porosity of PA6/Kevlar fibers, PA6/glass fibers and PA6/carbon fibers-based composites up to 1.7, 1 and 5.7% respectively and also increased interlayer shear strength up to 12, 22 and 33% respectively. Carbon black is one of the most common fillers used for improving the thermal and electrical conductivity of polymer composites. Espera Jr *et al.*[22] manufactured mechanically robust complex parts from PA12/carbon black powder composites using SLS-based 3D printing. The amount of carbon black directly affected the bulk resistivity of the composites. The addition of 1.5 and 3% carbon black in PA12 improved the blockage of crack growth on applied load. More than 3% carbon black was responsible for the reduction in mechanical properties due to hampering the physical contact between PA12 and carbon black. On the other hand, the thermal stability was improved as compared to that of PA12.

5.7. Poly(lactic acid) (PLA)

Poly lactic acid belongs to the thermoplastic aliphatic polyester family and can be synthesized from lactides and lactic acid monomer (2-hydroxypropanoic acid) using various polymerization routes such as condensation polymerization and ring opening polymerization.[278] Lactic acid is educed from natural resources such as corn, sweet potato, cassava, sugar beet pulp, and sugarcane *via* traditional fermentation process.[279] PLA properties vary by changing polymer chain orientation. Based on the chain arrangement, PLA can be classified into amorphous, semicrystalline, and highly crystalline polymer.[278] PLA can be widely used as a feedstock material for 3D printing due to its industrially compostable, and recyclable properties. Benwood *et al.*[56] conducted an experimental optimization of FFF-based 3D printing parameters for PLA to improve the impact strength and heat resistance and found out the correlation among chemical structure, properties and processing. Various parameters such as sample annealing, melt temperature, bed temperature, and raster angle were studied and concluded that the annealed samples showed superior properties due to the change in the crystalline phase of PLA. Significant increments in tensile strength, modulus, impact strength (80%), and heat deflection temperature were observed at higher bed temperatures ~105 °C. The 3D printing of PLA was investigated with various fillers in order to check the effect on the analytical properties. Keeping all these properties targeted, Wu *et al.*[280] prepared biocomposites from PLA with renewable rice husk (RH) by using melt extrusion followed by specimens prepared using FFF-based 3D printing. In experimental, PLA was grafted with acrylic acid (AA) and RH was treated with coupling agent to prepare treated rice husk (TRH). Finally, two types of composites (*i.e.*, PLA/RH and AA-*g*-PLA/TRH) were used for melt extrusion followed by 3D printing. AA-*g*-PLA and TRH were used in place of PLA and RH to increase the compatibility between

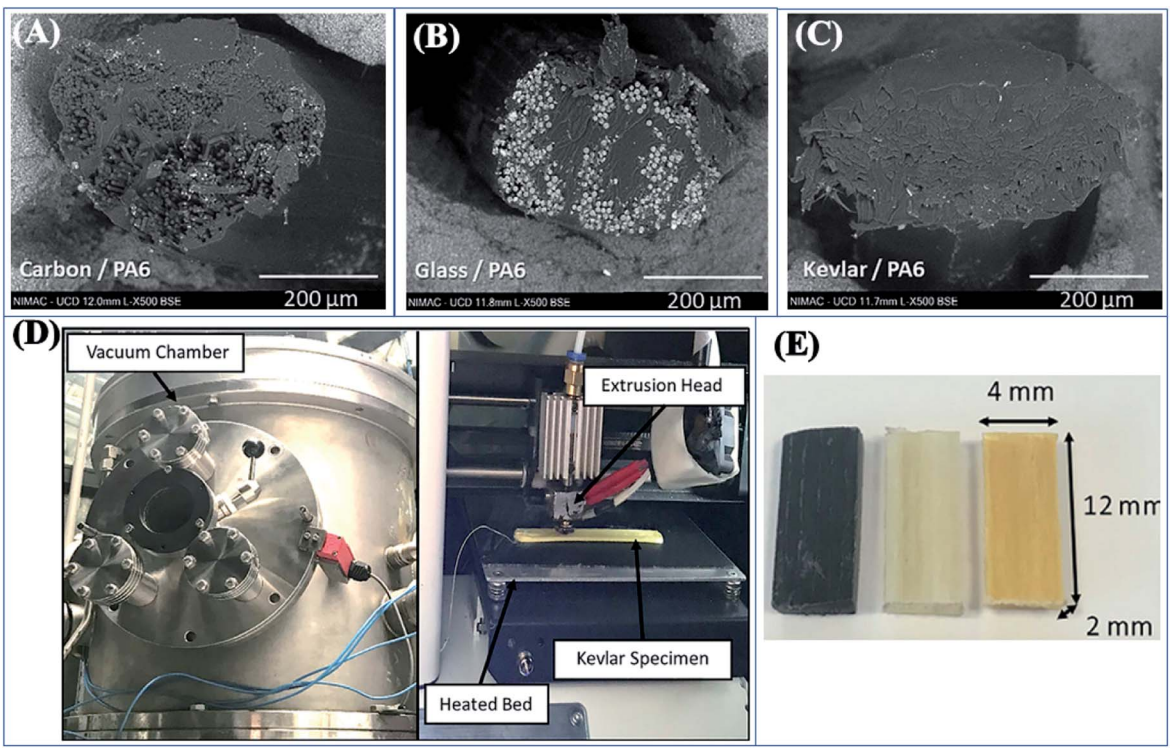

Fig. 10 Micrographs of PA6 filaments with (A) carbon fibers, (B) glass fibers and (C) Kevlar fibers, (D) vacuum chamber (left) containing 3D printer (right) showing printing of Kevlar reinforced PA6 on heated bed using extrusion head and (E) 3D printed carbon, glass, and Kevlar based composite specimens (adapted with permission).[277] Copyright 2019, John Wiley and Sons, License Number: 5143640032911.

matrix and reinforcement phase. It was detected that the mechanical behavior of AA-*g*-PLA/TRH were improved due to the uniform dispersion of filler in the matrix, increased branching, and three-dimensional network structure. Lebedev *et al.*[281] also performed similar type of work with PLA with different types of fillers such as single walled carbon nanotubes, wood flour, bronze and copper to compare mechanical properties of hot-pressed specimens *vs.* 3D printed specimens. The results suggested that % elongation and yield strength of 3D printed samples were declined by 15–60% as compared to that of hot-pressed samples. However, mechanical properties are independent on the deposition scheme. As far as the filler or reinforcing agent is concerned, few types of macromolecular materials such as CNTs were used to drastically improve the conductive, mechanical strength, and modulus due to have a single function. Luo *et al.*[189] fabricated conductive composite complex shaped products from PLA and various proportions of multi-walled carbon nanotubes (MWCNTs) based nanocomposites using FFF-based 3D printing as MWCNTs are highly rich in terms of carbon content. The high value of conductivity, tensile strength, and elongation from 3D printed PLA parts were observed after the addition of 5% MWCNTs; it can therefore be used in the fabrication of 3D printed consumables in our daily life. Similar to nanotubes, natural fibers were also explored as filler or reinforcement with PLA to identify the printing quality and other related properties. Dong *et al.*[282] utilized wood fibers as filler in PLA matrix to print the specimens for examining the mechanical properties. The design of experiments was performed to optimize various printing parameters such as layer height, infill density, and the number of shells. It was observed that material type and shell number were the critical parameters in designing the specimen, which also maximized the mechanical properties. PLA based materials and composites were investigated as fire retardants, which help to minimize the fire hazards in various applications.[283] The distribution of fire retardant (ammonium polyphosphate) and two types of phyllosilicates (organically modified Cloisite 30B and unmodified Sepiolite) in 3D printed and injection molded PLA were analyzed using cone calorimeter test and concluded that the 3D printed samples exhibited significantly reduced ignition time as compared to injection molded samples. The released heat in 3D printed samples was also reduced due to higher porosity as compared to injection molded samples. Nanoclays showed considerable synergy with fire retardants and have become one of the most promising PLA based fire retardant. PLA-based binary blends with and without filler or reinforcement also showed potential performance and to be used in 3D printing to increase their utilization in various applications. Ou-Yang *et al.*[284] used FFF-based 3D printing to fabricate complex parts with the blends of PLA and PBS in various proportions. The addition of more than 40% PLA in PBS was capable to produce higher melt viscosity, higher tensile strength, and modulus with negligible distortion. The blend ratio also showed good dimensional stability and gloss. One important point to note in this article is that the blends ratio with low degree of crystallinity, moderate viscosity, and high modulus are most suitable for 3D printing. Cork, a renewable and biodegradable material was blended in various proportions with PLA to fabricate pellets for preparing compression molded samples to analyze thermal, mechanical, and morphological properties and the filaments were fabricated using optimized formulation for FFF-based 3D printing to compare mechanical properties.[285] It was suggested that the increment in cork content reduced the tensile strength and density of PLA based composites. The reason behind reduced density of PLA/cork composites was the very low density of cork because of its closed cell morphology. Whereas the impact strength, specific tensile strength, and specific modulus were improved. The inherent brittleness of PLA can be overcome by the addition of a biodegradable plasticizer called tributyl citrate (TBC). The addition of TBC resulted in the improvement in the ductility of PLA/cork based composites, whereas tensile yield strength and modulus were compromised. The mechanical results (tensile yield strength and elastic modulus) of 3D printed PLA/cork based composite samples were lowered as compared to compression molded samples. However, the % elongation was improved slightly for 3D printed samples due to the selected printing conditions and closed cell morphology of cork, which increased the amorphous phase in the composites as compared to that of compression moulded samples. Better improvement in the analytical properties of 3D printed samples containing continuous fibers reinforced polymer matrix was observed as compared to that of short fibers. The effect of fiber arrangement design on tensile, compressive and flexural properties of 3D printed continuous fiber reinforced heterogeneous composites (CFRHCs) were analyzed. The total fiber volume content (%) in CFRHCs was 15% that was distributed layer-by-layer and distinguished in terms of G1, G2, G3 and G4 as shown in Fig. 11(A).[286] G1 represented the low fiber content in the upper 3D printed layer and higher fiber content in lower 3D printed layer. However, G3 represented the reverse order of fiber distribution to G1, which means that high fiber content in the upper 3D printed layer and low fiber content in the lower 3D printed layer. G2 represented the low fiber content in the outer layers (upper and lower both) and high fiber content in the intermediate layer. However, G4 represented the uniform distribution of fibers throughout the layers. The flexural strength and modulus were improved in the case of G1 type of fiber content loading as shown in Fig. 11(B). However, the failure of CFRHCs was also analyzed with the help of simulation model as shown in Fig. 11(C). The surface morphology of cross sections of printed CFRHCs was performed and observed better dispersion. Liu *et al.*[187] extracted cellulose fibers from sugarcane bagasse (SCB) by chemical treatment methods and utilized as filler in PLA matrix to fabricate filaments followed by FFF-based 3D printing for preparing specimens to analyze the outcome of printing orientation on mechanical behavior. The performance of 3D printed PLA/SCB based composites revealed that the addition of 6 wt% SCB in PLA matrix provided the best tensile strength. Whereas further addition of SCB in the PLA matrix reduced the mechanical behavior – particularly flexural modulus, tensile, and flexural strength. It was also concluded that the modification in G code affects the printing performance. Hence, the sample printed by "parallel" method showed better tensile strength as compared to the sample printed by

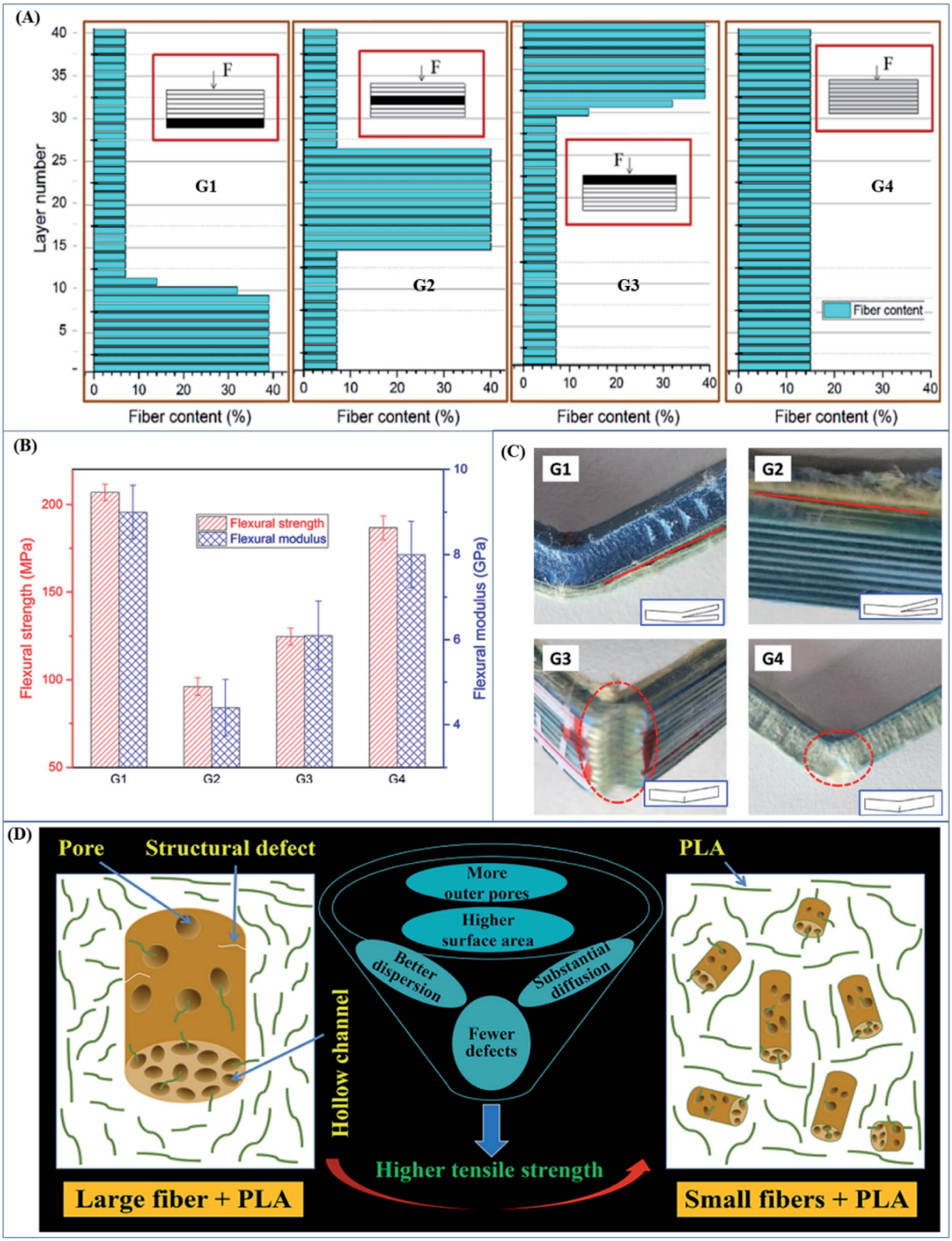

Fig. 11 (A) Illustration of CFRHCs fabricated using 3D printing, (B) effect of nonuniform fiber distribution on flexural properties and (C) failure mode of printed CFRHCs (adapted with permission).[286] Copyright 2020, Elsevier, License Number: 5143640554902. (D) Illustration of proposed dispersion of poplar fibers and PLA (adapted with permission).[287] Copyright 2019, American Chemical Society.

"vertical" method. SCB increased the thermal stability of composites which supported in the melt processing of PLA. In other research, the effect of longer and short poplar fibers derived from biomass were used as reinforcement into PLA matrix and the mechanical properties of FFF-based 3D printed specimens were analyzed.[287] The mechanical strength of PLA/poplar fibers was improved from 34 to 54 MPa based on fiber size due to its dispersion as illustrated in Fig. 11(D).

Biocarbon, one of the promising sustainable fillers, is produced from the heat treatment or pyrolysis of biomass at a wide range of temperatures under inert atmosphere. At higher temperatures, biomass is converted into highly carbonaceous biocarbon. Generally, the top temperatures for biomass conversion into biocarbon can vary up to 700 °C under inert atmosphere.[288,289] The pyrolysis produces solids biocarbon as product, gases, and oil as by-products. The surface structure of produced biocarbon depends on the pyrolysis temperature. As per the literature survey, the research on biocarbon has not been explored much. While biocarbon can be used in automotive and electronics applications due to its high modulus and high carbon content, it is also used as filler in various petroleum-based and biobased polymer matrices in 3D printing. In this direction, Ertane *et al.*[288] used biogenic carbon (5, 15 and 30 vol%) as a filler into PLA and fabricated filaments followed by 3D printing to analyze the processing and wear behaviour. Biocarbon was produced from wheat stems at 800 °C using pyrolysis in vacuum oven, and it was observed that the higher content of biocarbon created nozzle blocking problems and hindered the printing process. However, the uniform dispersion of biocarbon particles was observed in the PLA

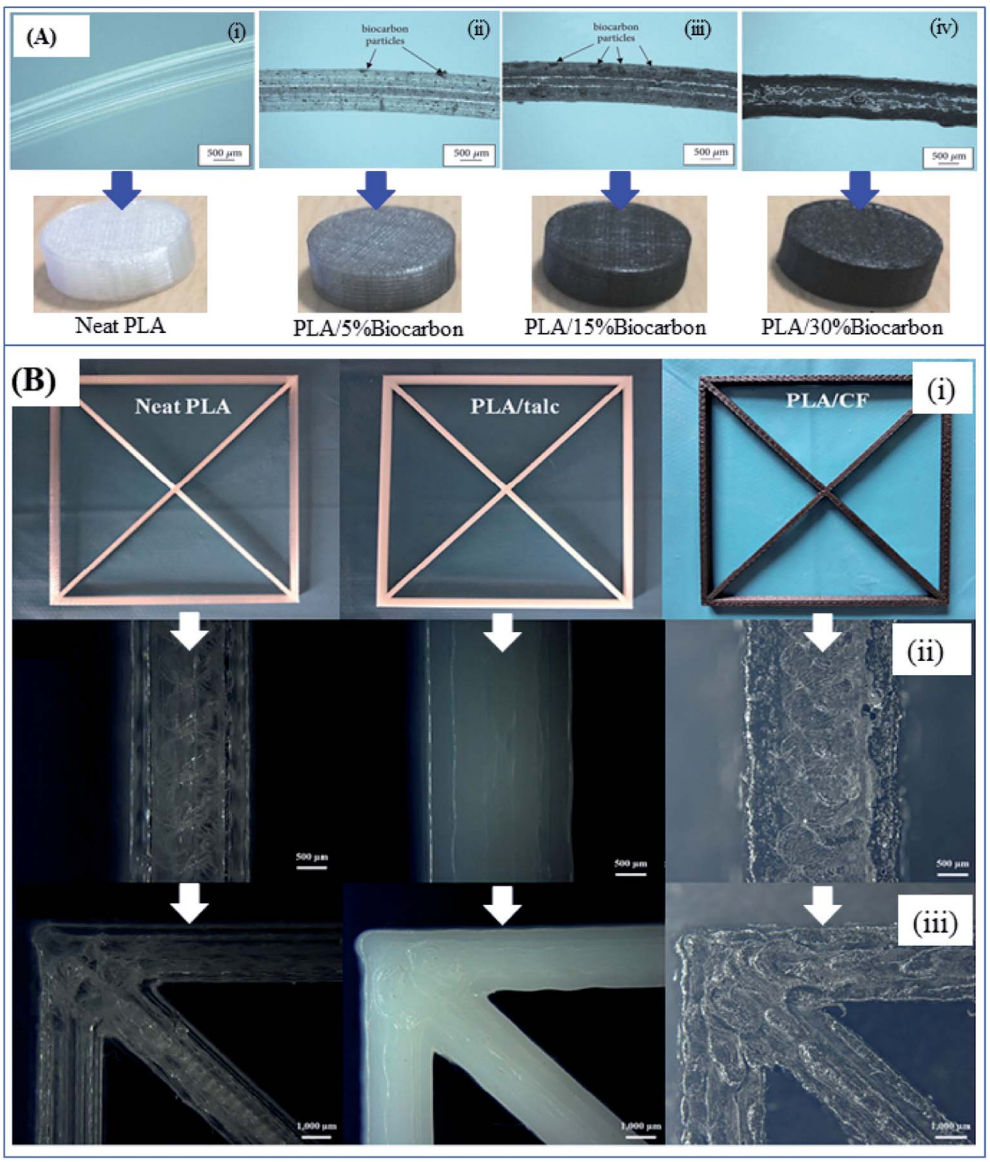

Fig. 12 (A) Microscopic images of fabricated filaments (above) and pictures of their respective 3D printed objects (below): (i) neat PLA, (ii) PLA/5 vol% biocarbon, (iii) PLA/15 vol% biocarbon and (iv) PLA/30 vol% biocarbon (adapted from Hindawi[288] open access 2021). (B) 3D printed square shaped objects (above), microscopic images of printed straight lines of the objects (middle) and corners (below) using (i) neat PLA, (ii) PLA/talc and (iii) PLA/carbon fibers filaments (adapted with permission).[290] Copyright 2019, John Wiley and Sons, License Number: 5144150098005.

Table 4 Traditional polymers and their composites in 3D printing applications

Materials used	Printing method	Targeted application	Research output	Sources
ABS	FFF	Automotive application	Decrease in melt flow, increase in glass transition temperature, reduction in tensile and compressive strengths and carbonyl groups generation in ABS after recycling	292
ABS/polycarbonate	FFF	Automotive application	Void formation, proves compatibility between ABS and polycarbonate, improved hardness and strength of ABS with increase in polycarbonate	220
ABS/coir fibers	FFF	Biomedical application	Good mechanical properties due to good dispersion	293
ABS/acrylonitrile-butadiene rubber/lignin/carbon fibers	FFF	Shape memory and other high-performance applications	Highly interfused and 100% improved inter-layer adhesion, reduced degree of chemical crosslinking	294
ABS/PLA	FFF	Cartilage tissue regeneration	Well proliferation of articular chondrocytes cells and nucleus pulposus (NP) cells, sustained scaffold stability due to good mechanical properties	295
ABS/polyethylene oxide/lignin/short carbon fibers	FFF	Automotive application	Slightly improved tensile strength of ABS/lignin at lower lignin wt%. Improved dispersion of lignin after adding PEO in ABS. Addition of carbon fibers maintained the mechanical properties of ABS	225
ABS/poly(methyl methacrylate)/methacrylate-butadiene-styrene	FFF	Automotive application	Effectively improved melt flow rate, elongation, impact strength, optical, scratch resistant and surface gloss properties	221
ABS/rice straw	FFF	Structural application	Tensile and flexural properties decreased with increment in rice straw content. However, water absorption increased	296
ABS/macadamia nutshells	FFF	Lightweight product applications	Lower density and similar mechanical properties as compared to commercial wood polymer composite filaments	297
Polypropylene (PP)	FFF	Automotive application	Demonstrated a variation of crystallinity across individual layers, more crystallinity of printed polymer in bulk of layer and less crystallinity in the vicinity of interfaces, improved mechanical performance of 3D-printed objects	298
PP/hemp fibers	FFF	Packaging	Effective shrinkage reduction	299
PP/hydrocarbon resin	FFF	Automotive	Lowered crystallization temperature and delayed crystallization of PP due to adding hydrocarbon resins, which provided longer time for relaxation of residual stresses and also allows additional diffusion through solidification process, improved tensile strength	233
Recycled PP/cellulose waste materials	FFF	Automotive and household goods	20–30% increment in storage modulus and 38% increment in elastic modulus with addition of cellulose materials, no significant improvement in tensile strength, weaker interfacial strength as compared to filler strength	20
Nylon/carbon fibers, Nylon/glass fibers, Nylon/Kevlar fibers	FFF	Automotive and aerospace applications	5.7, 1.0, and 1.7% reduction in porosity and 33, 22, and 12% increment in interlaminar shear strength for polyamide reinforced with carbon, glass and kevlar fibers respectively, 3D printed at low pressure (1 Pa) conditions as compared to that of atmospheric pressure	277
Polyether ether ketone (PEEK)/carbon nanotubes/graphene nanoplatelets	FFF	Automotive, space, orthopedics and electronics applications	Young's and storage modulus improved by 20 and 66% after adding 3% carbon nanotubes. However, the same properties were improved by 23 and 72% after adding 5% graphene nanoplatelets respectively. CLTE value reduced by 26 and 18% by adding 5% graphene nanoparticles and 3% carbon nanotubes into PEEK, respectively	300
PEEK/laser-induced graphene	FFF	Smart components and fabrication of structure self-monitoring systems	Working process with self-monitoring ability, stretching and bidirectional bending types deformations in real time with accuracy, hold good reliability (>1000 cycles), fast recovery time (247 ms) and response time (60 ms)	301

Table 4 (*Contd.*)

Materials used	Printing method	Targeted application	Research output	Sources
Methacrylate oligomers/graphene nanoplatelets	SLA	Sports equipments, automotive and aerospace	Same improvement in Young's modulus in stereolithographic 3D printing technique by using ~10 times less graphene loading as compared to other processing techniques due to assimilation of aligned graphene platelets into polymer matrix	302
Methacrylate polymer/ functionalized graphene oxide	SLA	Drone parts manufacturing, medical applications	Enhanced tensile strength and fracture energy due to stronger adhesion between matrix and filler, good antimicrobial properties	180
Recycled PET/biochar	FFF	Automotive application	Excellent dimensional stability, 32% improvement in tensile strength by adding 0.5% biochar and 60% improvement in tensile modulus by adding 5% biochar	253

matrix, which enhanced nozzle wear during printing. The increment in nozzle wear with increasing biocarbon content was due to the sticking out of biocarbon particles from the filament surface. The microscopic images of fabricated filaments of neat PLA, PLA/5 vol% biocarbon, PLA/15 vol% biocarbon, PLA/30 vol% biocarbon and their respective 3D printed objects are shown in Fig. 12(A). One ultimate advantage of PLA/biocarbon composite was its use as structural material to improve the soil quality due to its biodegradable nature. Similarly, Gao *et al.*[290] fabricated 3D parts using FFF-based technology from PLA with various fillers (talc and carbon fibers) and observed an usual behaviour of lowering in tensile strength as compared to that of injection molded counterparts. The 3D printed square shaped objects, microscopic images of printed straight lines of the objects, and corners using neat PLA, PLA/talc and PLA/carbon fibers were shown in Fig. 12(B).

The degree of mechanical anisotropy was affected by the addition of filler in PLA matrix. The dispersion of filler facilitated the molecular diffusion across the bond interface. Kalinke *et al.*[291] used nickel oxyhydroxide supported activated biochar to fabricate an electrode which was coupled with a electroanalytical device for the determination of non-enzymatic glucose. Castor oil cake was pyrolyzed at 400 °C in the presence of nitric acid to produce biochar, which increased surface area, functional groups, and porosity. Activated biochar (AB) demonstrated an outstanding performance for spontaneous measurement of Ni(II) ions.

Overall, Table 4 explains the utilization of traditional polymers and their composites in various AM techniques, effect on various properties and their possible applications in various commercial fields.

6. Real-world application of 3D printed polymeric materials through commercialization

AM opens a new era of industrialization in various sectors such as medical, automotive and electronics.[303] However, it impacts the medical sector particularly, where it provides a freedom of design selection and product creation to the manufacturer in a faster and cost-effective way.[31] It is particularly important for disabled people who can easily find a solution based on their specific requirement.[304] The 3D technologies are one of the efficient and cheapest solutions, which includes the creation of artificial prosthetic arm, hand, leg or foot.[305] A 3D printed real functional prosthetic can help the people with disabilities to perform their daily routine work and can change their daily lives.[306]

In Fig. 13(A), various custom-made orthotics such as forearm static fixation (Fig. 13(A)-i), hand prosthetic (Fig. 13(A)-ii), spinal braces (Fig. 13(A)-iii) and ankle-foot orthosis (Fig. 13(A)-iv) were developed on demand using various polymers in 3D printing technique.[307] The German manufacturer has provided the online platform to the patients to customize his/her prosthesis and the 3D printed prosthesis is delivered in just one week.[308] The manufacturer is trying to reduce the delivery time from one week to just 48 h. This can only be possible with the help of AM technologies. Presently, E-nable is an association, which is situated in United States. The motive of this association is to create a network of enthusiastic manufacturers, who can help to generate customized designs of prostheses in the world and those digital designs can be printed in 3D. The main goal of this association is to help disabled people who need the prosthesis most, thus the cost of 3D printed prosthesis has been set lower as compared to the traditional prosthesis.

The other example of the use of AM technologies in medical sector is the manufacturing of clear dental aligners as shown in Fig. 13(B).[309] The use of 3D printers makes it easier to print customized dental aligners, which helps both the manufacturers and the consumers. It was also observed that 3D printing has increased the company's capacity ~30% to produce custom-made orthodontic aligners.[310]

The automotive industrial sector has been influenced drastically by the advancement and introduction of AM technologies as it opens the door to improve the parts properties which was not possible earlier with traditional manufacturing techniques such as injection molding. More robust and complex designs can be manufactured along with the improved properties particularly lightweight and strength in the reduced cost and

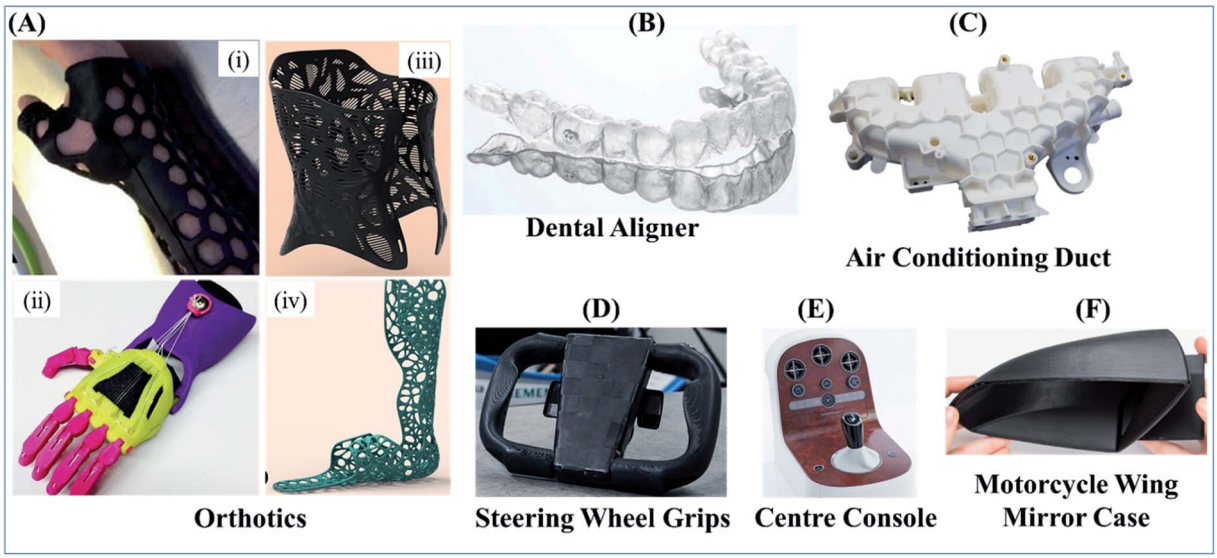

Fig. 13 3D printed polymeric products used in various applications; (A) orthotics[307] (adapted from MDPI 2020, open access), (B) dental aligners[309] (adapted from MDPI 2021, open access), (C) air conditioning duct,[311] (D) steering wheel grips,[311] (E) centre console[311] and (F) motorcycle wing mirror case[311] (adapted with copyright permission 2021 by http://www.hubs.com).

lead time. Among those, the weight reduction in printed components is one of the critical aspects in automotive industry. The utilization of advanced engineering materials, complex geometries and infill patterns are the key factors to reduce the weight and improve performance of the printed automotive parts. Few of the commercially available 3D printed automotive parts have been shown in Fig. 13(C)–(F). Internal channels are often required to cover various aspects such as conformal cooling, thin walls, complex curved surfaces and fine meshes in automotive parts.[311] AM can produce highly customized structures which can be still lightweight and extremely stable. It is also noteworthy that AM technologies provide a digital route to utilize high degree of freedom in designing, optimization and incorporation of functional features, which can be manufactured in small batches at realistic unit cost and also high degree of customization in continuous production. Heat deflection temperature of polymers in automotive application is also critically required to measure to avoid system failure due to dimensional inaccuracy at higher temperature near engine component. Few of the engineering thermoplastics such as nylon and PET can withstand at higher temperature and are suitable to be used in engine components at high temperature. Mostly, SLS-based 3D printing is used to produce highly complex single-piece part such as non-structural low volumes ducting for aerospace and performance racing. It is also possible with SLS to manufacture a single component having variable wall thickness with increased strength to weight ratio. Such an arrangement will be very costly to design for traditional manufacturing techniques. However, SLS doesn't require any extra cost for increased complexity. The automotive parts can be printed at high level of accuracy without using any support material in SLS-based 3D printing. Unlike traditional manufacturing techniques, AM technologies has a provision to produce multicolored designs with an aesthetic surface finish.

AM technology and cloth designing are a great combination which was explored by Sculpteo.[312] 3D printing is growing and getting more precise in terms of application. Great advantages of 3D printing have been observed for fashion industry, from 3D printed flexible fabrics/cloths to 3D printed footwear and other accessories. Hence the possibilities of AM in fashion industry are endless. Earlier, 3D printing was used for an artistic touch, but now, the fashion industry has shown interest to develop 3D printed wearable flexible clothes[313] as shown in Fig. 14(A). This technology gives freedom to create intricate designs in the fashion industry. Some of the cost-effective cloths with complex designing pattern have been fabricated using 3D printing, which may be expensive while prepare using other manufacturing methods. AM is now used as manufacturing method which is a sustainable way to produce a collection of customizable and comfortable regular clothes for the body and its movements. The goal of fashion industry is to develop a supply chain and to print more comfortable and durable clothes on demand. It was noticed that the material waste in fashion industry has been reduced up to ~35% by using eco-friendly 3D printing technology.[312]

Indeed, AM is one of the best methods to produce complex shaped functional objects including 3D printed watches, which are already available in the market. Even if AM leads towards invention in numerous engineering divisions, there are still few limitations to face. The watches prepared by 3D printing technique are one of them due to their complicated mechanism. This fabrication process permits us to produce on-demand designs and can be a center of attraction for watchmakers. One of the main advantages is customization, which can be exploited with the help of 3D printing by watchmakers as the lower price of customized watches can be possible now. In this

case, ALB Watches fabricated four different watch models using 3D printing. The fabricated watches must be very precise, and there must not be any possibility for approximation. It is still very difficult to 3D print a small and wearable watch with a 3D printed gear. The lightness and resistance of PA12 could be very useful. Two types of plastics: polyethylene terephthalate glycol (PETG) and PLA were used to print watches.[314] The clockmakers also tried to print the case with PETG and internal the mechanism of a watch with PLA.

Few manufacturers used plastic wastes in 3D printing to fabricate sustainable furniture (stools, lounge chairs and tables). The printed furniture was lightweight and can easily be transferred from one place to other. Such concept of using recycled plastics in 3D printing can compete with the current industrial processes and also satisfy the circular economy approach.[315] It should be noted that the furniture has been printed using minimum material and within a limited time frame and energy. As discussed before, the design of the printed specimens is critically important for its performance. Hence, the selected closed-loop shape of the printed furniture provides additional mechanical strength and durability.

The 3D printing of bike helmets is also an emerging area for the automotive industries. The 3D printed helmets with entirely customized and comfortable designs are ready to be marketed. The silent features of 3D printed helmets are lightweight, comfortability and safety.[316] For the last two years, Québec Company Kupol has been fine-tuning the design of helmets. Its unique and innovative safety ideas combined with the advent of 3D printing have enabled the company to create a truly avant-garde design. Advances in 3D-printing technology have given the experts a better way to explore and design safety features to create superior helmets when it comes to aesthetics, adjustments, and function. 3D printing has improved the degree of accuracy that's revolutionizing traditional bike helmets and streamlining design. The Kupol helmet is designed to react to impacts from any angle and absorb rotational forces – the characteristics of most cycling accidents.

AM industry has made great progress in developing complex shaped drones. The drones are unmanned aerial vehicle, which was very costly to purchase earlier. However, the cost-effective and custom-made drones can be prepared now using 3D printing. Hence, the advantages of 3D printing technique make it appropriate for fabricating such a vehicle. Indeed, drones are attractive to several industries as they handle with plentiful degrees of independence. The decent thing about using AM to fabricate drones is that nearly all the parts of drones can be 3D printed, excluding electronic components. These comprise the propellers, frames, antenna mounts, prop protectors, and battery housing.[317] Besides the main parts of the drone, other fixtures like mounts, boosters or cases can also be generated by 3D printing. This technology delivers several benefits when generating prototypes or functional models. With 3D printing, ~40% of the time can be saved in the prototype designing. The total weight of the drone was also decreased by 20% by using 3D printing.

The various parts of violin can also be 3D printed and assembled together to fabricate violin. Violins are used from centuries and the design has hardly changed. The efforts are needed in designing an acoustic instrument which needs to create an authentic sound without the help of any other things.[318]

The various other products such as eyewear glasses, razor handles, shoes, toys, air ducts, shower heads and furnitures (as shown in Fig. 14B)[319] are used in our day-to-day life those can be 3D printed with improved customization and aesthetic designs. Mostly, FFF-based 3D printing is used to produce eyeglasses to bring more innovation in designing part. AM technology

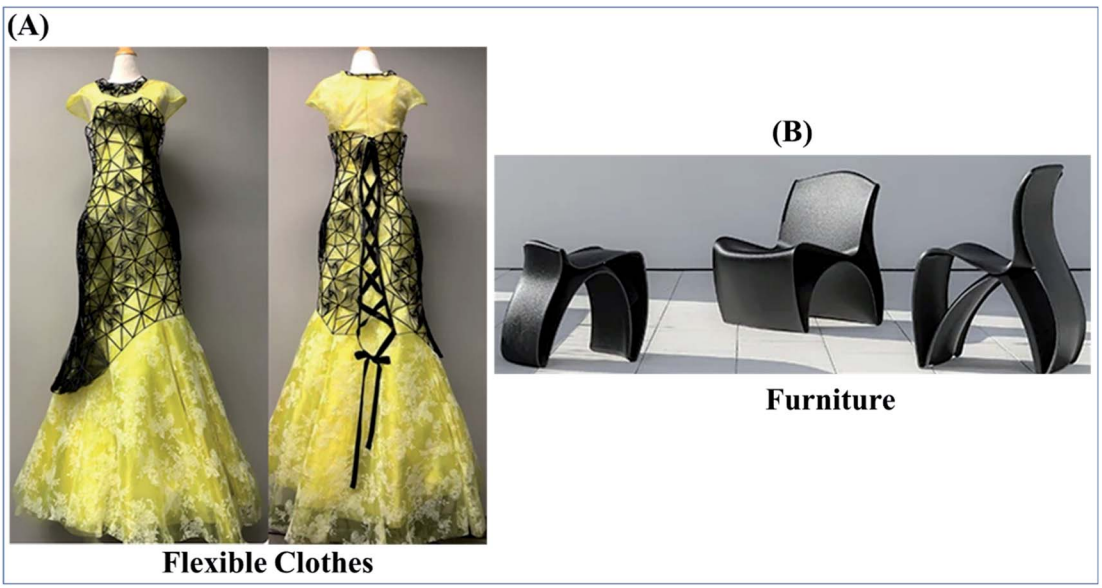

Fig. 14 3D printed polymeric products used in various applications; (A) flexible clothes[313] (adapted from Springer Nature 2019, open access), (B) furniture[319] (adapted with copyright permission 2021 provided by Strat Collection, recycled furniture designed by Joachim Froment, FutureWave, Photography: MAD, Home of Creators, Brussels from http://www.joachimfroment.com/strats-furniture).

permits to produce extremely complex structures, and in few cases, the designs could not even possible to prepare without 3D printing due to the limited constraints in traditional manufacturing. In the eyewear industry, the glasses frames are mainly custom-made and ultra-light weight using 3D printing.[320] Many eyewear manufacturers have adopted this technology to improve their design and help to optimize the supply chain.

Custom-made 3D printed razor handles have been developed by a collaboration of Gillette Company and Formlabs.[321] The focus behind 3D printed razor handle was to provide best look, cost-effective, grooming preference, color and style. Three ranges of razor handles based on the level of 3D printing are available in market. Those are partially printed razors, fully printed razors and with a chrome effect. The pricing of the razor handle varies based on the level of 3D printing.

The AM also contributes to developing shoes midsoles, sandals and insoles with increased design freedom at industrial scale as shown in Fig. 15(A).[322] The shoes midsoles are manufactured using a blend of polyurethane and UV-curable resin.[323] The blend is arranged in a complex lattice structure which provides strength to the midsole.

The manufacturing of 3D printed toys offers more flexibility (as shown in Fig. 15(B)) and cost-effectiveness as compared to injection molding.[324] Toys manufacturing is one of the major markets for plastic products in the world, which is nearly 89

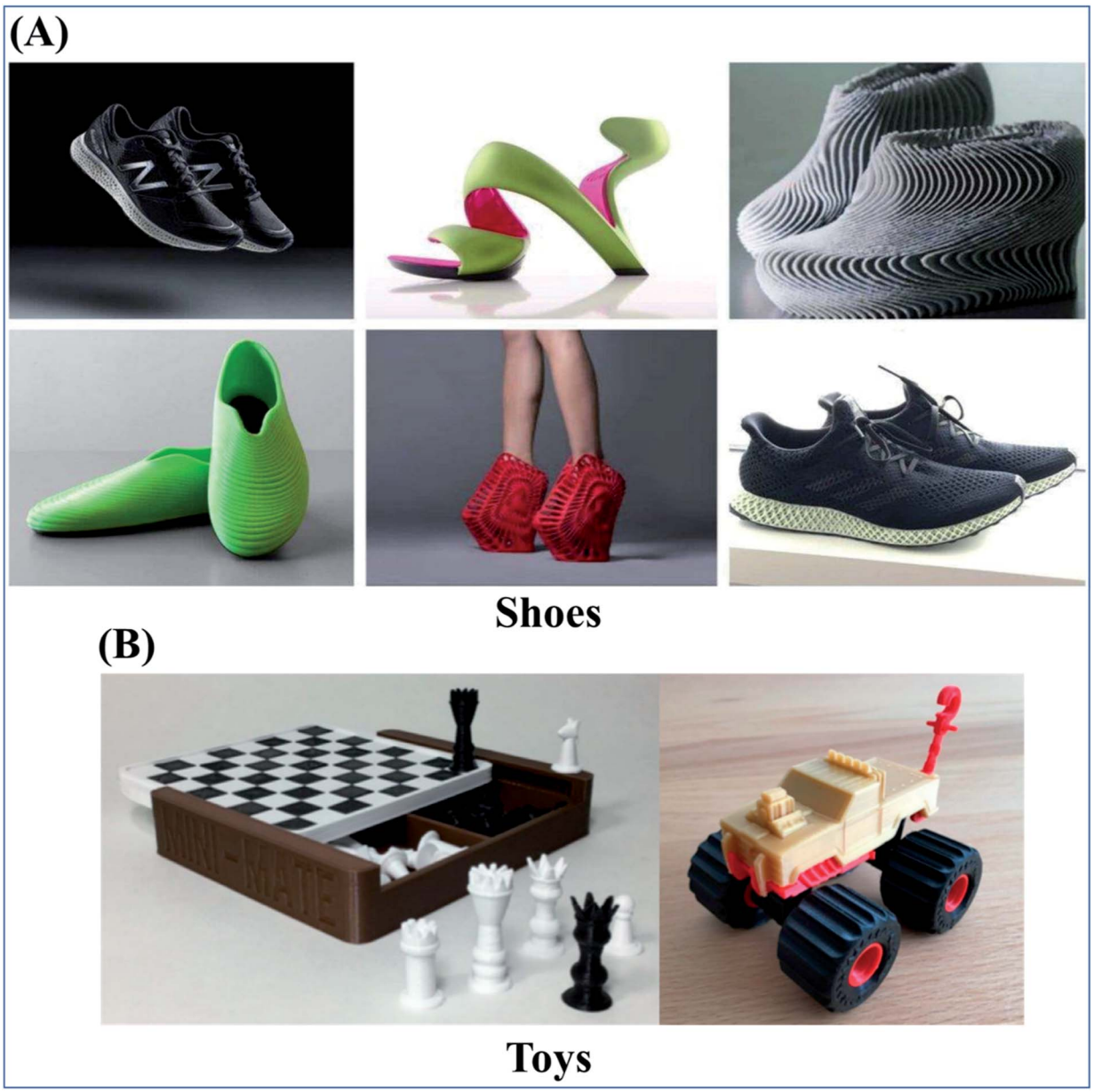

Fig. 15 3D printed polymeric products used in various applications; (A) shoes (adapted from Taylor & Francis online[322] open access 2021), and (B) toys (adapted from MDPI[324] open access 2017).

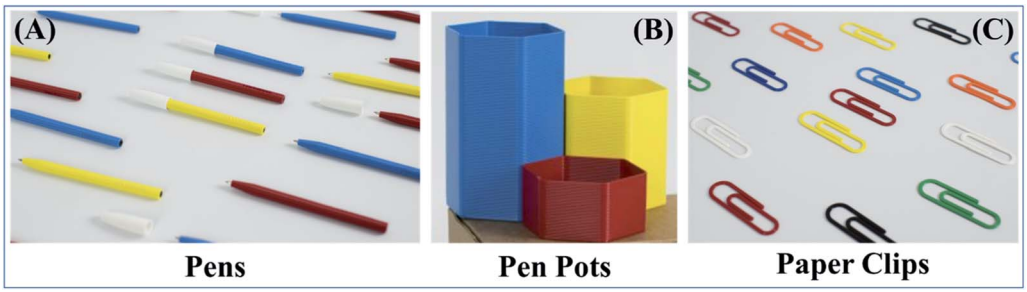

Fig. 16 3D printed stationery items; (A) biodegradable pens,[328] (B) biodegradable pen pots,[328] and (C) biodegradable paper clips.[328] (Adapted with copyright permission 2021 by Batch.Works from http://www.batch.works).

Billion dollars per year.[325] The toys industry produces a great deal of profit and also risky as the interest of the consumers may change time to time. As far as traditional manufacturing is concerned, the main cost is involved in tooling, which can be reduced significantly by using AM. The benefit of using AM is its digital process to create optimized 3D model of the product, which is not possible in traditional manufacturing. The other benefit of the digital process is that if the specimen needs to be updated or replaced, then only change in digital file will be required with no external tooling cost. The air duct was also printed using 3D printing technique and was approved by flights to be used for air-conditioning.[326] PLA polymer has been used in FFF-based 3D printing to manufacture custom-made shower-head designs in different colors.[327]

The stationery items such as ballpoint pens, pen pots and paper clips has also been produced by FFF-based 3D printing technique using biodegradable plastics. The examples of 3D printed ballpoint pens, pen pots and paper clips are shown in Fig. 16(A)–(C) respectively. Batch.Works manufactured 30 000 stationery products using AM within two months.[328] It was estimated that each paper clip and pen pot take 2 and 20 minutes, respectively to print.

A cosmetic product called mascara brush has been manufactured using SLS-based 3D printing technology. A mass-production of 3D printed mascara brushes has been started at industrial scale last year by Chanel in collaboration with Erpro Group and manufactured up to 50 000 pieces in a day.[329] SLS-based 3D printing generates pores or microcavities on the brush during printing, which is capable to hold higher amount of mascara as compared to the brushes produced from traditional manufacturing process. A granular texture on the 3D printed brush's strands increases their surface area, which improves the ability to adhere to eyelashes.

7. Critical challenges and future opportunities in 3D printing

7.1. Critical challenges

The worldwide demand of AM is increasing due to its ability to produce more challenging customized objects, design flexibility and ease of use based on the process parameters for particular applications.[330] In general, the restrictions of AM can be seen on the basis of areas need to be explored and indeed AM technology will be the only response of existing limitations where the majority of new and innovative developments have risen.[331] However, AM is still not matured enough for its utilization in all real-world applications. Numerous challenges and drawbacks exist in AM which need to be investigated for advanced technological development. The existing limitations on specimen size, warping, poor accuracy, air gaps in top printed layers, anisotropic mechanical properties, layer misalignment, building of overhang surfaces, low manufacturing efficiency, under and over-extrusion, pillowing, stringing, mass production and material's limitation are the critical challenges that require further investigation and exploration.[13,42] However, significant amount of research is going on various 3D processes to overcome the above-mentioned limitations. In detail, the engineering plastics such as nylon, PP and their blends show various issues such as non-uniform filament diameter, warping, extrusion difficulties, nozzle clogging and layer delamination during 3D printing. These printing related problems can be solved by optimizing the operating conditions such as print temperature, build platform temperature, printing speed, cooling speed, flowability, infill density and % overlap. Ahn *et al.*[332] revealed that the quality of 3D printed specimens can be upgraded by fine-tuning the printing conditions namely layer thickness, chamber temperature, raster angle, raster width and air gap. It is important to note that the variation in cooling speed of the molten filament at nozzle influences the printing quality and acts as driving force to warpage and shrinkage. A similar phenomenon was also described by Fitzharris *et al.*[333] for 3D printed polyphenylene sulfide (PPS). It was stated that the warping and shrinking of the printed polymer are the outcome of improper cooling settings, which stretches the polymer chains and forms a highly dense crystalline region. The higher cooling rate quickly reduces the molten polymer temperature, which develops stress on the printed part due to enhanced crystallization rate. Hence, the polymers with less crystalline region, such as PLA and ABS, are slightly affected by the change in cooling rates. The warping issues of polymers during 3D printing can also be resolved by increasing the number of brim layers.[334] More brim layers increased the contact area between printed layer and platform, as a result, the adhesion between the initial layer and platform increases and that improves the printed surface quality. The optimized distance between nozzle

and printing bed controls the interlayer adhesion and surface roughness of printing material.[335] It was concluded that 0.10 mm distance between nozzle and printing bed is appropriate for finest surface quality. The adhesion between build platform and first layer of printing part depends on the printing bed temperature. Spoerk *et al.*[336] stated that the printing bed temperature must be selected a little higher than the T_g value of the polymer. In AM process, the void formation between successive layers is also one of the major challenges, which occurs as a result of insufficient bonding between layers and shows inferior mechanical properties.[337] Certainly, this void formation issue depends on the type of AM technique and the material used. Hence, the void formation can be minimized by the geometry of nozzle used. Paul *et al.*[338] estimated the variation in nozzle geometry on the void formation and concluded that the rectangular shaped nozzles showed better performance as compared to cylindrical nozzles. The staircase effect is also one of the major drawbacks in AM technology, which shows significant effect on the quality of external surfaces and can be minimized by using post-processing methods like sand sintering.[339] The anisotropic mechanical properties of 3D printed specimen are another challenge in AM, which can be seen along the build direction as well as other directions.[332]

7.2. Future opportunities

3D printing technology has triggered a third industrial revolution because it offers creative and customized products used in various applications which expands economic, technical, and social impacts.[340] The current traditional manufacturing techniques such as injection molding and thermoforming will be severely affected after the establishment of 3D printing technology due to its reduced time, working cost, materials storage, labour requirement, semi-manufactured parts, and the easiness in relocating at the location of demand.[341] It will be based on enormous investments at small scales in distributed manufacturing sites unlike high investment costs for a few centralized manufacturing sites. On the spot manufacturing by 3D printing techniques will improve the supply chain efficiently and will make the logistics availability easier. Only transportation of raw materials will be needed. However, the requirement of raw materials will be reduced due to minimized production wastes and on-demand production. In most of the cases, the virtual design of complex shaped products from software will be made an open source so that many people can access across the world without investing money. Although this paradigm shift in manufacturing technology will take time, it is inevitable due to its economic feasibility and ease of operation.

8. Conclusion

The leading-edge research related to product designing, materials used, and manufacturing processes may advance the manufacturing industry. Based on the increment in product complexity, there is a demand to develop a new and innovative manufacturing technique. At the commencement of the 21st century, AM offers an adaptable platform for digital designing and manufacturing of innovative functional materials. The researchers have utilized newly developed AM techniques for rapid prototyping of complex shaped components. Such advancement in manufacturing techniques helped to modify the commercial instruments and made them more reliable, affordable and cost-effective. An intensive investigation and detailed review are required by the researchers to explore the benefits of AM technology and to overcome drawbacks/challenges. In this paper, a comprehensive literature review on various 3D printing techniques has been performed. The execution of all types of 3D printing techniques has been explained along with their benefits and limitations based on working principle and materials used. AM is a technique in which all types of plastics from petroleum-based resources and natural resources can be used. The recycled plastics can also be used in AM to develop sustainable products. The differences between traditional manufacturing technique such as injection molding and AM technique conclude that the highly complex structures can't be manufactured cost-effectively using injection molding as compared to AM. A comprehensive literature review on the effect of various printing conditions on the quality of the printed parts has been explained in this review article. Various parameters such as nozzle temperature, print bed temperature, print speed, and raster angle have been reviewed in detail. The application of AM technique in various industrial sectors such as automotive, biomedical and electronics has been explained well. The key feature of this review article is the detailed description of 3D printing and its application based on various traditional polymers. The real-world application of 3D printed polymeric materials has been explained which showed a promising aspect of mass customization of 3D printed products in various industrial sectors. Apart from the utilization of AM in various applications, there are few challenges, need to be resolved in order to industrialization of 3D printed products. Based on the detailed literature survey, the observed challenges such as specimen size, warping, poor accuracy, air gaps in top printed layers, anisotropic mechanical properties, layer misalignment, building of overhang surfaces, low manufacturing efficiency, under and over-extrusion, pillowing, stringing, mass production and material's limitation need exhaustive research and observation. It was noted that the 3D printing research on hybrid polymers is limited and need to be explored much, which can further expand the applications of AM technology. Hence, the development of innovative materials for AM has been productive, and continuous efforts will be required further innovation in this direction.

Abbreviation

3D	Three-dimensional
AM	Additive manufacturing
FFF	Fused filament fabrication
SLS	Selective laser sintering
SLA	Stereolithography
EBDM	Electron beam direct manufacturing
BJP	Binder jetting 3D printing

IJP	Inkjet 3D printing
3DP	3D plotting or polyjet printing
LOM	Laminated object manufacturing
ABS	Acrylonitrile butadiene styrene
PP	Polypropylene
PE	Polyethylene
PET	Polyethylene terephthalate
PC	Polycarbonate
TPE	Thermoplastic elastomers
PA	Polyamide
PTT	Poly(trimethylene terephthalate)
PLA	Poly(lactic acid)
RP	Rapid prototyping
CAD	Computer-aided design
PCL	Polycaprolactone
ASTM	American society for testing and materials
UV	Ultraviolet
TPU	Thermoplastic polyurethane
EBM	Electron beam melting
CT	Computerized tomography
CNT	Carbon nanotubes
LED	Light emitting diode
SA-GMA	Poly(styrene-acrylic-*co*-glycidyl methacrylate)
EBA-GMA	Poly(ethylene-*n*-butylene-acrylate-*co*-glycidyl methacrylate)
GO	Graphene oxide
MWCNTs	Multi-walled carbon nanotubes
PBS	Polybutylene succinate
ZrO_2	Zirconium dioxide
PMMA	Poly(methyl methacrylate)
MBS	Methacrylate-butadiene-styrene
PA	Polyamide
PEO	Poly(ethylene oxide)
MOF	Metal organic framework
FH	Fully hydrogenated
PH	Partially hydrogenated
POM	Polarized optical microscopy
CF	Carbon fibers
SEBS	Styrene-(ethylene-butylene)-styrene
MAPP	Maleated polypropylene
EPP	Expanded polypropylene
LDPE	Low density polyethylene
LLDPE	Linear low-density polyethylene
HDPE	High-density polyethylene
HMWPE	High molecular weight polyethylene
UHMWPE	Ultra high molecular weight polyethylene
CLTE	Coefficient of linear thermal expansion
SEM	Scanning electron microscopy
PEI	Polyetherimide
SBC	Styrene block copolymers
TPPOE	Thermoplastic polyolefinelastomers
TPCP	Thermoplastic copolyesters
TPPA	Thermoplastic polyamides
TPV	Thermoplastic vulcanizate
PBBSI	Poly(1,4-butanediol/2,3-butanediol/succinate/itaconic acid)
PDMS	Polydimethylsiloxane
WF	Wood flour
EPDM-*g*-MAH	Ethylene propylene diene monomer-*grafted*-maleic anhydride
MTT	3-(4,5-Dimethylthiazol-2-Yl)-2,5-diphenyltetrazoliumbromid
RH	Rice husk
AA	Acrylic acid
TRH	Treated rice husk
TBC	Tributyl citrate
SCB	Sugarcane bagasse
PHA	Polyhydroxyalkanoate
NP	Nucleus pulposus
PEG	Polyethylene glycol
PEEK	Polyether ether ketone
HPMC	Hydroxypropyl methylcellulose
MCC	Microcrystalline cellulose
CMC	Carboxymethyl cellulose
DCS	Diclofenac sodium
LID	Lidocaine
AB	Activated biochar
SMA	Styrene-maleic anhydride copolymer
MBS	Methyl methacrylate butadiene styrene
CB	Carbon black
cFF	Continuous flex fibers
TMP	Thermomechanical pulp
rPLA	Recycled poly(lactic acid)
MFI	Melt flow index
PVA	Polyvinyl alcohol
ABR	Acrylonitrile-butadiene rubber
OPF	Oil palm fibers
DPPH	2,2-Diphenyl-1-picrylhydrazyl
PLGA	Poly L-lactide-glycolic acid
PLLA	Poly-L-lactide
PDLA	Poly-D-lactide
HA	Hydroxyapatite
MNC	Micro-nanocellulose
Ox-SCG	Oil-extracted spent coffee grounds
PU	Polyurethane
PEGDA	Polyethylene glycol diacrylate
PETG	Polyethylene terephthalate glycol
PPS	Polyphenylene sulfide

Conflicts of interest

The authors declare no competing financial interest.

Acknowledgements

The authors are thankful for the financial support from: (i) the Ontario Research Fund, Research Excellence Program (ORF-RE09-078) from the Ontario Ministry of Economic Development, Job Creation and Trade, Canada (Project No. 053970 and 054345); (ii) the Ontario Ministry of Agriculture, Food and Rural Affairs (OMAFRA), Canada University of Guelph, Bioeconomy Industrial Uses Research Program Theme (Project No. 030252 and 030485); and (iii) the Natural Sciences and Engineering Research Council of Canada (NSERC), Canada Research Chair (CRC) Program Project No. 460788. This study has also benefited

from the facility funding to the Bioproducts Discovery and Development Centre, University of Guelph supported by FedDev Ontario, Canada; OMAFRA Canada; the Canada Foundation for Innovation (CFI); Federal Post-Secondary Institutions Strategic Investment Fund (SIF), Canada; and Bank of Montreal (BMO).

References

1 X. Wang, L. Zhao, J. Y. H. Fuh and H. P. Lee, *Polymers*, 2019, **11**, 1154–1174.
2 S. H. Huang, P. Liu, A. Mokasdar and L. Hou, *Int. J. Adv. Manuf. Technol.*, 2013, **67**, 1191–1203.
3 S. Ford and M. Despeisse, *J. Clean. Prod.*, 2016, **137**, 1573–1587.
4 S. C. Daminabo, S. Goel, S. A. Grammatikos, H. Y. Nezhad and V. K. Thakur, *Mater. Today Chem.*, 2020, **16**, 100248.
5 Y. Zhou, X. Xia, X. Liu, B. Huang, L. Xiao, Q. Qian and Q. Chen, *Macromol. Mater. Eng.*, 2019, **304**, 1900021.
6 G. W. Melenka, B. K. O. Cheung, J. S. Schofield, M. R. Dawson and J. P. Carey, *Compos. Struct.*, 2016, **153**, 866–875.
7 S. A. Tofail, E. P. Koumoulos, A. Bandyopadhyay, S. Bose, L. O'Donoghue and C. Charitidis, *Mater. Today*, 2018, **21**, 22–37.
8 M. Lille, A. Nurmela, E. Nordlund, S. Metsä-Kortelainen and N. Sozer, *J. Food Eng.*, 2018, **220**, 20–27.
9 J. Liu, L. Sun, W. Xu, Q. Wang, S. Yu and J. Sun, *Carbohydr. Polym.*, 2019, **207**, 297–316.
10 M. Somireddy, A. Czekanski and C. V. Singh, *Mater. Today Commun.*, 2018, **15**, 143–152.
11 I. Anderson, *3D Print. Addit. Manuf.*, 2017, **4**, 110–115.
12 M. Jorfi and E. J. Foster, *J. Appl. Polym. Sci.*, 2015, **132**, 41719–41738.
13 S. C. Ligon, R. Liska, J. Stampfl, M. Gurr and R. Mülhaupt, *Chem. Rev.*, 2017, **117**, 10212–10290.
14 X. Wang, M. Jiang, Z. Zhou, J. Gou and D. Hui, *Compos. B Eng.*, 2017, **110**, 442–458.
15 E. S. Bishop, S. Mostafa, M. Pakvasa, H. H. Luu, M. J. Lee, J. M. Wolf, G. A. Ameer, T.-C. He and R. R. Reid, *Genes Dis.*, 2017, **4**, 185–195.
16 A. D. Valino, J. R. C. Dizon, A. H. Espera, Q. Chen, J. Messman and R. C. Advincula, *Prog. Polym. Sci.*, 2019, **98**, 101162.
17 H. Wu, W. P. Fahy, S. Kim, H. Kim, N. Zhao, L. Pilato, A. Kafi, S. Bateman and J. H. Koo, *Prog. Mater. Sci.*, 2020, **111**, 100638.
18 M. S. Huda, L. T. Drzal, A. K. Mohanty and M. Misra, *Compos. Sci. Technol.*, 2008, **68**, 424–432.
19 J. H. Song, R. J. Murphy, R. Narayan and G. B. Davies, *Philos. Trans. R. Soc. Lond. B Biol. Sci.*, 2009, **364**, 2127–2139.
20 N. E. Zander, J. H. Park, Z. R. Boelter and M. A. Gillan, *ACS Omega*, 2019, **4**, 13879–13888.
21 R. Singh, R. Kumar and N. Ranjan, *J. Inst. Eng. (India): Ser. C*, 2018, **100**, 351–360.
22 A. H. Espera Jr, A. D. Valino, J. O. Palaganas, L. Souza, Q. Chen and R. C. Advincula, *Macromol. Mater. Eng.*, 2019, **304**, 1800718–1800726.
23 H. Zeidler, D. Klemm, F. Böttger-Hiller, S. Fritsch, M. J. Le Guen and S. Singamneni, *Procedia Manuf.*, 2018, **21**, 117–124.
24 P. Laurén, PhD, Doctoral Dissertation, Division of Pharmaceutical Biosciences, Faculty of Pharmacy, University of Helsinki, 2018.
25 Z. Sheikh, S. Najeeb, Z. Khurshid, V. Verma, H. Rashid and M. Glogauer, *Materials*, 2015, **8**, 5744–5794.
26 M. S. B. Reddy, D. Ponnamma, R. Choudhary and K. K. Sadasivuni, *Polymers*, 2021, **13**, 1105–1156.
27 C. M. B. Ho, S. H. Ng and Y.-J. Yoon, *Int. J. Precis. Eng. Manuf.*, 2015, **16**, 1035–1046.
28 B. C. Gross, J. L. Erkal, S. Y. Lockwood, C. Chen and D. M. Spence, *Anal. Chem.*, 2014, **86**, 3240–3253.
29 W. J. Sames, F. List, S. Pannala, R. R. Dehoff and S. S. Babu, *Int. Mater. Rev.*, 2016, **61**, 315–360.
30 Z. Chen, Z. Li, J. Li, C. Liu, C. Lao, Y. Fu, C. Liu, Y. Li, P. Wang and Y. He, *J. Eur. Ceram. Soc.*, 2019, **39**, 661–687.
31 T. D. Ngo, A. Kashani, G. Imbalzano, K. T. Nguyen and D. Hui, *Compos. B Eng.*, 2018, **143**, 172–196.
32 S. Liu, S. Qin, M. He, D. Zhou, Q. Qin and H. Wang, *Compos. B Eng.*, 2020, **199**, 108238.
33 A. Ghilan, A. P. Chiriac, L. E. Nita, A. G. Rusu, I. Neamtu and V. M. Chiriac, *J. Polym. Environ.*, 2020, **28**, 1345–1367.
34 C. Hu and Q.-H. Qin, *Curr. Opin. Solid State Mater. Sci.*, 2020, **24**, 100867.
35 I. Sibikin and J. Karger-Kocsis, *Advanced Industrial and Engineering Polymer Research*, 2018, **1**, 48–60.
36 American Society for Testing and Materials (ASTM), *ASTM F2792 – 12a: Standard Terminology for Additive Manufacturing Technologies*, ASTM International, 2012.
37 *3D printing market size worldwide from 2013 to 2021 (in billion U.S. dollars)*, http://www.statista.com/statistics/796237/worldwide-forecast-growth-3d-printing-market/, accessed September 17 2021.
38 E. Babaie and S. B. Bhaduri, *ACS Biomater. Sci. Eng.*, 2018, **4**, 1–39.
39 S. S. Alghamdi, S. John, N. R. Choudhury and N. K. Dutta, *Polymers*, 2021, **13**, 753–792.
40 J. Oliveira, V. Correia, H. Castro, P. Martins and S. Lanceros-Mendez, *Addit. Manuf.*, 2018, **21**, 269–283.
41 W. Grzesik, *Journal of Machine Engineering*, 2018, **18**, 5–24.
42 O. Abdulhameed, A. Al-Ahmari, W. Ameen and S. H. Mian, *Adv. Mech. Eng.*, 2019, **11**, 1–27.
43 A. Pasricha and R. Greeninger, *Fash. Tex.*, 2018, **5**, 30–48.
44 V. Petrovic, J. Vicente Haro Gonzalez, O. Jordá Ferrando, J. Delgado Gordillo, J. Ramón Blasco Puchades and L. Portolés Griñan, *Int. J. Prod. Res.*, 2011, **49**, 1061–1079.
45 B. Berman, *Bus. Horiz.*, 2012, **55**, 155–162.
46 B. Gross, S. Y. Lockwood and D. M. Spence, *Anal. Chem.*, 2016, **89**, 57–70.
47 S. S. Crump, *US Pat.*, 5121329, 1992.
48 G. Campana, R. J. Howlett, R. Setchi and B. Cimatti, *Sustainable design and manufacturing 2017: selected papers on sustainable design and manufacturing*, Springer International Publishing, 2017, p. 68.

49 American Society for Testing and Materials (ASTM), *ASTM52900-15: Standard Terminology for Additive Manufacturing—General Principles—Terminology*, ASTM International, 2015.
50 R. Jones, P. Haufe, E. Sells, P. Iravani, V. Olliver, C. Palmer and A. Bowyer, *Robotica*, 2011, **29**, 177–191.
51 M. B. Burn, A. Ta and G. R. Gogola, *J. Hand Surg.*, 2016, **41**, e103–e109.
52 A. Goyanes, J. Wang, A. Buanz, R. Martínez-Pacheco, R. Telford, S. Gaisford and A. W. Basit, *Mol. Pharm.*, 2015, **12**, 4077–4084.
53 N. Aliheidari, J. Christ and A. Ameli, in *Proceedings of Annual Technical Conference - ANTEC, Anaheim, CA*, 2017, Society of Plastics Engineers, Bethel, CT, pp. 89—93.
54 N. Herbert, D. Simpson, W. D. Spence and W. Ion, *J. Rehabil. Res. Dev.*, 2005, **42**, 141–146.
55 M. Nadgorny and A. Ameli, *ACS Appl. Mater. Interfaces*, 2018, **10**, 17489–17507.
56 C. Benwood, A. Anstey, J. Andrzejewski, M. Misra and A. K. Mohanty, *ACS Omega*, 2018, **3**, 4400–4411.
57 J. W. Stansbury and M. J. Idacavage, *Dent. Mater.*, 2016, **32**, 54–64.
58 S. Shaffer, K. Yang, J. Vargas, M. A. Di Prima and W. Voit, *Polymer*, 2014, **55**, 5969–5979.
59 Y. Yang, Y. Chen, Y. Wei and Y. Li, *Int. J. Adv. Manuf. Technol.*, 2016, **84**, 2079–2095.
60 C. B. Highley, C. B. Rodell and J. A. Burdick, *Adv. Mater.*, 2015, **27**, 5075–5079.
61 G. Postiglione, G. Natale, G. Griffini, M. Levi and S. Turri, *Compos. Appl. Sci. Manuf.*, 2015, **76**, 110–114.
62 M. Lay, N. L. N. Thajudin, Z. A. A. Hamid, A. Rusli, M. K. Abdullah and R. K. Shuib, *Compos. B Eng.*, 2019, **176**, 107341.
63 M. Picard, A. K. Mohanty and M. Misra, *RSC Adv.*, 2020, **10**, 36058–36089.
64 J. F. Christ, N. Aliheidari, A. Ameli and P. Pötschke, *Mater. Des.*, 2017, **131**, 394–401.
65 M. Nikzad, S. Masood and I. Sbarski, *Mater. Des.*, 2011, **32**, 3448–3456.
66 P. H. Daniels, *J. Vinyl Addit. Technol.*, 2007, **13**, 22–25.
67 K. Tappa and U. Jammalamadaka, *J. Funct. Biomater.*, 2018, **9**, 17.
68 B. Vayre, F. Vignat and F. Villeneuve, *Mech. Ind.*, 2012, **13**, 89–96.
69 T. Q. Tran, A. Chinnappan, J. K. Y. Lee, N. H. Loc, L. T. Tran, G. Wang, V. V. Kumar, W. A. D. M. Jayathilaka, D. Ji, M. Doddamani and S. Ramakrishna, *Metals*, 2019, **9**, 756.
70 S. Liu and Y. C. Shin, *Mater. Des.*, 2019, **164**, 107552.
71 W. J. Sames, K. A. Unocic, R. R. Dehoff, T. Lolla and S. S. Babu, *J. Mater. Res.*, 2014, **29**, 1920–1930.
72 B. Wysocki, P. Maj, R. Sitek, J. Buhagiar, K. J. Kurzydłowski and W. Świeszkowski, *Appl. Sci.*, 2017, **7**, 657–677.
73 E. Martinez, L. E. Murr, J. Hernandez, X. Pan, K. Amato, P. Frigola, C. Terrazas, S. Gaytan, E. Rodriguez and F. Medina, *Metallogr. Microstruct. Anal.*, 2013, **2**, 183–189.
74 J. P. Kruth, P. Mercelis, J. Van Vaerenbergh, L. Froyen and M. Rombouts, *Rapid Prototyp. J.*, 2005, **11**, 26–36.
75 E. O. Olakanmi, R. Cochrane and K. Dalgarno, *Prog. Mater. Sci.*, 2015, **74**, 401–477.
76 S. F. S. Shirazi, S. Gharehkhani, M. Mehrali, H. Yarmand, H. S. C. Metselaar, N. A. Kadri and N. A. A. Osman, *Sci. Technol. Adv. Mater.*, 2015, **16**, 033502.
77 F. Fina, A. Goyanes, S. Gaisford and A. W. Basit, *Int. J. Pharm.*, 2017, **529**, 285–293.
78 A. Jansson and L. Pejryd, *Addit. Manuf.*, 2016, **9**, 7–13.
79 K. O. Ogila, M. Shao, W. Yang and J. Tan, *Express Polym. Lett.*, 2017, **11**, 778–798.
80 E. O. Cisneros-López, A. A. Pérez-Fonseca, Y. González-García, D. E. Ramírez-Arreola, R. González-Núñez, D. Rodrigue and J. R. Robledo-Ortíz, *Adv. Polym. Technol.*, 2018, **37**, 2528–2540.
81 J. Li, C. Wu, P. K. Chu and M. Gelinsky, *Mater. Sci. Eng. R Rep.*, 2020, **140**, 100543.
82 S. Mubarak, D. Dhamodharan, M. B. Kale, N. Divakaran, T. Senthil, S. P, L. Wu and J. Wang, *Nanomaterials*, 2020, **10**, 217–241.
83 G. Burke, D. M. Devine and I. Major, *Polymers*, 2020, **12**, 2015–2038.
84 Z. Wang, R. Abdulla, B. Parker, R. Samanipour, S. Ghosh and K. Kim, *Biofabrication*, 2015, **7**, 045009.
85 E. M. Costabeber, Stereolithography Machine with Improved Optical Unit, *US Pat.*US9969129B2, 2018.
86 I. Donderwinkel, J. C. M. van Hest and N. R. Cameron, *Polym. Chem.*, 2017, **8**, 4451–4471.
87 S. Nayar, S. Bhuminathan and W. M. Bhat, *J. Pharm. BioAllied Sci.*, 2015, **7**, S216–S219.
88 Z. Weng, Y. Zhou, W. Lin, T. Senthil and L. Wu, *Compos. Appl. Sci. Manuf.*, 2016, **88**, 234–242.
89 A. Ronca and L. Ambrosio, *Advanced Biomaterials and Devices in Medicine*, 2017, **4**, 1–15.
90 K.-H. Choi, D. B. Ahn and S.-Y. Lee, *ACS Energy Lett.*, 2017, **3**, 220–236.
91 D. Tian, Y. Song and L. Jiang, *Chem. Soc. Rev.*, 2013, **42**, 5184–5209.
92 B. Y. Ahn and J. A. Lewis, *Mater. Chem. Phys.*, 2014, **148**, 686–691.
93 R. E. Sousa, C. M. Costa and S. Lanceros-Méndez, *ChemSusChem*, 2015, **8**, 3539–3555.
94 B. Derby, *Annu. Rev. Mater. Res.*, 2010, **40**, 395–414.
95 W. Xu, X. Wang, N. Sandler, S. Willför and C. Xu, *ACS Sustain. Chem. Eng.*, 2018, **6**, 5663–5680.
96 F. P. Melchels, M. A. Domingos, T. J. Klein, J. Malda, P. J. Bartolo and D. W. Hutmacher, *Prog. Polym. Sci.*, 2012, **37**, 1079–1104.
97 B. Utela, D. Storti, R. Anderson and M. Ganter, *J. Manuf. Process.*, 2008, **10**, 96–104.
98 C. J. Ferris, K. G. Gilmore and G. G. Wallace, *Appl. Microbiol. Biotechnol.*, 2013, **97**, 4243–4258.
99 S. V. Murphy and A. Atala, *Nat. Biotechnol.*, 2014, **32**, 773.
100 X. Cui, K. Breitenkamp, M. Finn, M. Lotz and D. D. D'Lima, *Tissue Eng.*, 2012, **18**, 1304–1312.
101 D. Pech, M. Brunet, P.-L. Taberna, P. Simon, N. Fabre, F. Mesnilgrente, V. Conédéra and H. Durou, *J. Power Sources*, 2010, **195**, 1266–1269.

102 M. Guvendiren, J. Molde, R. M. Soares and J. Kohn, *ACS Biomater. Sci. Eng.*, 2016, **2**, 1679–1693.
103 E. L. Kyser and S. B. Sears, *US Pat.*, 3946398, 1976.
104 R. Bhardwaj, X. Fang, P. Somasundaran and D. Attinger, *Langmuir*, 2010, **26**, 7833–7842.
105 H. Yoo and C. Kim, *Colloids Surf., A*, 2015, **468**, 234–245.
106 H. Gothait, *US Pat.*, US6259962B1, 2001.
107 A. Van Wijk and I. Van Wijk, *3D printing with biomaterials: Towards a sustainable and circular economy*, IOS Press, Amsterdam, 2015, DOI: 10.3233/978-1-61499-486-2-i.
108 N. Bhattacharjee, A. Urrios, S. Kang and A. Folch, *Lab Chip*, 2016, **16**, 1720–1742.
109 A. Waldbaur, H. Rapp, K. Länge and B. E. Rapp, *Anal. Methods*, 2011, **3**, 2681–2716.
110 I. Sander, T. Liepert, E. Doney, W. Leevy and D. Liepert, *J. Funct. Biomater.*, 2017, **8**, 13.
111 N. N. Zein, I. A. Hanouneh, P. D. Bishop, M. Samaan, B. Eghtesad, C. Quintini, C. Miller, L. Yerian and R. Klatte, *Liver Transplant.*, 2013, **19**, 1304–1310.
112 J. I. Gear, C. Cummings, A. J. Craig, A. Divoli, C. D. Long, M. Tapner and G. D. Flux, *Eur. J. Nucl. Med. Mol. Imaging*, 2016, **3**, 17–33.
113 A. Aimar, A. Palermo and B. Innocenti, *J. Healthc. Eng.*, 2019, **2019**, 5340616–5340627.
114 S. Marconi, L. Pugliese, M. Botti, A. Peri, E. Cavazzi, S. Latteri, F. Auricchio and A. Pietrabissa, *Surg. Endosc.*, 2017, **31**, 4102–4110.
115 Y. He, Y. Wu, J.-z. Fu, Q. Gao and J.-j. Qiu, *Electroanalysis*, 2016, **28**, 1658–1678.
116 K. M. Meess, R. L. Izzo, M. L. Dryjski, R. E. Curl, L. M. Harris, M. Springer, A. H. Siddiqui, S. Rudin and C. N. Ionita, *Proc. SPIE-Int. Soc. Opt. Eng.*, 2017, **10138**, 101380P–101394P.
117 M. Feygin and S. S. Pak, *US Pat.*5876550, 1999.
118 D. V. Mahindru, M. S. R. Priyanka and G. L. Tewari, *Global J. Comput. Sci. Technol.*, 2013, **13**, 1–13.
119 F. Rengier, A. Mehndiratta, H. Von Tengg-Kobligk, C. M. Zechmann, R. Unterhinninghofen, H.-U. Kauczor and F. L. Giesel, *Int. J. Comput. Assist. Radiol. Surg.*, 2010, **5**, 335–341.
120 J. Park, M. J. Tari and H. T. Hahn, *Rapid Prototyp. J.*, 2000, **6**, 36–50.
121 B. Mueller and D. Kochan, *Comput. Ind.*, 1999, **39**, 47–53.
122 K. V. Wong and A. Hernandez, *International Scholarly Research Network*, 2012, **2012**, 1–11.
123 J. Saroia, Y. Wang, Q. Wei, M. Lei, X. Li, Y. Guo and K. Zhang, *Int. J. Adv. Manuf. Technol.*, 2019, **106**, 1695–1721.
124 A. Ambrosi and M. Pumera, *Chem. Soc. Rev.*, 2016, **45**, 2740–2755.
125 X. Y. Ali Kazemian, E. Cochran and B. Khoshnevis, *Constr. Build. Mater.*, 2017, **145**, 639–647.
126 M. E. Prendergast and J. A. Burdick, *Adv. Mater.*, 2019, **32**, 1902516.
127 B. Gross, S. Y. Lockwood and D. M. Spence, *Anal. Chem.*, 2017, **89**, 57–70.
128 Y. Li, Z. Feng, L. Hao, L. Huang, C. Xin, Y. Wang, E. Bilotti, K. Essa, H. Zhang, Z. Li, F. Yan and T. Peijs, *Adv. Mater. Technol.*, 2020, **5**, 1900981–1901013.
129 D. Appleyard, *Met. Powder Rep.*, 2015, **70**, 285–289.
130 M. Invernizzi, G. Natale, M. Levi, S. Turri and G. Griffini, *Materials*, 2016, **9**, 583–595.
131 P. Geng, J. Zhao, Z. Gao, W. Wu, W. Ye, G. Li and H. Qu, *3D Print. Addit. Manuf.*, 2021, **8**, 33–41.
132 S. Zhou, Q. Zhang, C. Wu and J. Huang, *Mater. Des.*, 2013, **44**, 493–499.
133 J. Gu, J. Du, J. Dang, W. Geng, S. Hu and Q. Zhang, *RSC Adv.*, 2014, **4**, 22101–22105.
134 A. El Magri, K. El Mabrouk, S. Vaudreuil and M. Ebn Touhami, *J. Appl. Polym. Sci.*, 2020, **138**, 49625.
135 V. Kishore, X. Chen, A. A. Hassen, J. Lindahl, V. Kunc and C. Duty, *Addit. Manuf.*, 2020, **35**, 101387.
136 E. Macdonald, R. Salas, D. Espalin, M. Perez, E. Aguilera, D. Muse and R. B. Wicker, *IEEE Access*, 2014, **2**, 234–242.
137 J. H. Kim, S. Lee, M. Wajahat, H. Jeong, W. S. Chang, H. J. Jeong, J. R. Yang, J. T. Kim and S. K. Seol, *ACS Nano*, 2016, **10**, 8879–8887.
138 K. Huang, S. Dong, J. Yang, J. Yan, Y. Xue, X. You, J. Hu, L. Gao, X. Zhang and Y. Ding, *Carbon*, 2019, **143**, 63–72.
139 S. J. Leigh, R. J. Bradley, C. P. Purssell, D. R. Billson and D. A. Hutchins, *PLoS One*, 2012, **7**, e49365.
140 R. D. Farahani, H. Dalir, V. Le Borgne, L. A. Gautier, M. A. El Khakani, M. Levesque and D. Therriault, *Nanotechnology*, 2012, **23**, 085502.
141 A. Joe Lopes, E. MacDonald and R. B. Wicker, *Rapid Prototyp. J.*, 2012, **18**, 129–143.
142 X. Jin, Y. Deng, W.-r. Cai, W.-m. Lau, D. Hui, H. Yan, J. Mei and Y. Liu, *Compos. B Eng.*, 2016, **105**, 111–115.
143 I. Cooperstein, M. Layani and S. Magdassi, *J. Mater. Chem. C*, 2015, **3**, 2040–2044.
144 M. Saari, B. Cox, E. Richer, P. S. Krueger and A. L. Cohen, *3D Print. Addit. Manuf.*, 2015, **2**, 32–39.
145 H. N. Chia and B. M. Wu, *J. Biol. Eng.*, 2015, **9**, 1–14.
146 M. Mehrali, S. Bagherifard, M. Akbari, A. Thakur, B. Mirani, M. Mehrali, M. Hasany, G. Orive, P. Das and J. Emneus, *Adv. Sci.*, 2018, **5**, 1700931.
147 H. Zhao, F. Yang, J. Fu, Q. Gao, A. Liu, M. Sun and Y. He, *ACS Biomater. Sci. Eng.*, 2017, **3**, 3083–3097.
148 J. Li, B. Esteban-Fernandez de Avila, W. Gao, L. Zhang and J. Wang, *Sci. Rob.*, 2017, **2**, 6431–6451.
149 M. H. Michalski and J. S. Ross, *Jama*, 2014, **312**, 2213–2214.
150 H. Scheidbach, C. Tamme, A. Tannapfel, H. Lippert and F. Köckerling, *Surgical Endoscopy and Other Interventional Techniques*, 2004, vol. 18, pp. 211–220.
151 P. Lichte, H. Pape, T. Pufe, P. Kobbe and H. Fischer, *Injury*, 2011, **42**, 569–573.
152 N. E. Fedorovich, J. Alblas, J. R. de Wijn, W. E. Hennink, A. J. Verbout and W. J. Dhert, *Tissue Eng.*, 2007, **13**, 1905–1925.
153 J. Zuniga, D. Katsavelis, J. Peck, J. Stollberg, M. Petrykowski, A. Carson and C. Fernandez, *BMC Res. Notes*, 2015, **8**, 1–9.
154 J. Ten Kate, G. Smit and P. Breedveld, *Disabil. Rehabilitation Assist. Technol.*, 2017, **12**, 300–314.
155 S. M. Fuller, D. R. Butz, C. B. Vevang and M. V. Makhlouf, *J. Hand Surg.*, 2014, **39**, 1840–1845.

156 S. Sankar, J. Paulose and N. Thomas, *ASME 2017 International Mechanical Engineering Congress and Exposition*, 2017, V014T007A008.
157 J. Giannatsis and V. Dedoussis, *Int. J. Adv. Manuf. Technol.*, 2009, **40**, 116–127.
158 T. Xu, J. Olson, W. Zhao, A. Atala, J.-M. Zhu and J. J. Yoo, *J. Manuf. Sci. Eng.*, 2008, **130**, 021013.
159 R. K. Jackler, W. M. Luxfor and W. F. House, *Laryngoscope*, 1987, **97**, 2–14.
160 P. I. Branemark, B. Kasemo and J. Lausmaa, *US Pat.*4712681, 1987.
161 C. W. Scarantino, H. T. Nagle, L. C. Hall, J. Mueller and C.-S. Kim, *US Pat.*US6402689B1, 2002.
162 S. Bose, S. Vahabzadeh and A. Bandyopadhyay, *Mater. Today*, 2013, **16**, 496–504.
163 S. J. Hollister, *Nat. Mater.*, 2005, **4**, 518.
164 D. Puppi, F. Chiellini, A. Piras and E. Chiellini, *Prog. Polym. Sci.*, 2010, **35**, 403–440.
165 R. A. Perez and G. Mestres, *Mater. Sci. Eng., C*, 2016, **61**, 922–939.
166 N. Vidakis, M. Petousis, E. Velidakis, N. Mountakis, P. E. Fischer-Griffiths, S. A. Grammatikos and L. Tzounis, *Adv. Compos. Mater.*, 2021, 1–22.
167 M. Jin, C. Neuber and H.-W. Schmidt, *Addit. Manuf.*, 2020, **33**, 101101–101114.
168 V. Mazzanti, L. Malagutti and F. Mollica, *Polymers*, 2019, **11**, 1094–1116.
169 X. Peng, H. He, Y. Jia, H. Liu, Y. Geng, B. Huang and C. Luo, *J. Mater. Sci.*, 2019, **54**, 9235–9246.
170 A. K. Singh, B. Saltonstall, B. Patil, N. Hoffmann, M. Doddamani and N. Gupta, *JOM*, 2018, **70**, 310–314.
171 J. T. Belter and A. M. Dollar, *PLoS One*, 2015, **10**, e0122915.
172 H. L. Tekinalp, V. Kunc, G. M. Velez-Garcia, C. E. Duty, L. J. Love, A. K. Naskar, C. A. Blue and S. Ozcan, *Compos. Sci. Technol.*, 2014, **105**, 144–150.
173 F. L. Weihong Zhonga, Z. Zhang, L. Song and Z. Li, *Mater. Sci. Eng. A*, 2001, **301**, 125–130.
174 B. Huang, H. He, S. Meng and Y. Jia, *Polym. Int.*, 2019, **68**, 1351–1360.
175 S. Meng, H. He, Y. Jia, P. Yu, B. Huang and J. Chen, *J. Appl. Polym. Sci.*, 2017, **134**, 44470–44479.
176 F. V. Der Klift, Y. Koga, A. Todoroki, M. Ueda, Y. Hirano and R. Matsuzaki, *Open J. Compos. Mater.*, 2016, **06**, 18–27.
177 A. M. Abdullah, T. Rahim, W. Hamad, D. Mohamad, H. M. Akil and Z. A. Rajion, *Dent. Mater.*, 2018, **34**, e309–e316.
178 M. E. Spreeman, H. A. Stretz and M. D. Dadmun, *Addit. Manuf.*, 2019, **27**, 267–277.
179 E. V. Diederichs, M. C. Picard, B. P. Chang, M. Misra, D. F. Mielewski and A. K. Mohanty, *ACS Omega*, 2019, **4**, 20297–20307.
180 J. O. Palaganas, N. B. Palaganas, L. J. I. Ramos and C. P. C. David, *ACS Appl. Mater. Interfaces*, 2019, **11**, 46034–46043.
181 L. Chaunier, S. Guessasma, S. Belhabib, G. Della Valle, D. Lourdin and E. Leroy, *Addit. Manuf.*, 2018, **21**, 220–233.
182 V. Gaikwad, A. Ghose, S. Cholake, A. Rawal, M. Iwato and V. Sahajwalla, *ACS Sustainable Chem. Eng.*, 2018, **6**, 14432–14440.
183 R. D. Chen, C. F. Huang and S. H. Hsu, *Carbohydr. Polym.*, 2019, **212**, 75–88.
184 F. Ibrahim, D. Mohan, M. S. Sajab, S. B. Bakarudin and H. Kaco, *Polymers*, 2019, **11**, 1544–1556.
185 N. Ayrilmis, M. Kariz, J. H. Kwon and M. Kitek Kuzman, *Int. J. Adv. Manuf. Technol.*, 2019, **102**, 2195–2200.
186 D. Filgueira, S. Holmen, J. K. Melbø, D. Moldes, A. T. Echtermeyer and G. Chinga-Carrasco, *ACS Sustainable Chem. Eng.*, 2017, **5**, 9338–9346.
187 H. Liu, H. He, X. Peng, B. Huang and J. Li, *Polym. Adv. Technol.*, 2019, **30**, 910–922.
188 E. Gkartzou, E. P. Koumoulos and C. A. Charitidis, *Manuf. Rev.*, 2017, **4**, 1–14.
189 J. Luo, H. Wang, D. Zuo, A. Ji and Y. Liu, *Micromachines*, 2018, **9**, 635–648.
190 D. Zhang, B. Chi, B. Li, Z. Gao, Y. Du, J. Guo and J. Wei, *Synth. Met.*, 2016, **217**, 79–86.
191 Q. Chen, J. D. Mangadlao, J. Wallat, A. De Leon, J. K. Pokorski and R. C. Advincula, *ACS Appl. Mater. Interfaces*, 2017, **9**, 4015–4023.
192 R. Matsuzaki, M. Ueda, M. Namiki, T. K. Jeong, H. Asahara, K. Horiguchi, T. Nakamura, A. Todoroki and Y. Hirano, *Sci. Rep.*, 2016, **6**, 23058.
193 Y. Guo, C.-C. Chang, G. Halada, M. A. Cuiffo, Y. Xue, X. Zuo, S. Pack, L. Zhang, S. He, E. Weil and M. H. Rafailovich, *Polym. Degrad. Stab.*, 2017, **137**, 205–215.
194 D. Rasselet, A. S. Caro-Bretelle, A. Taguet and J. M. Lopez-Cuesta, *Materials*, 2019, **12**, 485–503.
195 H. Long, Z. Wu, Q. Dong, Y. Shen, W. Zhou, Y. Luo, C. Zhang and X. Dong, *Polym. Eng. Sci.*, 2019, **59**, E247–E260.
196 N. Vidakis, M. Petousis, L. Tzounis, A. Maniadi, E. Velidakis, N. Mountakis, D. Papageorgiou, M. Liebscher and V. Mechtcherine, *Sustainability*, 2020, **13**, 159.
197 H. A. Little, N. G. Tanikella, M. J. Reich, M. J. Fiedler, S. L. Snabes and J. M. Pearce, *Materials*, 2020, **13**, 4273–4295.
198 K. Mikula, D. Skrzypczak, G. Izydorczyk, J. Warchol, K. Moustakas, K. Chojnacka and A. Witek-Krowiak, *Environ. Sci. Pollut. Res.*, 2021, **28**, 12321–12333.
199 M. J. Reich, A. L. Woern, N. G. Tanikella and J. M. Pearce, *Materials*, 2019, **12**, 1642–1660.
200 D. Mohan, Z. K. Teong, A. N. Bakir, M. S. Sajab and H. Kaco, *Polymers*, 2020, **12**, 1876–1907.
201 A. Folino, A. Karageorgiou, P. S. Calabrò and D. Komilis, *Sustainability*, 2020, **12**, 6030.
202 J. V. Rutkowski and B. C. Levin, *Fire Mater.*, 1986, **10**, 93–105.
203 S. Wang, Y. Hu, L. Song, Z. Wang, Z. Chen and W. Fan, *Polym. Degrad. Stab.*, 2002, **77**, 423–426.
204 N. G. Morales, T. J. Fleck and J. F. Rhoads, *Addit. Manuf.*, 2018, **24**, 243–248.

205 G. Li, J. Zhao, J. Jiang, H. Jiang, W. Wu and M. Tang, *Int. J. Adv. Manuf. Technol.*, 2018, **96**, 2747–2755.
206 A. Tofangchi, P. Han, J. Izquierdo, A. Iyengar and K. Hsu, *Polymers*, 2019, **11**, 315.
207 Y. Y. Aw, C. K. Yeoh, M. A. Idris, P. L. Teh, K. A. Hamzah and S. A. Sazali, *Materials*, 2018, **11**, 466.
208 C. R. Rocha, A. R. T. Perez, D. A. Roberson, C. M. Shemelya, E. MacDonald and R. B. Wicker, *J. Mater. Res.*, 2014, **29**, 1859–1866.
209 Z. Weng, J. Wang, T. Senthil and L. Wu, *Mater. Des.*, 2016, **102**, 276–283.
210 M. Alexandre and P. Dubois, *Mater. Sci. Eng. R Rep.*, 2000, **28**, 1–63.
211 T. P. Pasanen, G. von Gastrow, I. T. S. Heikkinen, V. Vähänissi, H. Savin and J. M. Pearce, *Mater. Sci. Semicond. Process.*, 2019, **89**, 59–67.
212 R. M. Cardoso, D. M. H. Mendonça, W. P. Silva, M. N. T. Silva, E. Nossol, R. A. B. da Silva, E. M. Richter and R. A. A. Muñoz, *Anal. Chim. Acta*, 2018, **1033**, 49–57.
213 R. S. Arulmozhi, M. Vaidya, M. G. Poojalakshmi, D. Ashok Kumar and K. Anuraag, *Biomed. Eng. - Appl. Basis Commun.*, 2018, **30**, 1850032–1850041.
214 R. Singh, H. Singh, I. Farina, F. Colangelo and F. Fraternali, *Compos. B Eng.*, 2019, **156**, 259–265.
215 M. Bible, M. Sefa, J. A. Fedchak, J. Scherschligt, B. Natarajan, Z. Ahmed and M. R. Hartings, *3D Print. Addit. Manuf.*, 2018, **5**, 63–72.
216 E. Provaggi, C. Capelli, B. Rahmani, G. Burriesci and D. M. Kalaskar, *Mater. Des.*, 2019, **163**, 107540.
217 M. Dawoud, I. Taha and S. J. Ebeid, *J. Manuf. Process.*, 2018, **35**, 337–342.
218 R. I. Haque, O. Chandran, S. Lani and D. Briand, *Nano Energy*, 2018, **52**, 54–62.
219 B. Khatri, K. Lappe, M. Habedank, T. Mueller, C. Megnin and T. Hanemann, *Polymers*, 2018, **10**, 666.
220 M. Kumar, R. Ramakrishnan and A. Omarbekova, *J. Mech. Sci. Technol.*, 2019, **33**, 5219–5226.
221 S. Chen, J. Lu and J. Feng, *Ind. Eng. Chem. Res.*, 2018, **57**, 3923–3931.
222 J. Ren and J. Y. Yin, *Materials*, 2018, **11**, 1249.
223 W. Zhang, C. Cotton, J. Sun, D. Heider, B. Gu, B. Sun and T.-W. Chou, *Compos. B Eng.*, 2018, **137**, 51–59.
224 D. Young, N. Wetmore and M. Czabaj, *Addit. Manuf.*, 2018, **22**, 508–515.
225 K. Akato, C. D. Tran, J. Chen and A. K. Naskar, *ACS Sustainable Chem. Eng.*, 2015, **3**, 3070–3076.
226 M. C. Kreider, M. Sefa, J. A. Fedchak, J. Scherschligt, M. Bible, B. Natarajan, N. N. Klimov, A. E. Miller, Z. Ahmed and M. R. Hartings, *Polym. Adv. Technol.*, 2018, **29**, 867–873.
227 A. Woern, D. Byard, R. Oakley, M. Fiedler, S. Snabes and J. Pearce, *Materials*, 2018, **11**, 1413.
228 D. Lee, Y. Lee, K. Lee, Y. Ko and N. Kim, *J. Manuf. Sci. Eng.*, 2019, **141**, 021007.
229 G. Natta and P. Corradini, *Il Nuovo Cimento*, 1960, **15**, 40–51.
230 H. A. Maddah, *Am. J. Polym. Sci.*, 2016, **6**, 1–11.
231 A. Graziano, C. Garcia, S. Jaffer, J. Tjong and M. Sain, *Compos. Sci. Technol.*, 2020, **188**, 107958–107967.
232 W. S. Tan, C. K. Chua, T. H. Chong, A. G. Fane and A. Jia, *Virtual Phys. Prototyp.*, 2016, **11**, 151–158.
233 A. Das, A. E. C. Marnot, J. J. Fallon, S. M. Martin, E. G. Joseph and M. J. Bortner, *ACS Appl. Polym. Mater.*, 2019, **2**, 911–921.
234 P. J. Kitson, S. Glatzel, W. Chen, C. G. Lin, Y. F. Song and L. Cronin, *Nat. Protoc.*, 2016, **11**, 920–936.
235 M. Spoerk, C. Savandaiah, F. Arbeiter, G. Traxler, L. Cardon, C. Holzer and J. Sapkota, *Compos. Appl. Sci. Manuf.*, 2018, **113**, 95–104.
236 B. Kaynak, M. Spoerk, A. Shirole, W. Ziegler and J. Sapkota, *Macromol. Mater. Eng.*, 2018, **303**, 1800037.
237 M. Spoerk, F. Arbeiter, I. Raguž, G. Weingrill, T. Fischinger, G. Traxler, S. Schuschnigg, L. Cardon and C. Holzer, *Macromol. Mater. Eng.*, 2018, **303**, 1800179.
238 P. Parandoush, L. Tucker, C. Zhou and D. Lin, *Mater. Des.*, 2017, **131**, 186–195.
239 N. E. Zander, M. Gillan, Z. Burckhard and F. Gardea, *Addit. Manuf.*, 2019, **25**, 122–130.
240 S. S. Banerjee, S. Burbine, N. Kodihalli Shivaprakash and J. Mead, *Polymers*, 2019, **11**, 347.
241 A. Agkathidis, Y. Berdos and A. Brown, *Int. J. Architect. Comput.*, 2019, **17**, 74–87.
242 P. Sauerbier, J. Anderson and D. J. Gardner, *Coatings*, 2018, **8**, 457.
243 C. J. Yoo, B. S. Shin, B. S. Kang, C. Y. Gwak, C. Park, Y. W. Ma and S. M. Hong, *Procedia Eng.*, 2017, **184**, 10–15.
244 S. V. Panin, L. A. Kornienko, V. O. Alexenko, D. G. Buslovich and Y. V. Dontsov, *AIP Conf. Proc.*, 2017, **1915**, 020005.
245 P. N. Khanam and M. A. A. AlMaadeed, *Adv. Manuf.: Polym. Compos. Sci.*, 2015, **1**, 63–79.
246 S. Hou, S. Qi, D. A. Hutt, J. R. Tyrer, M. Mu and Z. Zhou, *J. Mater. Process. Technol.*, 2018, **254**, 310–324.
247 S. Chong, G.-T. Pan, M. Khalid, T. C. K. Yang, S.-T. Hung and C.-M. Huang, *J. Polym. Environ.*, 2016, **25**, 136–145.
248 S. Wojtyla, P. Klama and T. Baran, *J. Occup. Environ. Hyg.*, 2017, **14**, D80–D85.
249 L. N. Ji, *Appl. Mech. Mater.*, 2013, **312**, 406–410.
250 A. L. Woern, D. J. Byard, R. B. Oakley, M. J. Fiedler, S. L. Snabes and J. M. Pearce, *Materials*, 2018, **11**, 1413–1432.
251 N. E. Zander, M. Gillan and R. H. Lambeth, *Addit. Manuf.*, 2018, **21**, 174–182.
252 J. Gu, M. Wensing, E. Uhde and T. Salthammer, *Environ. Int.*, 2019, **123**, 476–485.
253 M. Idrees, S. Jeelani and V. Rangari, *ACS Sustainable Chem. Eng.*, 2018, **6**, 13940–13948.
254 Z. Bashir, H. Gu and L. Yang, *Polym. Eng. Sci.*, 2018, **58**, 1888–1900.
255 M. Parvin and J. G. Williams, *J. Mater. Sci.*, 1975, **10**, 1883–1888.
256 C. M. Shemelya, A. Rivera, A. T. Perez, C. Rocha, M. Liang, X. Yu, C. Kief, D. Alexander, J. Stegeman, H. Xin, R. B. Wicker, E. MacDonald and D. A. Roberson, *J. Electron. Mater.*, 2015, **44**, 2598–2607.

257 A. S. Alaboodi and S. Sivasankaran, *J. Manuf. Process.*, 2018, **35**, 479–491.
258 F. Blaya, P. S. Pedro, J. L. Silva, R. D'Amato, E. S. Heras and J. A. Juanes, *J. Med. Syst.*, 2018, **42**, 54.
259 I. Blanco, G. Cicala, G. Ognibene, M. Rapisarda and A. Recca, *Polym. Degrad. Stab.*, 2018, **154**, 234–238.
260 F. Peng, Z. Zhao, X. Xia, M. Cakmak and B. D. Vogt, *ACS Appl. Mater. Interfaces*, 2018, **10**, 16087–16094.
261 Z. Liu, J. Zhan, M. Fard and J. L. Davy, *Mater. Lett.*, 2016, **181**, 296–299.
262 S. Rohde, J. Cantrell, A. Jerez, C. Kroese, D. Damiani, R. Gurnani, L. DiSandro, J. Anton, A. Young, D. Steinbach and P. Ifju, *Exp. Mech.*, 2018, **58**, 871–884.
263 Y. Gao, Y. Li, X. Hu, W. Wu, Z. Wang, R. Wang and L. Zhang, *Polymers*, 2017, **9**, 694–709.
264 A. Woern and J. Pearce, *Technologies*, 2017, **5**, 71.
265 J. M. G. Farstad, Ø. Netland and T. Welo, *Procedia CIRP*, 2017, **60**, 247–252.
266 J. Wang, C. McMullen, P. Yao, N. Jiao, M. Kim, J.-W. Kim, L. Liu and S. Tung, *Microfluid. Nanofluid.*, 2017, **21**, 105–118.
267 G. Ellson, X. Carrier, J. Walton, S. F. Mahmood, K. Yang, J. Salazar and W. E. Voit, *J. Appl. Polym. Sci.*, 2018, **135**, 45574.
268 H. Bi, M. Xu, G. Ye, R. Guo, L. Cai and Z. Ren, *Polymers*, 2018, **10**, 1234–1246.
269 T. N. A. T. Rahim, A. M. Abdullah, H. Md Akil, D. Mohamad and Z. A. Rajion, *Express Polym. Lett.*, 2017, **11**, 963–982.
270 D. Zhu, Y. Ren, G. Liao, S. Jiang, F. Liu, J. Guo and G. Xu, *J. Appl. Polym. Sci.*, 2017, **134**, 45332.
271 A. C. de Leon, B. J. Rodier, C. Bajamundi, A. Espera, P. Wei, J. G. Kwon, J. Williams, F. Ilijasic, R. C. Advincula and E. Pentzer, *ACS Appl. Energy Mater.*, 2018, **1**, 1726–1733.
272 S. Balzereit, F. Proes, V. Altstädt and C. Emmelmann, *Addit. Manuf.*, 2018, **23**, 347–354.
273 G. Chabaud, M. Castro, C. Denoual and A. Le Duigou, *Addit. Manuf.*, 2019, **26**, 94–105.
274 T. Brugo, R. Palazzetti, S. Ciric-Kostic, X. T. Yan, G. Minak and A. Zucchelli, *Polym. Test.*, 2016, **50**, 301–308.
275 F. Neugebauer, V. Ploshikhin, J. Ambrosy and G. Witt, *J. Therm. Anal. Calorim.*, 2016, **124**, 925–933.
276 N. Lammens, M. Kersemans, I. De Baere and W. Van Paepegem, *Polym. Test.*, 2017, **57**, 149–155.
277 H. J. O'Connor and D. P. Dowling, *Polym. Compos.*, 2019, **40**, 4329–4339.
278 D. Garlotta, *J. Polym. Environ.*, 2001, **9**, 63–84.
279 A. Komesu, J. A. Rocha de Oliveira, L. H. d. S. Martins, M. R. W. Maciel and R. M. Filho, *BioResources*, 2017, **12**, 4364–4383.
280 C.-S. Wu and C.-H. Tsou, *J. Polym. Res.*, 2019, **26**, 44–53.
281 S. M. Lebedev, O. S. Gefle, E. T. Amitov, D. V. Zhuravlev, D. Y. Berchuk and E. A. Mikutskiy, *Int. J. Adv. Manuf. Technol.*, 2018, **97**, 511–518.
282 Y. Dong, J. Milentis and A. Pramanik, *Adv. Manuf.*, 2018, **6**, 71–82.
283 A. Regazzi, M. F. Pucci, L. Dumazert, B. Gallard, S. Buonomo, R. Ravel and J.-M. Lopez-Cuesta, *Polym. Degrad. Stab.*, 2019, **163**, 143–150.
284 Q. Ou-Yang, B. Guo and J. Xu, *ACS Omega*, 2018, **3**, 14309–14317.
285 F. Daver, K. P. M. Lee, M. Brandt and R. Shanks, *Compos. Sci. Technol.*, 2018, **168**, 230–237.
286 Z. Hou, X. Tian, J. Zhang, L. Zhe, Z. Zheng, D. Li, A. V. Malakhov and A. N. Polilov, *Compos. Struct.*, 2020, **237**, 111945.
287 X. Zhao, H. Tekinalp, X. Meng, D. Ker, B. Benson, Y. Pu, A. J. Ragauskas, Y. Wang, K. Li, E. Webb, D. J. Gardner, J. Anderson and S. Ozcan, *ACS Appl. Bio Mater.*, 2019, **2**, 4557–4570.
288 E. G. Ertane, A. Dorner-Reisel, O. Baran, T. Welzel, V. Matner and S. Svoboda, *Adv. Tribol.*, 2018, **2018**, 1–11.
289 X. He, Z. Liu, W. Niu, L. Yang, T. Zhou, D. Qin, Z. Niu and Q. Yuan, *Energy*, 2018, **143**, 746–756.
290 X. Gao, D. Zhang, S. Qi, X. Wen and Y. Su, *J. Appl. Polym. Sci.*, 2019, **136**, 47824.
291 C. Kalinke, V. Wosgrau, P. R. Oliveira, G. A. Oliveira, G. Martins, A. S. Mangrich, M. F. Bergamini and L. H. Marcolino-Junior, *Talanta*, 2019, **200**, 518–525.
292 M. I. Mohammed, D. Wilson, E. Gomez-Kervin, B. Tang and J. Wang, *ACS Sustainable Chem. Eng.*, 2019, **7**, 13955–13969.
293 J. Šafka, M. Ackermann, J. Bobek, M. Seidl, J. Habr and L. Behálek, *Mater. Sci. Forum*, 2016, **862**, 174–181.
294 N. A. Nguyen, C. C. Bowland and A. K. Naskar, *Appl. Mater. Today*, 2018, **12**, 138–152.
295 D. H. Rosenzweig, E. Carelli, T. Steffen, P. Jarzem and L. Haglund, *Int. J. Mol. Sci.*, 2015, **16**, 15118–15135.
296 M. A. Osman and M. R. A. Atia, *Rapid Prototyp. J.*, 2018, **24**, 1067–1075.
297 J. Girdis, L. Gaudion, G. Proust, S. Löschke and A. Dong, *JOM*, 2016, **69**, 575–579.
298 A. Nogales, E. Gutiérrez-Fernández, M.-C. García-Gutiérrez, T. A. Ezquerra, E. Rebollar, I. Šics, M. Malfois, S. Gaidukovs, E. Gēcis, K. Celms and G. Bakradze, *Macromolecules*, 2019, **52**, 9715–9723.
299 D. Stoof and K. Pickering, *Compos. B Eng.*, 2018, **135**, 110–118.
300 M. F. Arif, H. Alhashmi, K. M. Varadarajan, J. H. Koo, A. J. Hart and S. Kumar, *Compos. B Eng.*, 2020, **184**, 107625.
301 W. Yang, W. Zhao, Q. Li, H. Li, Y. Wang, Y. Li and G. Wang, *ACS Appl. Mater. Interfaces*, 2020, **12**, 3928–3935.
302 K. Markandan and C. Q. Lai, *Compos. Appl. Sci. Manuf.*, 2020, **129**, 105726.
303 M. Jiménez, L. Romero, I. A. Domínguez, M. d. M. Espinosa and M. Domínguez, *Complexity*, 2019, **2019**, 1–30.
304 Y.-a. Jin, J. Plott, R. Chen, J. Wensman and A. Shih, *Procedia CIRP*, 2015, **36**, 199–204.
305 L. J. Marks and J. W. Michael, *BMJ*, 2001, **323**, 732–735.
306 A. Manero, P. Smith, J. Sparkman, M. Dombrowski, D. Courbin, A. Kester, I. Womack and A. Chi, *Int. J. Environ. Res. Public Health*, 2019, **16**, 1641–1656.
307 J. Barrios-Muriel, F. Romero-Sánchez, F. J. Alonso-Sánchez and D. Rodriguez Salgado, *Materials*, 2020, **13**, 295–310.
308 K. Niru, *Top 12 3D printed prostheses*, http://www.3dnatives.com/en/3d-prostheses-100420184/, accessed September 17, 2021.

309 G. M. Tartaglia, A. Mapelli, C. Maspero, T. Santaniello, M. Serafin, M. Farronato and A. Caprioglio, *Materials*, 2021, **14**, 1799–1810.
310 R. McComas, *Dental 3D Scanning and Printing*, http://www.cellular3d.com/index.php/dental-3d-printing/55-clearcorrect-expands-dental-alignment-product, accessed September 17, 2021.
311 B. Artley, *Automotive 3D printing applications*, http://www.3dhubs.com/knowledge-base/automotive-3d-printing-applications/, accessed September 17, 2021.
312 *3D printed clothes in 2020: What are the best projects?*, http://www.sculpteo.com/en/3d-learning-hub/applications-of-3d-printing/3d-printed-clothes/, accessed September 17, 2021.
313 S. Kim, H. Seong, Y. Her and J. Chun, *Fashion and Textiles*, 2019, **6**, 1–24.
314 L. Gaget, *3D printed watch: The most promising projects*, http://www.sculpteo.com/blog/2017/12/19/3d-printed-watch-is-everything-possible/, accessed September 17, 2021.
315 C. Gomez, *Joachim froment designs 3D printed furniture out of recycled plastic waste*, http://www.designboom.com/design/joachim-froment-3d-print-furniture-recycled-plastic-waste-strat-belgium-11-10-2019/, accessed September 17, 2021.
316 M. Ranum, *Kupol – 3D Printed Bike Helmet*, http://www.activegearreview.com/cycling-gear/bike-helmets/kupol-3d-printed-bike-helmet/, accessed September 17, 2021.
317 V. Carlota, *What benefits do 3D printed drones bring to our society?*, http://www.3dnatives.com/en/3d-printed-drone-150620204/#!, accessed September 17, 2021.
318 *Designing a 3D Printed Acoustic Violin*, http://www.formlabs.com/blog/designing-a-3d-printed-acoustic-violin/, accessed September 17, 2021.
319 J. Froment, *Strat Collection - 3D Printed Furniture out of Recycled Plastic, recycled furniture designed by Joachim Froment, FutureWave, Photography*, MAD, Home of Creators, Brussels, https://www.joachimfroment.com/strats-furniture/u7chkmuw3ry02vzwb3sgvmg68nxdb5, accessed September 16, 2021.
320 *3D Printed Glasses: Trends in the eyewear industry in 2020*, http://www.sculpteo.com/en/3d-learning-hub/applications-of-3d-printing/3d-printed-glasses/, accessed September 17, 2021.
321 *Gillette Stays Ahead of the Competition by Using 3D Printing to Unlock Consumer Personalization*, https://formlabs.com/blog/gillette-uses-3d-printing-to-unlock-consumer-personalization, accessed September 16, 2021.
322 D. Ukobitz and R. Faullant, *Res. Technol. Manag.*, 2021, **64**, 20–30.
323 *Reebok's 3D Printed Shoe Line Dashes into Production*, https://3dprintingindustry.com/news/reeboks-3d-printed-shoe-line-dashes-into-production-137497, accessed September 16, 2021.
324 E. E. Petersen, R. W. Kidd and J. M. Pearce, *Technologies*, 2017, **5**, 45–67.
325 *Manufacturing Toys with Production 3D Printing*, http://www.slant3d.com/slant3d-blog/manufacturing-toys-with-production-3d-printing8652532, accessed September 17, 2021.
326 U. Iftikhar, *Marshall ADG to 3D Print Functional Aircraft Parts with Stratasys Fortus 450MC*, http://www.3dprintingindustry.com/news/marshall-adg-to-3d-print-functional-aircraft-parts-with-stratasys-fortus-450mc-156673/, accessed September 17, 2021.
327 *The Best 3D Printed Consumer Products*, https://3dprintingindustry.com/news/the-best-3d-printed-consumer-products-148352, accessed September 16, 2021.
328 *3D Printed Products Made for You*, https://www.batch.works/, accessed September 16, 2021.
329 *Extreme Volume Mascara, 3D Printed Brush*, https://www.chanel.com/gb/makeup/p/191710/le-volume-revolution-de-chanel-extreme-volume-mascara-3d-printed-brush, accessed September 16, 2021.
330 P. Wu, J. Wang and X. Wang, *Autom. ConStruct.*, 2016, **68**, 21–31.
331 B. Ahuja, M. Karg and M. Schmidt, Laser 3D Manufacturing II, *Int. Soc. Opt. Photonics*, 2015, **9353**, 935304–935314.
332 S. H. Ahn, M. Montero, D. Odell, S. Roundy and P. K. Wright, *Rapid Prototyp. J.*, 2002, **8**, 248–257.
333 E. R. Fitzharris, N. Watanabe, D. W. Rosen and M. L. Shofner, *Int. J. Adv. Manuf. Technol.*, 2017, **95**, 2059–2070.
334 L. Wang, J. Palmer, M. Tajvidi, D. J. Gardner and Y. Han, *J. Therm. Anal. Calorim.*, 2018, **136**, 1069–1077.
335 J. Y. Wang, D. D. Xu, W. Sun, S. M. Du, J. J. Guo and G. J. Xu, *IOP Conf. Ser. Mater. Sci. Eng.*, 2019, **479**, 012094.
336 M. Spoerk, J. Gonzalez-Gutierrez, J. Sapkota, S. Schuschnigg and C. Holzer, *Plast., Rubber Compos.*, 2017, **47**, 17–24.
337 L. Chen, Y. He, Y. Yang, S. Niu and H. Ren, *Int. J. Adv. Manuf. Technol.*, 2016, **89**, 3651–3660.
338 S. C. Paul, Y. W. D. Tay, B. Panda and M. J. Tan, *Arch. Civ. Mech. Eng.*, 2018, **18**, 311–319.
339 W. Oropallo and L. A. Piegl, *Eng. Comput.*, 2015, **32**, 135–148.
340 J. R. Castrejon-Pita, W. R. S. Baxter, J. Morgan, S. Temple, G. D. Martin and I. M. Hutchings, *Atomization Sprays*, 2013, **23**, 541–565.
341 H. Stahl, *J. Appl. Ecol.*, Institute for Applied Ecology, Oko-Institut e.V., Darmstadt, Tech. Rep., 2013, vol. 23, pp. 3–4.